

**Aus der Universitätsklinik für Anästhesiologie und  
Intensivmedizin Tübingen**

**Ärztlicher Direktor: Professor Dr. K. Unertl**

**Endothelial Catabolism of Extracellular Adenosine  
during Hypoxia:  
Role of Surface Adenosine Deaminase and CD26**

**Inaugural-Dissertation  
zur Erlangung des Doktorgrades  
der Medizin**

**der Medizinischen Fakultät  
der Eberhard-Karls-Universität  
zu Tübingen**

**vorgelegt von  
Simone Ulrike Knapp  
aus  
Heilbronn**

**2008**

Dekan: Professor Dr. I. B. Autenrieth

1. Berichterstatter: Professor Dr. H. Eltzhig

2. Berichterstatter: Privatdozent Dr. V. Kempf





## List of contents

---

Abbreviations .....	7
1 Introduction .....	9
1.1 Transendothelial migration of polymorphonuclear leukocytes .....	9
1.2 Structural and functional elements of the vascular barrier .....	10
1.3 Vascular barrier during inflammation .....	12
1.4 Increased adenosine production during hypoxia .....	19
1.5 Role of adenosine deaminase in vascular inflammation during hypoxia ....	20
1.6 Aims of the study .....	22
2 Materials and Methods.....	23
2.1 Equipment.....	23
2.2 Materials .....	24
2.3 Chemicals .....	26
2.4 Methods .....	31
2.4.1 Endothelial cell culture: .....	31
2.4.2 Endothelial cell culture in hypoxia unit (5% CO <sub>2</sub> , 2% O <sub>2</sub> , 37°C):.....	34
2.4.3 RNA isolation: .....	35
2.4.4 Photometric measurement of RNA: .....	36
2.4.5 DNase digestion: .....	36
2.4.6 cDNA synthesis / reverse transcription: .....	38
2.4.7 Real - time RT-PCR: .....	38
2.4.8 Gel electrophoresis: .....	40
2.4.9 Immunblotting experiments: .....	40
2.4.10 Measurement of ADA activity in cell culture experiments: .....	44
2.4.11 Macromolecule paracellular permeability assay: .....	46
2.4.12 In vivo hypoxia model:.....	47
3 Results .....	50
3.1 Endothelial ADA mRNA and protein are induced by hypoxia.....	50
3.2 Functional results for hypoxia induced ADA .....	54
3.3 Transcriptional induction of the ADA complexing protein CD26 is coordinated by hypoxia .....	60
3.4 Influence of ADA activity on endothelial adenosine signaling .....	65
3.5 In vivo model for endothelial permeability and PMN tissue accumulation ..	71
4 Discussion .....	77

5 Summary .....	83
6 References .....	87
7 Danksagung .....	99
8 Lebenslauf .....	100

## Abbreviations

ADA.....	adenosine deaminase
AdoRA <sub>2A</sub> .....	A <sub>2A</sub> -adenosine receptor
AdoRA <sub>2B</sub> .....	A <sub>2B</sub> -adenosine receptor
ADP.....	adenosine diphosphate
AMP.....	adenosine monophosphate
APCP.....	5'-alpha, beta-methylenediphosphate
ARDS.....	adult respiratory distress syndrome
ATP.....	adenosine triphosphate
cAMP.....	cyclic adenosine monophosphate
CNT.....	concentrative nucleoside transporter
ENT.....	equilibrative nucleoside transporter
fMLP.....	peptide formyl-Met-Leu-Phe
mGluR.....	metabotropic glutamate receptor
BMK1 (= ERK5).....	big mitogen-activated protein kinase1 gene
HBP (= CAP37).....	heparin-binding protein
HIF.....	hypoxia-inducible factor
MAPK.....	mitogen-activated protein kinase
MEF2C.....	myocyte enhancer factor 2C
MPO.....	myeloperoxidase
PKA.....	protein kinase A
PMN.....	polymorphonuclear leukocyte
TEM.....	transendothelial migration
JAM.....	junctional adhesion molecule
SIRS.....	systemic inflammatory response syndrome
VASP.....	vasodilator-stimulated phosphoprotein





## 1 Introduction

### 1.1 Transendothelial migration of polymorphonuclear leukocytes

About 70 million polymorphonuclear leukocytes (PMN) exit the vasculature per minute (1). These inflammatory cells move into underlying tissue by passing between endothelial cells that line the inner surface of blood vessels. This process, referred to as transendothelial migration (TEM), is particularly prevalent in inflamed tissues, but also occurs as a natural process of leukocyte mobilization (e.g. bone marrow extravasation). Understanding the biochemical details of leukocyte - endothelial interactions is currently an area of concentrated investigation, and recent studies using genetically modified animals have identified specific molecules which function as "bottlenecks" in the control of the inflammatory response (2). For example, detailed studies have shown that the leukocyte TEM causes a concerted series of events involving intimate interactions of a series of leukocyte and endothelial glycoproteins that include selectins, integrins, and members of the immunoglobulin supergene family (3-5).

Histologic studies of TEM reveal that PMN initially adhere to endothelium, move to nearby inter-endothelial junctions via diapedesis, and insert pseudopodia into the inter-endothelial paracellular space (6).

Successful TEM is accomplished by temporary PMN self-deformation with localized widening of the inter-endothelial junction. Especially during episodes of inflammation, TEM has the potential to disturb vascular barrier function and give rise to fluid extravasation and edema. However, several innate mechanisms have been described to dampen fluid loss during PMN-endothelial interactions (7). For example, after transendothelial migration, adjacent endothelial cells appear to "reseat", leaving no residual inter-endothelial gaps (6). These histologic studies are consistent with the observation that leukocyte TEM may result in little or no change in endothelial permeability to macromolecules (8-12). In the absence of this tight and dynamic control of endothelial morphology and permeability, inter-endothelial

gap formation during leukocyte TEM could lead to marked increases in endothelial permeability.

However, only limited information exists regarding the biochemical events which maintain and dynamically regulate endothelial permeability in the setting of either PMN activation or TEM (5, 6). Studies have revealed that activated PMN release soluble factors which support maintenance of endothelial permeability during PMN-endothelial interactions (7, 13, 14). Several crosstalk pathways have been identified to protect endothelial function during inflammation and hypoxia and to dampen excessive fluid loss into the interstitium. Such innate protective pathways share the common strategy to increase intravascular adenosine concentrations and adenosine signaling within the inflamed or hypoxic vasculature (7, 13, 15-18).

## **1.2 Structural and functional elements of the vascular barrier**

Movement of macromolecules across a blood vessel wall is mainly inhibited by the endothelium (19, 20). Macromolecules can cross a cellular monolayer via either a paracellular route (i.e., between cells) or a transcellular route (i.e., through cells). In non-pathologic endothelium, macromolecules such as albumin (molecular weight ~40 kD) appear to cross the cell monolayer by passing between adjacent endothelial cells (i.e., paracellular) although some degree of transcellular passage may also occur (21, 22). Endothelial permeability is determined by cytoskeletal mechanisms that regulate lateral membrane intercellular junctions (23, 24). Tight junctions, also known as zona occludens, comprise one type of intercellular junction. Transmembrane proteins found within this region which function to regulate paracellular passage of macromolecules include the proteins occludin, and members of the junctional adhesion molecule (JAM) and claudin families of proteins (18). Tight junctions form narrow, cell-to-cell contacts with adjacent cells and comprise the predominant barrier to transit of macromolecules between adjacent endothelial cells (25). Endothelial macromolecular permeability is

inversely related to macromolecule size. Permeability is also dependent on the tissue of origin. For example, endothelial cells in the cerebral circulation (i.e., blood-brain barrier) demonstrate an exceptionally low permeability (26, 27). Endothelial permeability may increase markedly upon exposure to a variety of inflammatory compounds (e.g., histamine, thrombin, reactive oxygen species, leukotrienes, bacterial endotoxins) or adverse conditions (e.g., hypoxia, ischemia) (6, 19). Reversible increases in endothelial permeability are produced by administration of cytochalasin or other agents that disrupt cytoskeletal microfilaments (19, 28). Likewise, increases in endothelial permeability are accompanied by disruption of peripheral actin microfilaments and formation of gaps between adjacent endothelial cells (19, 28). Administration of compounds that decrease endothelial permeability result in an irregular endothelial cell contour, greater convolution of cell margins, closer cell-to-cell contact, and increased surface area and cell perimeter (28). These changes in cell morphology are accompanied by a loss of F-actin in stress fibers, “ruffling” of dense peripheral bands of F-actin, and increase in the polymerized actin pool without significant changes in total F-actin endothelial cell content (23, 24). Interestingly, these changes in intracellular actin are similar to those observed during PMN transendothelial migration (29). By comparison, thrombin-induced increases in permeability result in a centralization and peripheral loss of F-actin. Both of these changes (permeability and F-actin distribution) are inhibited by isoproterenol (30). Phalloidin, an F-actin-stabilizing compound, also markedly attenuates thrombin-induced increases in permeability and accompanying morphologic changes.

In addition to the above components of the vascular barrier, the glycocalyx may play a role in determining movements of fluid and macromolecules across the endothelium. The endothelial glycocalyx is a dynamic extracellular matrix composed of cell surface proteoglycans, glycoproteins, and adsorbed serum proteins, implicated in the regulation and modulation of capillary tube hematocrit, permeability, and hemostasis (31). As such, increased paracellular permeability of such molecules as water, albumin and hydroxyethyl starch can be observed

following experimental degradation of the functional components of the glycocalyx (32), and functional components of this glycocalyx may be dynamically regulated by endogenous mediators such as adenosine (33).

### **1.3 Vascular barrier during inflammation**

Ongoing inflammatory responses are characterized by dramatic shifts in tissue metabolism. These changes include large fluctuations in energy supply and demand and diminished availability of oxygen (34). Such shifts in tissue metabolism result, at least in part, from profound recruitment of inflammatory cell types, particularly myeloid cells such as neutrophils (PMN) and monocytes. The majority of inflammatory cells are recruited to, as opposed to being resident at, inflammatory lesions, and myeloid cell migration to sites of inflammation are highly dependent on hypoxia-adaptive pathways (34, 35). Consequently, much recent attention has focused on understanding how metabolic changes (e.g. hypoxia) relate to the establishment and propagation of the inflammatory response.

As previously shown, many parallels exist between hypoxic and inflamed tissues (36). For example, during episodes of hypoxia, polymorphonuclear leukocytes (PMN) are mobilized from the intravascular space to the interstitium, and such responses may contribute significantly to tissue damage during consequent reperfusion injury (37-39). Moreover, emigration of PMN through the endo- and epithelial barrier may lead to a disruption of such tissue barriers (40-42) and such a setting creates the potential for extravascular fluid leakage and subsequent edema formation (43, 44).

#### **a) Barrier disruptive pathways**

Macromolecule transit across blood vessels has evolved to be tightly controlled. Relatively low macromolecular permeability of blood vessels is essential for maintenance of a physiologically optimal equilibrium between intravascular and

extravascular compartments (45, 46). Endothelial cells are primary targets for leukocytes during episodes of infection, ischemic or traumatic injury, which all together can result in an altered barrier function. Disturbance of endothelial barrier during these disease states can lead to deleterious loss of fluids and plasma protein into the extravascular compartment. Such disturbances in endothelial barrier function are prominent in disorders such as shock and ischemia-reperfusion and contribute significantly to organ dysfunction (47-51).

As outlined above, previous studies have indicated that activated PMN release a number of soluble mediators, which dynamically influence vascular permeability during transmigration. As such, PMN have been shown to liberate factors that can either disrupt or protect the endothelial barrier: For example, it was recently shown that activation of PMN through  $\beta_2$  integrins elicits the release of soluble factor(s) which induce endothelial cytoskeletal rearrangement, gap formation and increased permeability (52). This PMN-derived permeabilizing factor was subsequently identified as heparin-binding protein (HBP, also called azurocidin or CAP37) (52), a member of the serprocidin family of cationic peptides (53). HBP, but not other neutrophil granule proteins (e.g. elastase, cathepsin G), was shown to induce  $\text{Ca}^{2+}$ -dependent cytoskeletal changes in cultured endothelia and to trigger macromolecular leakage in vivo. Interestingly, HBP regulation of barrier may not be selective for PMN, and in fact, endothelial cells themselves are now a reported source of HPB (54). It is therefore possible that endothelia may self-regulate permeability through HBP under some conditions, and that mediators found within the inflammatory milieu may also increase endothelial permeability.

Similarly, PMNs were observed to significantly alter endothelial permeability by release of glutamate, following FMLP activation. This crosstalk pathway appears to be of particular importance for the regulation of the vascular barrier of the brain ("blood brain barrier"). In fact, treatment of human brain endothelia with glutamate or selective mGluR group I or III agonists resulted in a time-dependent loss of phosphorylated vasodilator-stimulated phosphoprotein (VASP) and significantly

increased endothelial permeability. Glutamate-induced decreases in brain endothelial barrier function and phosphorylated VASP were significantly attenuated by pretreatment of human brain endothelia with selective mGluR antagonists. Even in an *in vivo* hypoxic mouse model, the pretreatment with mGluR antagonists significantly decreased fluorescein isothiocyanate-dextran flux across the blood-brain barrier, suggesting that activated human PMNs release glutamate and that endothelial expression of group I or III mGluRs function to decrease human brain endothelial VASP phosphorylation and barrier function (38).

A recently described gene regulatory pathway revealed a critical role for BMK1/ERK5 in maintaining the endothelial barrier and blood vessel integrity: A targeted deletion of big mitogen-activated protein kinase1 gene (BMK1) (also known as ERK5, member of the MAPK family) in adult mice leads to disruption of the vascular barrier. Histological analysis of these mice reveals that, after BMK1 ablation, hemorrhages occurred in multiple organs in which endothelial cells lining the blood vessels became round, irregularly aligned, and, eventually, apoptotic. *In vitro* removal of BMK1 protein also led to the death of endothelial cells partially due to the deregulation of transcriptional factor MEF2C, which is a direct substrate of BMK1. Additionally, endothelial-specific BMK1-KO leads to cardiovascular defects identical to that of global BMK1-KO mutants. Taken together, these studies identify the BMK1 pathway as critical role for endothelial function and for maintaining blood vessel integrity (55).

### **b) Barrier protective pathways**

Acute increases in vascular permeability to macromolecules closely coincides with tissue injury of many etiologies, and can result in fluid loss, edema, and organ dysfunction (19, 56, 57).

However, transcriptional pathways mediated by hypoxia-inducible factor (HIF) may serve as a barrier-protective element during inflammatory hypoxia. For example, experimental studies of murine inflammatory bowel diseases have revealed extensive mucosal hypoxia and concomitant HIF-1 activation during colitis. Mice

engineered to express decreased intestinal epithelial HIF-1 exhibit more severe clinical symptoms of colitis, while increased HIF levels were protective in these parameters. Furthermore, colons with constitutive activation of HIF displayed increased expression levels of HIF-regulated barrier-protective genes (multidrug resistance gene-1, intestinal trefoil factor, CD73), resulting in attenuated loss of barrier during colitis *in vivo*. Such studies identify HIF as a critical factor for barrier protection during mucosal inflammation and hypoxia (58).

Previous studies have also indicated that extracellular nucleotide metabolites may function as an endogenous protective mechanism during hypoxia and ischemia (59-61). One important factor may be an increased production of endogenous adenosine, a naturally occurring anti-inflammatory agent (61-63). Several lines of evidence support this assertion. First, adenosine receptors are widely expressed on target cell types as diverse as leukocytes, vascular endothelia, and mucosal epithelia and have been studied for their capacity to modulate inflammation (64). Second, murine models of inflammation provide evidence for adenosine receptor signaling as a mechanism for regulating inflammatory responses *in vivo*. For example, mice deficient in the  $A_{2A}$ -adenosine receptor ( $AdoRA_{2A}$ ) show increased inflammation-associated tissue damage (65). Third, hypoxia is a common feature of inflamed tissues (34) and is accompanied by significantly increased levels of adenosine (66-68). The source of adenosine is likely result from a combination of increased intracellular metabolism and amplified extracellular phosphohydrolysis of adenine nucleotides via surface ecto-nucleotidases (see below) (13).

The vascular endothelium is the primary interface between a hypoxic insult and the surrounding tissues. At the same time, the endothelium is central to the orchestration of leukocyte trafficking in response to chemotactic stimuli. This critical anatomic location places vascular endothelial cells in an ideal position to coordinate extracellular metabolic events important to endogenous anti-inflammatory responses. Recently there was identified a neutrophil-endothelial cell crosstalk pathway that is coordinated by hypoxia. This pathway utilizes extracellular nucleotide substrates, liberated from different cell types. Extracellular

ATP release has been shown from endothelial cells, particularly under sheer conditions or hypoxia. In addition, FMLP activated neutrophils can release ATP, however the exact mechanism through that these cells release ATP remains currently unknown (see below) (13, 69). Activated platelets comprise an additional source for extracellular adenine nucleotides (70, 71). The role of endothelial CD39 (Ecto-apyrase, conversion of ATP/ADP to AMP) has been viewed as a protective, thromboregulatory mechanism for limiting the size of the hemostatic plug (71, 72). Metabolism of adenine nucleotides derived from activated platelets is crucial in limiting excessive platelet aggregation and thrombus formation (73, 74). Similarly, excessive platelet accumulation and recruitment can be treated with the use of soluble forms of CD39 (75, 76). Moreover, a thromboregulatory role could be demonstrated in a model of stroke, where CD39-null mice showed increased sizes of infarction that could be reduced by treatment with soluble CD39 (77). Surprisingly, targeted disruption of CD39 resulted in prolonged bleeding and increased vascular leak and fibrin deposition in hypoxemia (78), suggesting a dual role for ATP metabolism by CD39 in modulating hemostasis and thrombotic reactions. Moreover, this observation may be related to an activation and desensitization of the purinergic type  $P_2Y_1$  receptor. Activation of the  $P_2Y_1$ -platelet receptor appears to be crucial in the activation process of platelets. As such,  $P_2Y_1$  deficient mice exhibit signs of prolonged bleeding time and resistance to thromboembolism (79).

Extracellular ATP is readily converted on the endothelial surface to adenosine, due to the enzymatic function of CD39 and CD73 (5'-Ecto-nucleotidase, conversion of AMP to adenosine). Such adenosine binds to surface expressed PMN adenosine receptors to limit excessive accumulation of PMN within tissues, and as such, functions as a feedback loop to attenuate potential tissue injury (69). With regard to this latter point, it was recently shown that hypoxia coordinates both, transcriptional and metabolic control of the surface ecto-nucleotidases CD39 and CD73 (15, 80, 81), and as such, significantly amplifies the extracellular production of adenosine from adenine nucleotide precursors. In fact when using CD39- and CD73-null



animals it was found that extracellular adenosine produced through adenine nucleotide metabolism during hypoxia is a potent anti-inflammatory signal for PMN *in vitro* and *in vivo*. These findings identify CD39 and CD73 as critical control points for endogenous adenosine generation and implicate this pathway as an innate mechanism to attenuate excessive tissue PMN accumulation (69).

In addition to a role in limiting excessive neutrophil tissue accumulation, CD39 and CD73 are also critical control points for vascular permeability. For the purpose of investigating overall organ vascular permeability, there was used Evan's blue dye, which tightly binds to plasma albumin (82). To do this, mice were administered 0.2% Evan's blue dye (0.5% in PBS) by intravenous tail vein injection and subjected to room air (normoxia) or normobaric hypoxia (8% O<sub>2</sub> / 92% N<sub>2</sub>). At the end of exposure, animals were anesthetized, heparinized (50 U by i.p. injection) and fluid overloaded (3 c.c. normal Ringer's solution i.p.). Animals were then exsanguinated by femoral cut-down to flush all vascular beds, and tissues were harvested. Tissues were rinsed in PBS, and Evan's blue was extracted with formamide at 56°C for 2 hours, and quantified at 610nm with subtraction of reference absorbance at 450nm. This model entails the quantification of formamide-extractable Evans blue (83) from tissues of mice as a readout for overall vascular permeability of different organs. In fact vascular permeability in tissues derived from animals subjected to normobaric hypoxia (8% O<sub>2</sub> / 92% N<sub>2</sub>) ranged from 2 - 4-fold more permanent to Evans blue than normoxic controls (13).

In order to identify the role of CD73 in vascular permeability, this model was used in mice that were administered with the CD73 inhibitor 5'-alpha, beta-methylenediphosphate (APCP) or in mice following targeted deletion of CD73. In fact, there was found dramatic increase of hypoxia-elicited dysfunction of the vascular barrier in different organs (lung, heart, intestine, kidneys) following CD73 inhibition or deletion. Vascular leak associated with hypoxia was, at least in part, reversed by reconstitution with soluble 5'-nucleotidase and adenosine receptor agonists in the CD73-null mice. Histological examination of lungs from hypoxic

CD73-null mice revealed perivascular interstitial edema associated with inflammatory infiltrates surrounding larger pulmonary vessels (84). Taken together, these studies have identified CD73 as a critical mediator of vascular permeability *in vivo*. When measuring vascular permeability during hypoxia in mice with targeted deletion of CD39, similar increases in vascular barrier function could be observed in different organs (13). Consequently, adenosine generation of the hypoxic vasculature via nucleotide-phosphohydrolysis is identified as a cellular strategy to maintain vascular barrier function.

### **c) Effect of adenosine receptor activation on endothelial barrier function**

*In vitro* studies of endothelial permeability suggested, that activation of a specific endothelial adenosine receptor, the AdoRA<sub>2B</sub>, leads to a barrier resealing response following PMN transmigration (7). It was shown that of the four different adenosine receptors that are expressed by endothelia, only the AdoRA<sub>2B</sub> is selectively induced by hypoxia (13). Activation of the AdoRA<sub>2B</sub> is associated with increases in intracellular cAMP concentration due to the activation of the adenylate cyclase (61). By inhibition of cAMP formation, the resealing of the endothelial barrier during PMN transmigration can be obviated (7). Such increases in cAMP following activation of the AdoRA<sub>2B</sub> lead to an activation of protein kinase A (PKA) (18). Further studies revealed a central role of PKA-induced phosphorylation of vasodilator-stimulated phosphoprotein (VASP), a protein responsible for controlling the geometry of actin-filaments (85). Adenosine-receptor mediated phosphorylation of VASP is responsible for changes in the geometry and distribution of junctional proteins, thereby affecting the characteristics of the junctional complex and promoting increases in barrier function (86, 87).

#### 1.4 Increased adenosine production during hypoxia

The exact metabolic steps for generation of extracellular adenosine in hypoxia are not well characterized, but hypoxia is likely involved in increased enzymatic phosphohydrolysis from precursor adenine nucleotides (ATP, ADP and AMP). For example, it was recently demonstrated that hypoxia coordinates both transcriptional and metabolic control of the surface ecto-nucleotidases CD39 and CD73 (15, 80, 81) and thereby amplifies extracellular accumulation of adenosine. Additional mechanisms also exist to amplifying adenosine signaling during hypoxia including coordinate changes at the adenosine receptor level. As shown above, the vascular endothelial adenosine receptor subtype AdoRA<sub>2B</sub> is selectively induced by hypoxia and such increases in receptor density are associated with increased vascular barrier responses to adenosine (81).

After generation in the extracellular milieu, adenosine is rapidly cleared through passive or active uptake through nucleoside transporters, termed equilibrative nucleoside transporters (ENT) and concentrative nucleoside transporters (CNT), respectively, which are expressed on a variety of cell types (88). The predominant nucleoside transporters of the vascular endothelium are ENT1 and ENT2 (89), bi-directional transporters functioning as diffusion-limited channels for transmembrane adenosine flux. Previous studies have suggested that vascular adenosine flux during hypoxia is predominantly inward (90), thereby extracellular adenosine signaling is terminated. However, more recent studies indicate that the expression of ENT1 may be transcriptionally regulated by hypoxia (91, 92), thereby functioning to fine tune extracellular levels of adenosine.

Therefore, considering that endothelial adenosine uptake could influence endothelial cell function during hypoxia, as well as a recent study suggesting that ENT1 and ENT2 gene-regulation are influenced by hypoxia in murine cardiomyocytes (91, 92), next examinations were the influence of hypoxia on vascular endothelial adenosine transport. Results from these studies revealed that endothelial ENT1 and ENT2 gene expression and function are attenuated by

hypoxia, so these results identified transcriptional repression of ENT as an innate mechanism to elevate extracellular adenosine during hypoxia. Further examination of the ENT1 promoter identified a hypoxia inducible factor 1 (HIF-1)-dependent repression of ENT1. These studies provide new molecular insight into endogenous mechanisms of tissue protection during hypoxia (93).

### **1.5 Role of adenosine deaminase in vascular inflammation during hypoxia**

The influence of hypoxia on cell physiology and pathophysiologic response are still areas of intense investigation and several reports suggest that both transcriptional and metabolic pathways may contribute to a broad range of diseases (64). For example, during periods of hypoxia / ischemia, polymorphonuclear leukocytes (PMN) are mobilized from the intravascular space to the interstitium (94, 95), and such responses may contribute significantly to tissue damage during consequent reperfusion injury (96). Emigration of PMN through the endothelial barrier is associated with a disruption of tissue barriers creating the potential for vascular fluid leakage and subsequent edema formation (13, 97). Examples for such “hypoxia-associated” disorders are the systemic inflammatory response syndrome (SIRS), sepsis, acute respiratory distress syndrome (ARDS) and acute myocardial infarction (36, 98-102).

Other studies have indicated that extracellular nucleotide metabolites (particularly adenosine) may function as an endogenous anti-inflammatory metabolite during hypoxia (13, 64, 95, 96, 103). Pathophysiologic changes like increased tissue permeability, accumulation of inflammatory cells, and transcriptional induction of pro-inflammatory cytokines during hypoxia have seemed to be dampened by vascular adenosine signaling during hypoxia (64, 104). Several lines of evidence support this assertion (105). First, adenosine receptors have been found numerously on vascular endothelial cells, and have been studied for their capacity to modulate inflammation (64, 95, 97). Second, murine models of inflammation

and/or hypoxia provide evidence for adenosine receptor signaling as a mechanism for regulating hypoxia responses *in vivo*. Indeed, mice genetically deficient in surface enzymes CD39 (conversion of ATP to AMP) and CD73 (conversion of AMP to adenosine) which are necessary for adenosine generation, show increased hypoxia-associated tissue damage and vascular leak syndrome during hypoxia (13, 97). Third, hypoxia accompanies the normal inflammatory response (34, 106, 107) and is associated with significantly increased levels of adenosine (90, 108). Even if the exact sources of adenosine are not well defined, it is likely a result from a combination of increased intracellular metabolism and amplified extracellular phosphohydrolysis of adenine nucleotides via surface ectonucleotidases (CD39 and CD73) (13, 97). As described above already, recent studies have revealed that the predominant nucleoside transporter ENT1 is transcriptionally repressed by hypoxia, thereby providing an additional mechanism to elevate vascular adenosine levels during hypoxia (109).

In spite of the central role of adenosine in inflammatory or hypoxic tissue, chronically increased levels of adenosine may be detrimental (110). One evidence for this assumption are increased levels of adenosine in the lungs of asthmatics (111), in which elevations of adenosine correlate with the degree of inflammatory insult (112). These findings suggest a stimulating role of adenosine in asthma or chronic obstructive pulmonary disease (113). Furthermore, mice suffering from deficiency of adenosine-deaminase (ADA [conversion of adenosine to inosine]) develop signs of chronic pulmonary injury in association with elevated pulmonary adenosine levels. ADA-deficient mice, in fact, die within weeks after birth from severe respiratory distress (114), and recent studies suggest that attenuation of adenosine signaling may reverse the severe pulmonary phenotypes in ADA-deficient mice, suggesting that chronic adenosine elevations can affect signaling pathways that mediate aspects of chronic lung disease (115, 116). Similarly, ADA deficiency in human beings is a well characterized severe combined immunodeficiency syndrome associated with T cell cytotoxicity by deoxyadenosine (117, 118).

So, adenosine-deaminase (ADA) induction may serve as innate adaptation to protect the organism from potentially deleterious effects of long exposure of adenosine or its metabolites.

### 1.6 Aims of the study

Extracellular levels of the nucleoside adenosine significantly increase during conditions of hypoxia to counterbalance excessive inflammation and vascular leakage. So levels of circulating adenosine can reach nearly micromolar concentrations in cases of severe hypoxia. On the other side, as described above, chronically increased adenosine concentrations may be deleterious. Based on these findings the following study will try to define whether mechanisms exist to degrade extracellular adenosine in models of hypoxia with increased adenosine.

Initial microarray analyses have revealed a nearly fifty-fold induction of endothelial adenosine deaminase (ADA) mRNA in hypoxia, so adenosine deaminase may work as clearance mechanism in hypoxic endothelia.

To certify this hypothesis, first studies will be done in endothelial cells with different hypoxic exposure time, next steps will be functional experiments in murine models of hypoxia with and without inhibition of the enzyme adenosine deaminase, and finally experiments will also be done in an *in vivo* model.

Further questions will be examined in detail:

Where is the enzyme localized, on cell surface or inside the cells?

Are other enzymes involved in this clearance mechanism, or are there other pathways to dampen elevated adenosine?

## 2 Materials and Methods

### 2.1 Equipment

**Blotting chamber:** Trans Blot Cell<sup>®</sup>, BIO-RAD Laboratories Inc. (Hercules, CA, USA)

**Centrifuge:** Biofuge fresco, Heraeus Instruments (Hanau, Germany)

**Centrifuge:** Megafuge 1.0 R, Heraeus Sepatech (Hanau, Germany)

**Centrifuge:** Model TJ-6, BECKMAN (Krefeld, Germany)

**Column thermometer:** Jetstream-II-Plus-Säulenthermostat, VDS Oplitlab (Berlin, Germany)

**Detector:** UVD 170S, Dionex GmbH (Idstein, Germany)

**Diana:** Raytest (Straubenhardt, Germany)

**Electrophoresis chamber:** Horizon 11.14, GIBCO Invitrogen (Paisley, Scotland)

**Electrophoresis chamber:** x-cell sure lock, GIBCO Invitrogen (Paisley, Scotland)

**End-over-end-rotator:** Heidolph (Schwabach, Germany)

**Fluorescence Reader:** Cytofluor 2300, Millipore Corp., Waters Chromatography (Bedford, MA, USA)

**Freezer (-20° C):** Bosch (Stuttgart, Germany)

**Freezer (-80° C):** Model MDF-592, Sanyo Electric Biomedical Co., Ltd. ( Bensenville, IL, USA)

**HPLC-pump:** P680-HPLC, Dionex GmbH (Idstein, Germany)

**Hypoxia unit:** Invivo2 Hypoxia Workstation 400 + Hypoxia Gas Mixer, RUSKINN Technology Limited (Leeds, United Kingdom)

**Ice machine:** ZIEGRA (Isernhagen, Germany)

**iCycler:** BIO-RAD Laboratories Inc. (Hercules, CA, USA)

**Incubator:** Cytoperm 2, Heraeus Instruments (Hanau, Germany)

**Laboratory software:** Chromeleon V-6.50, Dionex GmbH (Idstein, Germany)

**Light-optical microscope:** DMIL, LEICA (Wetzlar, Germany)

**Magnetic stirrer:** IKAMAG<sup>®</sup> RCT, IKA (Staufen, Germany)

**Microtiter plate reader:** BIO-RAD Laboratories Inc. (Hercules, CA, USA)

**Microwave:** SIEMENS (Stuttgart, Germany)

**Photometer:** Ultrospec 3000pro + DPU-414 Thermal Printer, amersham pharmacia biotech (Cambridge, United Kingdom)

**Pipettor:** Pipetboy acu, INTEGRA BIOSCIENCES (Fernwald, Germany)

**Pipettors (10-1000 µl):** Pipetman, Gilson (Middleton, WI, USA)

**Precision balance:** Mettler PK 4800 Delta Range<sup>®</sup>, Mettler-Toledo GmbH (Giessen, Germany)

**Refrigerator (+ 4° C):** Liebherr (Ochsenhausen, Germany)

**Reverse-phase column:** Grom-Sil 120-ODS-ST-5µ; 150x3 mm Grom, Maisch GmbH (Ammerbuch-Entringen, Germany)

**Sample encoder:** L 7200 autosampler, Merck-Hitachi (Darmstadt, Germany)

**Seasaw-rotator:** Heidolph (Schwabach, Germany)

**Shaker:** Block Scientific Inc. (Englewood, NJ, USA)

**Shrink-wrap machine impulse seater:** TEW Electric Heating Equipment (Taipei, Taiwan)

**Speed vac:** Vacufuge, Eppendorf (Westbury, NY, USA)

**Table-centrifuge:** SD/220VAC, Roth (Taiwan)

**Thermocycler:** Mastercycler gradient, Eppendorf (Wesseling-Berzdorf, Germany)

**Thermomixer:** 5436, Eppendorf (Hamburg, Germany)

**Vortexer:** Vortex-Genie 2/G-560E, Scientific Industries, Inc. (New York, USA)

**Water bath:** 1083, GFL (Burgwedel, Germany)

**Workbench:** LaminAir HB2472S, Heraeus Instruments (Hanau, Germany)

## 2.2 Materials

**10-well NuPAGE<sup>®</sup> Novex Bis-Tris gel 4-12%:** GIBCO Invitrogen (Paisley, Scotland); #NPO322BOX



**96-well 0.2 ml thin-wall PCR plate:** BIO-RAD Laboratories Inc. (Hercules, CA, USA); #223-9441

**Beakers:** Schott Duran (Stafford, United Kingdom)

**Cannulae:** BD Microlance, Becton Dickinson Labware (Heidelberg, Germany)

**Carbon dioxide bottle:** Messer Griesheim GmbH (Düsseldorf, Germany)

**Cell culture flasks 75 cm<sup>2</sup>:** TPP (Trasadingen, Switzerland); #90076

**Cell-scraper:** Corning Incorporated Life Sciences (Schiphol-Rijk, Netherlands); #3010

**Collagen coated cell culture flasks 75 cm<sup>2</sup>:** Becton Dickinson Labware (Heidelberg, Germany); #35-4485

**Eppendorf tubes (0.5, 1.5, 2.0 ml):** Eppendorf (Wesseling-Berzdorf, Germany)

**Erlenmeyer flasks:** Schott Duran (Stafford, United Kingdom)

**Falcon tubes 50 ml:** Becton Dickinson Labware (Heidelberg, Germany); #352070

**Gel blotting paper:** Whatman<sup>®</sup> Schleicher & Schuell (Dassel, Germany); #10426693

**Measuring cylinder:** Schott Duran (Stafford, United Kingdom)

**Mice:** C57BL/6/129 svj mice, Charles River Lab, Inc. (Wilmington, MA, USA)

**Nitrogen bottle:** Messer Griesheim GmbH (Düsseldorf, Germany)

**Optical sealing tape:** BIO-RAD Laboratories Inc. (Hercules, CA, USA); #223-9444

**Oxygen bottle:** Linde AG (Höllriegelskreuth, Germany)

**Petri dishes (10 cm):** Cellstar<sup>®</sup>, Greiner Bio-One GmbH (Frickenhausen, Germany); #663102

**Pipette tips:** Biozym Diagnostik GmbH (Hess. Oldendorf, Germany)

**Pipettes (1, 5, 10, 25, 50 ml):** Falcon<sup>®</sup>, Becton Dickinson Labware (Heidelberg, Germany)

**Plastic bags:** Fisher Scientific (Schwerte, Germany); #5706377

**Polycarbonate permeable inserts (0.4- $\mu$ m pore, 6.5-mm diam):** Costar Corp. (Cambridge, MA, USA)

**Power Pack 200:** BIO-RAD Laboratories Inc. (Hercules, CA, USA)

**Power Pack 3000:** BIO-RAD Laboratories Inc. (Hercules, CA, USA)

**PVDF membranes Immun-Blot™:** BIO-RAD Laboratories Inc. (Hercules, CA, USA); #1620177

**Quartz cuvettes:** Hellma GmbH & Co (Müllheim, Germany)

**Sterile tissue:** Kinidrape® , Mölnlycke (Erkrath, Germany)

**Syringes (5, 10, 20 ml):** Braun (Melsungen, Germany)

### 2.3 Chemicals

**2,2-Azino-di-(3-ethyl) di-thiazoline sulfonic acid (ABTS)** 10mg/tablet: Sigma (Taufkirchen, Germany); #A-9941

**Accutase** 100 ml: PAA Laboratories GmbH (Cölbe, Germany); #L11-007

**Acetonitrile** 1000 ml: Merck (Darmstadt, Germany); #100030

**Adenosine (> 99%):** Sigma (Taufkirchen, Germany); #A-9251

**Agarose** 100 g: Type I-A Low EEO, Sigma (Taufkirchen, Germany); #A-0169

**Ammonium chloride (NH<sub>4</sub>Cl)** 1000 g: Merck (Darmstadt, Germany); #1145

**Antibiotic/antimycotic solution** 100 ml: Sigma (Taufkirchen, Germany); #A-5955

**Biotin** 1 g: Applichem GmbH (Darmstadt, Germany); #A0969.0001

**Bovine adenosine deaminase:** Sigma (Taufkirchen, Germany); #A-5168

**BRADFORD protein solution:** BIO-RAD Laboratories Inc. (Hercules, CA, USA); #500-0201

**Bromphenolblue-sodium salt** 5 g: Applichem GmbH (Darmstadt, Germany); #A3640.0005

**BSA** 1000 g: Sigma (Taufkirchen, Germany); #A-7902

**CD26 primer** (sense primer 5'-AAA ATG AGT CCA AGG AAG TT-3' and antisense primer 5'-AGG CAG CTT GAA ACT GAG-3'), PCR product size 166 bp: Thermo Electron GmbH (Ulm, Germany)

**Chloroform (CHCl<sub>3</sub>)** 25 ml: Sigma (Taufkirchen, Germany); #C-2432

**Citrate buffer:** Sigma (Taufkirchen, Germany); #P-4922

**Collagenase A solution** 500 mg: Roche (Mannheim, Germany); #10103586001

**Complete proteinase inhibitor cocktail tablets:** Roche (Mannheim, Germany); #11836145001

**Deoxycoformycin:** Wyeth Pharma (Münster, Germany)

**Dipyridamole** (10 mg/2 ml): Bedford Laboratories<sup>TM</sup> (Bedford, OH, USA); #55390-555-10

**Distilled water:** self-made

**DNA ladder (100 bp)** 250 µl: Promega GmbH (Mannheim, Germany); #G2101

**D-PBS<sup>-</sup> (-CaCl<sub>2</sub> / -MgCl<sub>2</sub>)** 500 ml: GIBCO Invitrogen (Paisley, Scotland); #14190-094

**D-PBS<sup>+</sup> (+CaCl<sub>2</sub> / +MgCl<sub>2</sub>)** 500 ml: GIBCO Invitrogen (Paisley, Scotland); #14040-091

**EDTA** 250 g: Sigma (Taufkirchen, Germany); # E-5134

**Endothelial Cell Growth-medium (EGM-medium) Kit** 500 ml: PromoCell (Heidelberg, Germany); #C-22110

**Epidermal growth factor:** BD Biosciences (Bradford, MA, USA); #354001

**Ethanol absolute** 500 ml: AppliChem GmbH (Darmstadt, Germany); #A3678.0500

**Ethidium bromide** 1 g: Sigma (Taufkirchen, Germany); #E-7637

**Evan's blue** 10 g: Sigma (Taufkirchen, Germany); #206334

**Fetal calf serum (FCS)** 500 ml: Biochrom (Berlin, Germany); #S-0115

**FITC-dextran (70kD)** 100 mg: Sigma (Taufkirchen, Germany); #FD-70S

**Formamide** 100 ml: Sigma (Taufkirchen, Germany); #F-9037

**Goat-anti-mouse-IgG (hrp-labeled)** 500 µl: Stressgene (Victoria, B.C., Canada); #SAB-100

**Goat-anti-rabbit-IgG (hrp-labeled)** 500 µl: Stressgene (Victoria, B.C., Canada); #SAB-300

**H<sub>2</sub>O (RNase-free)** 1000 ml: Sigma (Taufkirchen, Germany); #W-4502

**H<sub>2</sub>O<sub>2</sub> (30%)** 1000ml: Merck (Darmstadt, Germany); #1.08597

**HBSS<sup>-</sup> (-CaCl<sub>2</sub> / -MgCl<sub>2</sub>)** 500 ml: GIBCO Invitrogen (Paisley, Scotland); #14185-045

**HBSS<sup>+</sup> (+CaCl<sub>2</sub> / +MgCl<sub>2</sub>)** 500 ml: GIBCO Invitrogen (Paisley, Scotland); #14025-050

**Hepes (1 Mol/l)** 100 ml: GIBCO Invitrogen (Paisley, Scotland); #15630-056

**HIV-1 gp120** (100 µg/ml): Protein Sciences Corp. (Meriden, CT, USA); #2003LAV

**Human adenosine deaminase primer** (sense primer 5'-CAC ACG TAT ACC TCG GCA TG-3' and antisense primer 5'-GCC ATG GGC TTC TTT ATT GA-3'), PCR product size 153 bp: Thermo Electron GmbH (Ulm, Germany)

**Human β-actin primer** (sense primer 5'-GGT GGC TTT TAG GAT GGC AAG-3' and antisense primer 5'-ACT GGA ACG GTG AAG GTG ACA G-3'), PCR product size 161 bp: Thermo Electron GmbH (Ulm, Germany)

**Hydrocortisone** 1 g: Sigma (Taufkirchen, Germany); #H-0888

**Isopropylalcohol** 25 ml: Sigma (Taufkirchen, Germany); #I-9516

**Lactated ringers solution** 1000 ml: Fresenius (Bad Homburg, Germany)

**Laemmli sample buffer (2X) (1:20 ME)**: BIO-RAD Laboratories Inc. (Hercules, CA, USA); #1610737

**L-Glutamine 200 mM (100X)** 100 ml: GIBCO Invitrogen (Paisley, Scotland); #25030-024

**Magic mark™ XP Westernstandard**: GIBCO Invitrogen (Paisley, Scotland); #LC5602

**MCDB 131-medium (1X) without L-glutamine** 500 ml: GIBCO Invitrogen (Paisley, Scotland); #10372-019

**Medium 199** 500 ml: Cambrex Bio Science (Verviers, Belgium); #BE12-117F

**Mercapto-ethanol** 100 ml: Sigma (Taufkirchen, Germany); #M-7522

**Message Clean Kit** (140 µl 10X reaction buffer, 20 µl GH-DNase I, 140 µl NaOAc (3M), 1 ml H<sub>2</sub>O (RNase-free)): GenHunter Corporation (Nashville, TN, USA); #M601

**Methanol** 2.5 l: Merck (Darmstadt, Germany); #1060018

**Microbiology slim milk powder** 1 kg: Merck (Darmstadt, Germany); #VM810263

**Mouse monoclonal β-actin antibody** 500 µl: abcam (Cambridge, MA, USA); #ab3280

**NP 40 (1X Electrophoresis Reagent Igepal CA630):** Sigma (Taufkirchen, Germany); #I-7771

**NuPAGE<sup>®</sup> antioxidant** 15 ml: GIBCO Invitrogen (Paisley, Scotland); #NP0005

**NuPAGE<sup>®</sup> MES SDS running buffer (20X)** 500 ml: GIBCO Invitrogen (Paisley, Scotland); #NP0002

**NuPAGE<sup>®</sup> transfer buffer (20X)** 1000 ml: GIBCO Invitrogen (Paisley, Scotland); #NP0006-1

**Oligo(dT)<sub>12-18</sub> Primer** 25 µg: GIBCO Invitrogen (Paisley, Scotland); #18418-012

**Omniscript-Kit (10X RT Buffer, dNTP Mix, Omniscript RT, H<sub>2</sub>O (RNase-free)):** QIAGEN (Hilden, Germany); #205113

**Phenol** 100 ml: GIBCO Invitrogen (Paisley, Scotland); #15513-039

**Potassium chloride (KCl)** 1000 g: Merck (Darmstadt, Germany); #4936

**Potassium dihydrogenphosphate (KH<sub>2</sub>PO<sub>4</sub>)** 1000 g: Merck (Darmstadt, Germany); #104873

**Protein G-sepharose beads:** Amersham Bioscience (Heidelberg, Germany); #17-6002-39

**Rabbit polyclonal ADA-antibody** 200 µg: Santa Cruz Biotechnology, Inc. (Santa Cruz, California, USA); #sc-25747

**Rabbit polyclonal CD26-antibody** 200 µg: Santa Cruz Biotechnology, Inc. (Santa Cruz, California, USA); #sc-9153

**Rainbow mark RPN800:** GIBCO Invitrogen (Paisley, Scotland); #W327134

**RNase Inhibitor** 1000 Units: GIBCO Invitrogen (Paisley, Scotland); #15518-012

**RNase Zap<sup>®</sup>** 250 ml: Ambion (Austin, TX, USA); #9780

**Saccharose** 500 g: Sigma (Taufkirchen, Germany); #S-9378

**SDS** 500 g: Fluka (Buchs, Schweiz); #71725

**Sodium chloride (NaCl)** 1000 g: Merck (Darmstadt, Germany); #106404

**Sodium dihydrogenphosphate (NaH<sub>2</sub>PO<sub>4</sub>)** 1000 g: Merck (Darmstadt, Germany); #106370

**Sodium hydroxide (1 Mol/l)** 1000 ml: Merck (Darmstadt, Germany); #9137

**Sodium pyruvate** 100 ml: Sigma (Taufkirchen, Germany); #S-8636

**Streptavidin (hrp-labeled)** 2 ml: GIBCO Invitrogen (Paisley, Scotland); #43-4323

**SuperSignal West Pico Chemiluminescent Substrate** 500 ml: Pierce Biotechnology (Rockford, IL, USA); #34080

**SYBR<sup>®</sup> Green Supermix** 1.25 ml: BIO-RAD Laboratories Inc. (Hercules, CA, USA); #170-8880

**TAE buffer (50X)** 5 l cube: BIO-RAD Laboratories Inc. (Hercules, CA, USA); #161-0773

**Tris-HCl** 1000 g: Applichem GmbH (Darmstadt, Germany); #A3452.1000

**Triton X-100** 100 ml: Sigma (Taufkirchen, Germany); #X-100

**Trizol** 100 ml: GIBCO Invitrogen (Paisley, Scotland); #15596-026

**Trypsin-EDTA** 100 ml: Cambrex Bio Science (Verviers, Belgium); #CC-5012

**Trypsin-Neutralizing-Solution (TNS)** 100 ml: Cambrex Bio Science (Verviers, Belgium); #CC-5002

**Tween20** 500 ml: Merck (Darmstadt, Germany); #822184

**Xylencyanol FF** 10 g: Applichem GmbH (Darmstadt, Germany); #A1408.0010

**Zinc chloride** 100 g: Sigma (Taufkirchen, Germany); #Z-4875

## 2.4 Methods

### 2.4.1 Endothelial cell culture:

Human microvascular endothelial cells (**HMEC-1**) are a kind gift of Francisco Candal, Centers for Disease Control, Atlanta, GA (120).

Cells are cultured in an incubator (*Cytoperm 2, Heraeus Instruments*) at 37° C, containing 5% CO<sub>2</sub> and medium has to be changed every other day. Medium is discarded, cells are washed with 10 ml D-PBS<sup>+</sup> (containing calcium and magnesium) and pipetted off again. Adding 20 ml fresh medium in the cell culture flasks (*TPP*).

Full confluency and endothelial cell purity can be assessed by light-optical microscope (*DMIL, LEICA*). When the cells are confluent (reached within 1 week), they are split as follows: At first medium is discarded, confluent cells are washed with 10 ml D-PBS<sup>-</sup> (no calcium, no magnesium) and pipetted off again. Then 4 ml accutase are added, gently swiveling the flask and incubating for 5-10 minutes at 37° C (*Cytoperm 2, Heraeus Instruments*). Detaching the cells from the bottom of the cell culture flask, the flask has to be knocked a bit to remove all cells from the bottom of the flask. Then 2 ml fresh medium are added and washing several times the bottom of the flask that all cells are in suspension. 3 new cell culture flasks 75cm<sup>2</sup> (*TPP*) are filled with 18 ml fresh medium and to each flask 2 ml cell suspension are added and swivelled gently once. Culturing again in the incubator (*Cytoperm 2, Heraeus Instruments*).

- D-PBS<sup>+</sup> (+CaCl<sub>2</sub> / +MgCl<sub>2</sub>)
- D-PBS<sup>-</sup> (-CaCl<sub>2</sub> / -MgCl<sub>2</sub>)
- HMEC- medium: 500 ml MCDB 131 without L-glutamine + 25 ml L-glutamine 5 mM + 50 ml FCS (fetal calf serum) 10% + 10 ml hydrocortisone 1 µg/500 ml + 250 µl epidermal growth factor 5 µg/500 ml + 5 ml antibiotic/antimycotic solution 1%
- Accutase

Human umbilical vein endothelial cells (**HUVECs**), received from the Department of Gynaecology of University Hospital, Tuebingen, are isolated from a 10-15 cm long “fresh” piece of umbilical cord (minimum 10 cm). The umbilical cord is transported on ice from the labor floor to the laboratory in a sterile bottle without any solution. The residual blood within the umbilical cord provides the best medium for the cells until isolation.

To isolate the HUVECs from the cord, the umbilical cord is first flushed with HBSS<sup>-</sup> (containing no calcium and no magnesium), working all the time under sterile conditions. The vein is identified by its larger size (compared to the arteries) and lack of a muscular tissue surrounding the lumen, and filled all the way up with collagenase A solution (1 mg/ml). Both ends of the umbilical cord are sealed with clips and the collagenase A filled umbilical cord is incubated in 37° C warm lactated ringers solution for exactly 5 minutes (*Water bath 1083, GFL*). The collagenase A solution (containing the umbilical vein endothelial cells) is then flushed out of the vein into a 50 ml falcon tube using modified Medium 199. The cells are centrifuged at 800 RPM for 8 minutes at room temperature without brake (*Megafuge 1.0 R, Heraeus Sepatech*). The supernatant is discarded and to wash the cells, the pellet is carefully re-suspended into 20 ml of modified Medium 199 and centrifuged again (800 RPM, 8 minutes, room temperature, no brake) (*Megafuge 1.0 R, Heraeus Sepatech*). After discarding the supernatant again, the pellet is re-suspended into 20 ml supplemented endothelial cell growth-medium (EGM-medium) and transferred into a collagen coated cell culture flask 75cm<sup>2</sup> (*Becton Dickinson Labware*). Cells are incubated at 37° C, containing 5% CO<sub>2</sub> (*Cytoperm 2, Heraeus Instruments*).

The medium has to be changed the day following the primary cell preparation, thereafter every other day. To change the medium, at first medium is pipetted off, cells are washed with warm HBSS<sup>+</sup> (37°C) twice and 20 ml supplemented EGM-medium (37°C) are added again.

The time until the first passage of the cells differs considerably, therefore, cells have to be observed carefully prior to the first passage. Full confluency is usually



reached within 1 to 2 weeks. At that time cells should be split.

At first cells are washed with 10 ml HBSS<sup>-</sup>, then 7 ml trypsin-EDTA (0,25 mg/ml) are added, the removing process has to be observed with the light-optical microscope (*DMIL, LEICA*) (maximum 3 minutes), when all cells are removed, immediately 7 ml TNS (Trypsin-Neutralizing-Solution) are added. Cell suspension is transferred in a 50 ml falcon tube and centrifuged at 1100 RPM for 5 minutes at 25° C, with brake (*Megafuge 1.0 R, Heraeus Sepatech*). The supernatant is discarded and the pellet is re-suspended with 6 ml warm supplemented EGM-medium. 3 new collagen coated cell culture flasks (*Becton Dickinson Labware*) are filled with 18 ml supplemented EGM-medium and to each flask 2 ml cell suspension are added and mixed well. Culturing in an incubator at 37°C and 5% CO<sub>2</sub> (*Cytoperm 2, Heraeus Instruments*).

HUVECs can be used up to four passages, then the cells should be discarded and new cells have to be freshly prepared from an umbilical cord.

- HBSS<sup>-</sup> (Hanks<sup>-</sup>) (without calcium and magnesium) containing 1% antibiotic solution
- HBSS<sup>+</sup> (Hanks<sup>+</sup>) (with calcium and magnesium) containing 1% antibiotic solution
- Collagenase A solution in HBSS<sup>-</sup> to 1 mg/ml
- Lactated ringers solution
- Modified Medium 199: 44 ml Medium 199 + 5 ml FCS (fetal calf serum) + 0,5 ml Na-pyruvat + 0,5 ml antibiotic solution
- Supplemented endothelial cell growth-medium (EGM-medium): 500 ml endothelial cell basal medium + 10 ml fetal calf serum + 2 ml endothelial cell growth supplement/Heparin + 0.05 µg/500 µl epidermal growth factor, rec., human + 0.5 µg/500 µl basic fibroblast growth factor, rec., human + 500 µg/500 µl hydrocortisone
- Trypsin-EDTA
- Trypsin-Neutralizing-Solution (TNS)

#### 2.4.2 Endothelial cell culture in hypoxia unit (5% CO<sub>2</sub>, 2% O<sub>2</sub>, 37°C):

For preparation of experimental HMEC-1 or HUVEC monolayers, confluent endothelial cells of two cell culture flasks are seeded onto six 10 cm petri dishes. Endothelial cell purity and full confluency are assessed by light-optical microscope (*DMIL, LEICA*).

Like described above, cells are washed with D-PBS<sup>-</sup> and removed with accutase or for HUVECs with HBSS<sup>-</sup>, Trypsin-EDTA and TNS. 2 ml of cell suspension are added onto each petri dish with 10 ml HMEC- / EGM-medium. Then cells are incubated again at 37°C and 5% CO<sub>2</sub> (*Cytoperm 2, Heraeus Instruments*) until full confluency. When full confluency is reached, 5 of the petri dishes are placed in the hypoxia unit (*Invivo2 Hypoxia Workstation 400 + Hypoxia Gas Mixer, RUSKINN Technology Limited*) for different time points. First petri dish is put in hypoxia unit for 48 hours, second for 24 hours, third for 12 hours, fourth for 6 hours and fifth for 2 hours. Before putting the petri dishes in the hypoxia unit, medium has to be changed and hypoxic HMEC- / EGM-medium is added. The sixth petri dish is left in normoxic conditions.

- D-PBS<sup>-</sup> (-CaCl<sub>2</sub> / -MgCl<sub>2</sub>)
- HMEC-medium: 500 ml MCDB 131 without L-glutamine + 25 ml L-glutamine 5mM + 50 ml FCS (fetal calf serum) 10% + 10 ml hydrocortisone 1 µg/500 ml + 250 µl epidermal growth factor 5 µg/500 ml + 5 ml antibiotic/antimycotic solution 1%
- Accutase
- Hypoxic HMEC-medium
- HBSS<sup>-</sup> (Hanks<sup>-</sup>) (without calcium and magnesium) containing 1% antibiotic solution
- Supplemented endothelial cell growth-medium (EGM-medium): 500 ml endothelial cell basal medium + 10 ml fetal calf serum + 2 ml endothelial cell growth supplement/Heparin + 0.05 µg/500 µl epidermal growth factor, rec., human + 0.5 µg/500 µl basic fibroblast growth factor, rec., human + 500

µg/500 µl hydrocortisone

- Trypsin-EDTA
- Trypsin-Neutralizing-Solution (TNS)
- Hypoxic EGM-medium

### 2.4.3 RNA isolation:

Before starting, the work bench and all equipment have to be cleaned with RNase Zap<sup>®</sup>. All petri dishes with hypoxic endothelial cells (HMEC-1 or HUVEC) are taken out of the hypoxia unit (*Invivo2 Hypoxia Workstation 400 + Hypoxia Gas Mixer, RUSKINN Technology Limited*) at the same time. All six petri dishes (five hypoxic and one normoxic) are put on a cool pad and left there for all the time. Hypoxic medium is discarded, 10 ml HBSS<sup>-</sup> are added to each petri dish carefully, swiveling once and pipetting off again. Then 1000 µl trizol are added to each petri dish, cells are scraped with a cool cell-scraper so that all cells are in solution. Cell suspension of each petri dish is filled in two labeled sterile 1.5 ml eppendorf tubes. To each eppendorf tube 250 µl chloroform are added, mixed carefully for 15 seconds manually and left at room temperature for 3 minutes. All 12 eppendorf tubes are centrifuged at 12900 RPM for 15 minutes at 4° C, with brake (*Biofuge fresco, Heraeus Instruments*). Thereafter three layers are formed, at the bottom of the tubes DNA and proteins are dissolved in chloroform, the middle layer contains the lipid and at the top RNA is found. Only RNA is pipetted off and collected in one tube for each hypoxic time. 500 µl cold isopropylalcohol are added and mixed manually. Thereafter all 6 eppendorf tubes are freezed at -80° C (*Model MDF-592, Sanyo Electric Biomedical Co., Ltd.*) for at least one hour (better for one night).

After that time RNA is thawed on ice again, centrifuged at 12900 RPM for 15 minutes at 4° C, with brake (*Biofuge fresco, Heraeus Instruments*). The supernatant is discarded cautiously; tubes are dried on a tissue upside down. 1000 µl cool 75% ethanol (RNase-free) are added to each tube, mixed well and

centrifuged at 12900 RPM for 5 minutes at 4° C, with brake (*Biofuge fresco, Heraeus Instruments*). The supernatant is removed carefully again and the pellets within the tubes have to be dried completely (lasts about 30-45 minutes). Each pellet is dissolved in 11 µl H<sub>2</sub>O (RNase-free), mixed well and centrifuged again for a few seconds (*SD/220VAC, Roth*). 10 µl of the RNA solution are freezed at –80° C again (*Model MDF-592, Sanyo Electric Biomedical Co., Ltd.*), the remaining 1 µl is used for photometric measurement to assess purity and concentration.

- RNase Zap<sup>®</sup>
- HBSS<sup>-</sup>
- Trizol
- Chloroform
- Isopropylalcohol
- 75% Ethanol (RNase-free): RNA-Ethanol diluted with H<sub>2</sub>O (RNase-free) 3:1
- H<sub>2</sub>O (RNase-free)

#### 2.4.4 Photometric measurement of RNA:

1 µl RNA solution is mixed with 199 µl H<sub>2</sub>O (RNase-free) (1:200). The extinction is measured (*Ultrospec 3000pro + DPU-414 Thermal Printer, amersham pharmacia biotech*) using quartz cuvettes, at 260 nm, 280 nm and 320 nm. If ratio is more than 1.7, purity of the RNA will be good. Also concentration is measured.

- H<sub>2</sub>O (RNase-free)

#### 2.4.5 DNase digestion:

DNase digestion is necessary to remove DNA contaminant from RNA after RNA isolation. RNA is removed from –80° C and thawed on ice. Each 10 µl RNA tube is mixed with 40 µl H<sub>2</sub>O (RNase-free). Then 5.7 µl 10X reaction buffer and 1.0 µl

DNase I are added, mixed well and incubated at 37° C for 30 minutes (*Thermomixer 5436, Eppendorf*). After that time 40 µl phenol / chloroform (3:1) are added, tubes are vortexed for 30 seconds (*Vortex-Genie 2 / G-560E, Scientific Industries, Inc.*) and let sit on ice for 10 minutes. Then all eppendorf tubes are centrifuged at 12900 RPM for 5 minutes at 4° C (*Biofuge fresco, Heraeus Instruments*). 2 phases are formed, only the upper phases are pipetted off and transferred into new eppendorf tubes. In each new tube 5 µl NaOAc (3M) and 200 µl 100% ethanol are added and freezed again at -80° C (*Model MDF-592, Sanyo Electric Biomedical Co., Ltd.*) for at least one hour (better one night).

After thawing all tubes are centrifuged again at 12900 RPM for 10 minutes at 4° C (*Biofuge fresco, Heraeus Instruments*). The supernatant is removed carefully and the RNA pellets are washed with 0.5 ml 70% ethanol. Again centrifugation at 12900 RPM for 5 minutes at 4° C (*Biofuge fresco, Heraeus Instruments*). Ethanol is removed and pellet is dried. RNA is redissolved with 11 µl H<sub>2</sub>O (RNase-free) and mixed well. 1 µl of the RNA suspension is diluted with 199 µl H<sub>2</sub>O (RNase-free) (1:200) and concentration of RNA is measured by photometer (*Ultrospec 3000pro + DPU-414 Thermal Printer, amersham pharmacia biotech*). Each of the 10 µl RNA suspension is diluted to 1 µg/µl with H<sub>2</sub>O (RNase-free) and freezed at -80° C (*Model MDF-592, Sanyo Electric Biomedical Co., Ltd.*) again.

- “Message clean kit” (140 µl 10X reaction buffer, 20 µl GH-DNase I, 140 µl NaOAc (3M), 1 ml H<sub>2</sub>O (RNase-free))
- Phenol / Chloroform 3:1
- 100% Ethanol (RNase-free)
- 70% Ethanol (RNase-free)
- H<sub>2</sub>O (RNase-free)

#### 2.4.6 cDNA synthesis / reverse transcription:

10 µg (= 10 µl) RNA are used as template for cDNA synthesis. RNA is thawed on ice, reagents are thawed at room temperature and stored on ice immediately after thawing. RNA and reagents are vortexed briefly (*Vortex-Genie 2 / G-560E, Scientific Industries, Inc.*) and centrifuged again (*SD/220VAC, Roth*) to collect residual liquid from the sides of the tubes. For one RNA sample (10 µg) 10 µl 10X RT Buffer, 10 µl dNTP Mix, 5 µl Oligo(dt)<sub>12-18</sub> Primer, 5µl RNase Inhibitor, 5 µl Omniscript RT and 55 µl H<sub>2</sub>O (RNase-free) are needed. All reagents are mixed carefully and the mixture is dispensed to each RNA tube on ice. At first all samples are incubated in a thermocycler (*Mastercycler gradient, Eppendorf*) at 37° C for 60 minutes then at 93° C for 5 minutes and afterthere cooled at 4° C very fast.

After transcription concentration of cDNA is measured photometrically as described above (*Ultrospec 3000pro + DPU-414 Thermal Printer, amersham pharmacia biotech*) and each cDNA sample is diluted to 1 µg/µl with H<sub>2</sub>O (RNase-free) and freezed again at -80° C (*Model MDF-592, Sanyo Electric Biomedical Co., Ltd.*).

- “Omniscript-Kit” (10X RT Buffer, dNTP Mix, Omniscript RT, H<sub>2</sub>O (RNase-free))
- Oligo(dT)<sub>12-18</sub> Primer
- RNase Inhibitor
- H<sub>2</sub>O (RNase-free)

#### 2.4.7 Real - time RT-PCR:

First dried primers are dissolved in H<sub>2</sub>O (RNase-free) according to the primer data sheet. For primer-mix 20 µl sense primer, 20 µl antisense primer and 160 µl H<sub>2</sub>O (RNase-free) are mixed.

Human β-actin primer (sense primer 5'-GGT GGC TTT TAG GAT GGC AAG-3' and antisense primer 5'-ACT GGA ACG GTG AAG GTG ACA G-3') is used in identical reactions for control.

The reaction mixture consists of 12.5  $\mu\text{l}$  SYBR<sup>®</sup> Green Supermix, 1  $\mu\text{l}$  primer-mix (see above) and 10.5  $\mu\text{l}$  H<sub>2</sub>O (RNase-free) for each sample. 24  $\mu\text{l}$  reaction mixture are added in each well of the 96-well plate which is used. 1  $\mu\text{l}$  cDNA for each well is used and dispensed according to the pipette pattern. One well is only filled with reaction mixture, without cDNA to control purity of the reagents. The well plate is covered with an optical sealing tape and is centrifuged at 4000 RPM for 3 minutes (*Model TJ-6, BECKMAN*). Afterthere the real-time RT-PCR is run in an iCycler (*BIO-RAD Laboratories Inc.*) with the following protocol: 1 cycle of 95° C for 3 minutes, 40 numbers of cycles of 95° C for 30 seconds, 56° C for 30 seconds and 72° C for 30 seconds, 1 cycle of 95° C for 1 minute, and finally 98 numbers of cycles of 51° C for 10 seconds (after second cycle temperature increased continuously for 0.5° C), hold on 25° C finally.

Real-time RT-PCR are run for human adenosine deaminase (ADA) (sense primer 5'-CAC ACG TAT ACC TCG GCA TG-3' and antisense primer 5'-GCC ATG GGC TTC TTT ATT GA-3') and for CD26 (Dipeptidylpeptidase 4) (sense primer 5'-AAA ATG AGT CCA AGG AAG TT-3' and antisense primer 5'-AGG CAG CTT GAA ACT GAG-3').

- H<sub>2</sub>O (RNase-free)
- SYBR<sup>®</sup> Green Supermix
- Human  $\beta$ -actin primer (sense primer 5'-GGT GGC TTT TAG GAT GGC AAG-3' and antisense primer 5'-ACT GGA ACG GTG AAG GTG ACA G-3')
- Human adenosine deaminase primer (sense primer 5'-CAC ACG TAT ACC TCG GCA TG-3' and antisense primer 5'-GCC ATG GGC TTC TTT ATT GA-3')
- CD26 primer (sense primer 5'-AAA ATG AGT CCA AGG AAG TT-3' and antisense primer 5'-AGG CAG CTT GAA ACT GAG-3')

### 2.4.8 Gel electrophoresis:

The PCR transcripts are visualized on a 1.5% agarose gel to control the primer size.

For production of an agarose gel 3 g agarose is dissolved in 200 ml TAE buffer (1X) (4 ml TAE buffer (50X) and 196 ml distilled water). Afterwards the agarose solution is boiled for 3 minutes in a microwave (*SIEMENS*) and cooled down with a magnetic stirrer (*IKAMAG<sup>®</sup> RCT, IKA*) to 60° C. 5 µl ethidiumbromide (10 mg/ ml) are added (cave: carcinogenic) and the solution is put into a prepared electrophoresis chamber (*Horizon 11.14, GIBCO Invitrogen*). To produce 1 l TAE buffer (1X) 20 ml TAE buffer (50X) are diluted with 980 ml distilled water. When the agarose gel is dried, 1 l TAE buffer (1X) is poured on the gel. 5 µl DNA loading buffer are added to each DNA sample and each DNA sample is transferred into one gel slot. 5 µl DNA ladder are also put in one of the gel slots. Voltage of 90 V is attached. After about 1.5 hours gel is viewed with 302 nm UV light (*Diana, Raytest*).

- TAE buffer (50X)
- Distilled water
- Agarose
- Ethidiumbromide (10 mg/ ml)
- DNA loading buffer: 40% (m/v) saccharose, 0.25% (m/v) xylencyanol and 0.25% (m/v) bromphenolblue-sodium salt diluted in distilled water
- DNA ladder

### 2.4.9 Immunblotting experiments:

HMEC-1 are analyzed by western blot (total protein) or by immunoprecipitation of biotinylated membranes (surface protein).



**a) Immunoprecipitation:**

To show expression or induction of a specific cellular protein on the endothelial surface, surface proteins can be labeled with biotin.

So HMEC-1 are grown to full confluency in 10 cm petri dishes and exposed to hypoxic conditions as described above (2.4.2). To stabilize surface proteins the labeling has to be performed in the cold (4° C). Therefore, petri dishes with confluent cells are taken to a cold room (4° C) and placed on a cold surface (4° C). Cells are washed with 10 ml ice cold HBSS<sup>+</sup>/Hepes (10 mM) and surface proteins are labeled with biotin (1 M) for 30 minutes and petri dishes are placed on a seasaw-rotator (*Heidolph*) (slow settings) for 20 minutes at 4° C. As next step cells are washed with 10 ml HBSS<sup>+</sup>/Hepes (10 mM) twice. Then endothelia are incubated with 10 ml NH<sub>4</sub>Cl (150 mM) at 4° C for 15 minutes and rinsed again with 10 ml HBSS<sup>+</sup>/Hepes (10 mM). 500 µl lysis buffer, containing RIPA buffer and proteinase inhibitor mix, are added and all cells are scraped with a cell-scraper and transferred into an eppendorf tube (avoid bubbles). All eppendorf tubes are rotated end over end for 30 minutes (*Heidolph*) and afterwards cell debris is removed by centrifugation (12900 RPM, 15 minutes, 4° C) (*Biofuge fresco, Heraeus Instruments*). Concentrations are measured according to BRADFORD at 595 nm. 1µg/ µl BSA is used as standard curve. 1 ml protein sample (2 mg/ ml) is mixed with 10 µg antibody (rabbit polyclonal CD26-antibody, rabbit polyclonal ADA-antibody) and all samples are incubated end over end at 4° C for 15 minutes (*Heidolph*). Protein-G-sepharose beads, washed with RIPA buffer three times for pre-equilibration, are added and proteins are washed and centrifuged at 12900 RPM for 5 minutes at 4° C (*Biofuge fresco, Heraeus Instruments*). Afterwards pellets are washed with 0.5 ml RIPA buffer, diluted in 150 µl laemmli sample buffer (2X) (1:20 ME) and boiled for 5 minutes (*Thermomixer 5436, Eppendorf*).

For protein electrophoresis 10-well NuPAGE<sup>®</sup> Novex Bis-Tris gel 4-12% and NuPAGE<sup>®</sup> MES SDS running buffer (1X) are used. 7 µl magic mark<sup>™</sup> XP Westernstandard and 3 µl rainbow mark RPN800 (protein ladder) are used for size

analysis and blotting control. Electrophoresis takes about 1 hour 30 minutes at 110 V (*electrophoresis chamber x-cell sure lock, GIBCO Invitrogen*).

By tank buffer system (*blotting chamber Trans Blot Cell<sup>®</sup>, BIO-RAD Laboratories Inc.*) proteins are transferred to PVDF membranes, which have been pre-incubated in methanol for 3 minutes. Electrophoresis takes about 1 hour 30 minutes at 110 V (*electrophoresis chamber x-cell sure lock, GIBCO Invitrogen*). 50 ml NuPAGE<sup>®</sup> transfer buffer (20X), 1 ml NuPAGE<sup>®</sup> antioxidant, 200 ml methanol and 749 ml distilled water are used as transfer buffer.

For immunoprecipitation analysis membranes are blocked in 5% BSA-blocking buffer (1.5 g BSA solublized in 30 ml washing buffer) for 1 hour at room temperature, incubated overnight in 5% BSA-blocking buffer and hrp-labeled streptavidin (1:100), docking at biotinylated proteins, and visualized by enhanced chemiluminescence (*Diana, Raytest*).

#### **b) Western blot:**

For western blot analysis PVDF membranes are blocked in 5% slim milk-blocking buffer (1.5 g slim milk powder solublized in 30 ml washing buffer) for 1 hour and incubated again in primary antibody (rabbit polyclonal CD26-antibody, rabbit polyclonal ADA-antibody) and 5% slim milk-blocking buffer (1:200) overnight. After that membranes are washed three times with washing buffer (0.05% TBST) for 10 minutes and are incubated in hrp-labeled secondary antibodies (1:5000) for 1 hour at room temperature. Before detection by chemiluminescence (*Diana, Raytest*) membranes are rinsed three times in 0.05% TBST again.

To control protein loading, blots are stripped and reprobed with  $\beta$ -actin. Therefore membranes are incubated in stripping buffer, consisting of 0.49 g Tris-HCl, 2 g SDS and 789  $\mu$ l mercaptoethanol, solublized in 100 ml PBS<sup>+</sup> for 30 minutes at 50° C. Then membranes are washed twice in 0.05% TBST for 15 minutes, blocked in 5% slim milk-blocking buffer for 1 hour and incubated in mouse monoclonal  $\beta$ -actin antibody overnight. Next day membranes are washed three times with 0.05%

TBST, incubated in hrp-labeled secondary antibody (1:5000) and washed again three times in 0.05% TBST and detected by chemiluminescence (*Diana, Raytest*).

- HBSS<sup>+</sup>/Hepes (10 mM): 1 l HBSS<sup>+</sup> plus 10 ml Hepes (1 M) → pH 7.4
- Biotin (1M): 244 mg biotin solublized in 1 ml NaOH (1 M)
- NH<sub>4</sub>Cl (150 mM): 0.8 g NH<sub>4</sub>Cl solublized in 100 ml HBSS<sup>+</sup>/Hepes (10 mM)
- RIPA buffer: 250 mM NaCl + 1 mM Tris-HCl (pH 8.1) + 1 mM EDTA + Triton X-100 1% + NP 40 (1X Electrophoresis Reagent Igepal CA630)
- Proteinase inhibitor mix: complete proteinase inhibitor cocktail tablets
- BRADFORD protein solution
- BSA
- Rabbit polyclonal CD26-antibody
- Rabbit polyclonal ADA-antibody
- Protein G-sepharose beads
- Laemmli sample buffer (2X) (1:20 ME)
- 10-well NuPAGE<sup>®</sup> Novex Bis-Tris gel 4-12%
- NuPAGE<sup>®</sup> MES SDS running buffer (1x): 50 ml NuPAGE<sup>®</sup> MES SDS running buffer (20X) + 950 ml distilled water
- Protein ladder: magic mark<sup>™</sup> XP Westernstandard + rainbow mark RPN800
- PVDF membranes Immun-Blot<sup>™</sup>
- Gel blotting paper
- Methanol
- Transfer buffer: 50 ml NuPAGE<sup>®</sup> transfer buffer (20X) + 1 ml NuPAGE<sup>®</sup> antioxidant + 200 ml methanol + 749 ml distilled water
- 5% BSA-blocking buffer: 1.5 g BSA solublized in 30 ml washing buffer for immunoprecipitation
- Washing buffer for immunoprecipitation: 10 ml Hepes (1M) + 30 g NaCl + 2 ml Tween20 + 988 ml distilled water
- Hrp-labeled streptavidin (1:100)

- 5% skim milk-blocking buffer: 1.5 g microbiology skim milk powder solubilized in 30 ml washing buffer for western blot
- Washing buffer (0.05% TBST) for western blot: 100 ml TBS (107 mM KCl, 495 mM Tris-HCl (pH 7,4), 2.7 M NaCl, 14.1 mM NaH<sub>2</sub>PO<sub>4</sub>) + 0.5 ml Tween20 + 900 ml distilled water
- Hrp-labeled secondary antibodies: goat-anti-rabbit-IgG (hrp-labeled) and goat-anti-mouse-IgG (hrp-labeled)
- Stripping buffer: 0.49 g Tris-HCl + 2 g SDS + 789 µl mercaptoethanol + 100 ml PBS<sup>+</sup>
- Mouse monoclonal β-actin antibody
- For detection: SuperSignal West Pico Chemiluminescent Substrate

#### 2.4.10 Measurement of ADA activity in cell culture experiments:

HMEC-1 are grown to full confluency and exposed to normoxia and different times of hypoxia (0 – 72 hours) as described above (2.4.2). In order to develop a model for kinetics of endothelial ADA activity, first adenosine conversion to inosine is measured in HMEC-1 monolayers with different adenosine concentrations (1-500 µM). Optimal resolution for adenosine metabolism to inosine is found when using 50 µM adenosine concentrations. These conditions are used throughout for further measurements.

To measure ADA activity on the endothelial surface, cells are washed in HBSS<sup>+</sup> and 10 µM dipyridamole (to prevent endothelial adenosine uptake by ENT1 and ENT2) is added. 5 minutes later, the concentration of adenosine in the supernatant is adjusted to 50 µM and petri dishes are incubated at 37° C (*Cytoperm 2, Heraeus Instruments*). 100 µl samples are collected at indicated time points (10, 15, 30, 45, 60 minutes) and inosine concentrations are measured by HPLC with a pump P680 (*Dionex GmbH*), an autosampler L7200 (*Merck-Hitachi*) and an UVD 170S detector (*Dionex GmbH*) on a reverse-phase column (Grom-Sil 120-ODS-ST-5µ; 150x3 mm

Grom; *Maisch GmbH*), using a mobile phase gradient (A: 1000 ml distilled water + 1 g  $\text{KH}_2\text{PO}_4$ , pH 5; B: 800 ml distilled water + 3.2 g  $\text{KH}_2\text{PO}_4$  + 250 ml acetonitrile, pH 5; gradient: A to 100% B in 2 min). Ultraviolet absorption spectra are measured at 260 nm at 37° C. The experiments are also done in addition of 100 nM deoxycoformycin (ADA inhibitor) before adding adenosine to demonstrate specificity for ADA.

In subsets of experiments, ADA secretion into the supernatant is measured. For this purpose, HMEC-1 are exposed to hypoxia over 44 hours. Then the cell medium is replaced with HBSS<sup>+</sup> supplemented with 10 mM HEPES (pH 7.4) and cells are placed back in the hypoxia unit (*Invivo2 Hypoxia Workstation 400 + Hypoxia Gas Mixer, RUSKINN Technology Limited*). 4 hours later, the supernatant (HBSS<sup>+</sup>/Hepes) is collected from the cells, its adenosine concentration is adjusted to 50  $\mu\text{M}$ , incubated at 37° C (*Cytoperm 2, Heraeus Instruments*) and inosine generation in the supernatant is measured at the same time points as above. Inosine concentrations are also measured in addition of deoxycoformycin to hypoxic supernatant.

Further experiments are done, to measure ADA activity in the lysates of endothelia. For this purpose, HMEC-1 are exposed to normoxia or 48 hours of hypoxia, cells are washed with HBSS<sup>+</sup> and then lysed with 1.35 ml ice-cold distilled water. Afterwards 0.15 ml HBSS<sup>+</sup> (10x) / Hepes (10x) + 10 mM zinc chloride are added and ADA activity is measured in cell lysate as above (in addition of deoxycoformycin as well).

One more experiment is done: ADA binding to the ADA complexing protein CD26 is inhibited with HIV-1 gp120. For this purpose, HMEC-1 are exposed to normoxia or hypoxia (48 hours), incubated with 100 nM HIV-1 gp120 in HBSS<sup>+</sup> for 10 minutes at 37°C (*Cytoperm 2, Heraeus Instruments*), then washed with HBSS<sup>+</sup> and 10  $\mu\text{M}$  dipyridamole (prevention of endothelial adenosine uptake) is added. Adenosine is adjusted to 50  $\mu\text{M}$  and ADA activity is measured as above.

- HBSS<sup>+</sup>
- Dipyridamole (10  $\mu\text{M}$ )

- Adenosine (50  $\mu\text{M}$ )
- Distilled water
- Potassium dihydrogenphosphate ( $\text{KH}_2\text{PO}_4$ )
- Acetonitrile
- Deoxycoformycin (100 nM)
- Hepes (10 mM)
- Zinc chloride (10 mM)
- HIV-1 gp120 (100 nM)

#### 2.4.11 Macromolecule paracellular permeability assay:

For investigation of endothelial barrier function, HMEC-1 endothelia are cultured on a permeable support system with a separate apical and basal portion (so called “insert”) and exposed to normoxic and hypoxic conditions. Approximately  $1 \times 10^5$  cells/  $\text{cm}^2$  HMEC-1 are seeded onto polycarbonate permeable inserts (0.4- $\mu\text{m}$  pore, 6.5-mm diam). Therefore, fully confluent HMECs from a 75  $\text{cm}^2$  cell culture flask (TPP) are detached with trypsin and suspended in 20 ml HMEC-medium. 1 ml HMEC-medium is placed on the basal portion of the insert and 80  $\mu\text{l}$  of the cell suspension is carefully placed on the apical portion of the insert. Then a few drops of medium are added to the apical portion. As soon as a confluent monolayer is formed of the cultured endothelia (7-10 days after seeding), inserts are placed in 0.9 ml HBSS<sup>+</sup>-containing wells, and 100  $\mu\text{l}$  HBSS<sup>+</sup> (alone or with indicated concentrations of adenosine) are added to the apical portions. In subsets of experiments, bovine adenosine deaminase, deoxycoformycin and HIV-1 gp120 are used in concentrations as indicated.

At the start of the assay ( $t = 0$ ), FITC-labeled dextran 70 kD (concentration 3.5  $\mu\text{M}$ ) is added to fluids within the apical portion of the insert. Fluids from the opposing well (basal portion) are sampled (50  $\mu\text{l}$ ) over 60 minutes ( $t = 20, 40$  and 60 minutes). Fluorescence intensity of each sample is measured (excitation: 485 nm;

emission: 530 nm) (*Cytofluor 2300, Millipore Corp., Waters Chromatography*) and FITC-dextran concentrations are determined from standard curves generated by serial dilution of FITC-dextran. Paracellular flux is calculated by linear regression of sample fluorescence.

- Trypsin
- HMEC-medium
- HBSS<sup>+</sup>
- Adenosine
- Bovine adenosine deaminase
- Deoxycoformycin
- HIV-1 gp120
- FITC-labeled dextran 70kD (3.5  $\mu$ M)

#### **2.4.12 In vivo hypoxia model:**

Mice (C57BL/6/129 svj) are matched according to sex, age and weight. Then they are exposed to normobaric hypoxia (8% O<sub>2</sub>, 92% N<sub>2</sub>) or room air for 4 hours ( $n = 6$  animals per condition). Following hypoxia/normoxia exposure, the animals are sacrificed and plasma samples are obtained via cardiac puncture. Plasma ADA activity is measured as described above (2.4.10).

In subsets of experiments, pulmonary edema is assessed in normoxia and hypoxia. For this purpose, animals are injected with deoxycoformycin (1 mg/ kg intraperitoneally and 1 mg/ kg subcutaneously) or PBS<sup>+</sup> for control. Then mice are exposed to either normoxia or normobaric hypoxia (8% O<sub>2</sub>, 92% N<sub>2</sub>) for 4 hours. After that animals ( $n = 6$  animals per condition) are sacrificed and lungs are collected, weighed (*Mettler-Toledo GmbH*) and dried by speed vac (*Vacufuge, Eppendorf*). Weight differences before and after drying are used to calculate lung water content.

Additional experiments are done to quantify total organ vascular permeability by intravascular administration of Evan's blue as described by Barone et al. (121). As first, animals are injected with deoxycoformycin (1 mg/ kg i.p. and 1 mg/ kg s.c.) or PBS<sup>+</sup>. For the purpose of quantifying vascular permeability, 0.2 ml of Evan's blue (0.2 ml of 0.5% in PBS<sup>+</sup>) is administered intravenously. Animals are then exposed to normobaric hypoxia (8% O<sub>2</sub>, 92% N<sub>2</sub>) or room air for 4 hours ( $n = 6$  animals per condition). After hypoxia/normoxia exposure, the animals are sacrificed and the lungs, liver and colon are harvested. Organ Evan's blue concentrations are quantified following formamide extraction (55° C for 2 hours) by measuring absorbances at 610 nm with subtraction of reference absorbance at 450 nm (*Cytofluor 2300, Millipore Corp., Waters Chromatography*).

For the purpose of quantifying PMN tissue concentrations, the animals are exposed to normobaric hypoxia (8% O<sub>2</sub>, 92% N<sub>2</sub>) or room air for 4 hours ( $n = 6$  animals per condition) after administration of deoxycoformycin or PBS<sup>+</sup> for control. Following hypoxia/normoxia exposure the animals are sacrificed, organs are harvested and the PMN marker myeloperoxidase (MPO) is quantified. Therefore MPO has to be released by solubilization of the organs in 1 ml HBSS<sup>+</sup> containing 0.5% Triton X-100. The pH is then adjusted to 4.2 with 100 µl of 1 M citrate buffer (pH 4.2). Each sample is mixed with equal parts of a solution containing 1 mM 2,2-azino-di-(3-ethyl) di-thiazoline sulfonic acid and 10 mM H<sub>2</sub>O<sub>2</sub> in 100 mM citrate buffer (pH 4.2, 20° C). After that the colour development is measured at 405 nm on a microtiter plate reader (*BIO-RAD Laboratories Inc.*).

These experiments were done in the laboratories of Sean P. Colgan (Center for Experimental Therapeutics and Reperfusion Injury, Brigham and Women's Hospital, Harvard Medical School, Boston, MA 02115, USA) and are in accordance with NIH guidelines for use of live animals and are approved by the Institutional Animal Care and Use Committee at Brigham and Women's Hospital.

- C57BL/6/129 svj mice
- Adenosine



- Evan's blue
- Formamide
- Deoxycoformycin
- PBS<sup>+</sup>
- HBSS<sup>+</sup>
- Triton X-100 (0.5%)
- Citrate buffer (1 M), pH 4.2
- 2,2-Azino-di-(3-ethyl) di-thiazoline sulfonic acid (1 mM)
- H<sub>2</sub>O<sub>2</sub> (10 mM)
- Citrate buffer (100 mM), pH 4.2

**Data analysis:** Data were compared by two-factor ANOVA, or by Student's *t* test where appropriate. Values are expressed as the mean  $\pm$  st. dev. from at least three separate experiments.

## 3 Results

### 3.1 Endothelial ADA mRNA and protein are induced by hypoxia

Potential adenosine catabolic mechanisms induced by hypoxia were hypothesized. In addition recent studies from the study group of PD Dr. med. H. K. Eltzschig revealed significant changes in a number of nucleotide and nucleoside deaminase transcripts (Figure 1a). The transcriptional profile of HMEC-1 was assessed from total RNA derived from hypoxic HMEC-1 (24 hours) using quantitative GeneChip expression arrays (*Affymetrix Inc., Santa Clara, California, USA*). For example, these studies revealed transcriptional repression of AMP deaminase (AMPD<sub>1</sub>, 55 ± 9.1% decrease) and cytidine deaminase (CDA, 64 ± 11.2% decrease). By contrast, myoadenylate deaminase (AMPD<sub>2</sub>) and deoxycytidine deaminase (DCTD) were induced (9 ± 1.1 fold and 4 ± 0.3 fold, respectively). Most dramatically, these analyses identified a 47 ± 8.8 fold increase in ADA mRNA by hypoxia. Based on these results, further experiments were now necessary to verify ADA induction by hypoxia.

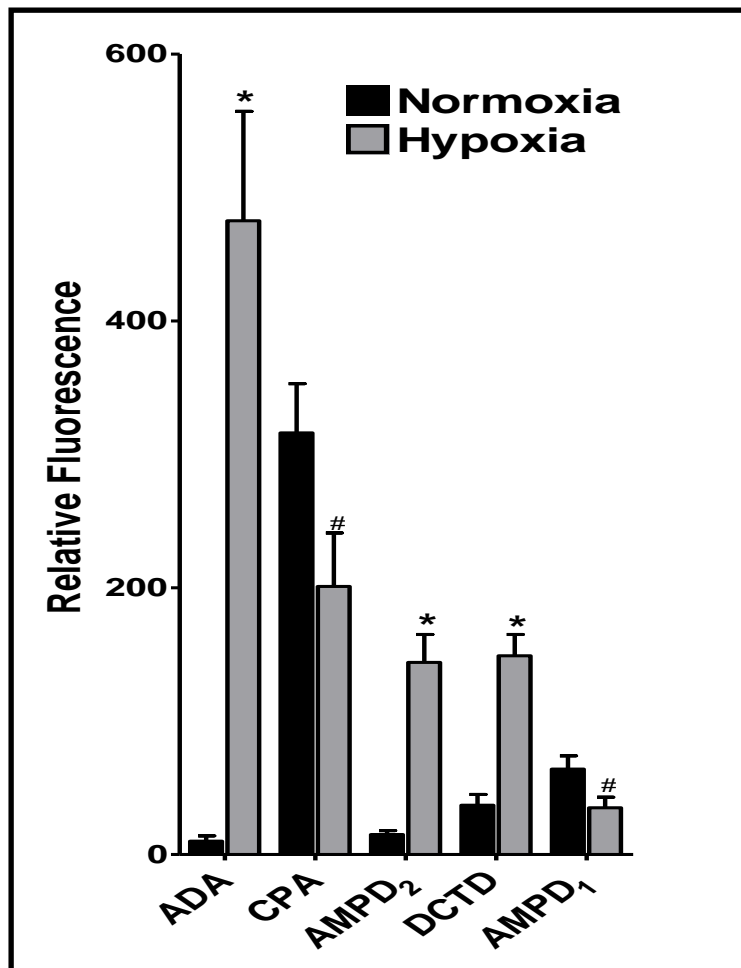


**Figure 1a:** Microarray analysis of individual nucleotide deaminases in response to hypoxia (ADA [adenosine deaminase], CPA [cytidine deaminase], AMPD<sub>2</sub> [AMP deaminase], DCTD [deoxycytidine deaminase] and AMPD<sub>1</sub> [myoadenylate deaminase]). Confluent HMEC-1 were exposed to normoxia or hypoxia (24-hours exposure) and the relative expression of individual nucleotide deaminases was quantified from total RNA by microarray analysis (\* indicates increased fluorescence,  $p < 0.01$ , and # indicates decreased fluorescence,  $p < 0.01$ ).

So confluent HMEC-1 and HUVEC monolayers were exposed to normoxia or hypoxia for different times (2, 6, 12 and 24 hours), total RNA was isolated and ADA

mRNA levels were measured by real-time RT-PCR. These results confirmed the microarray findings that ADA mRNA is prominently induced by hypoxia (Figure 1b).

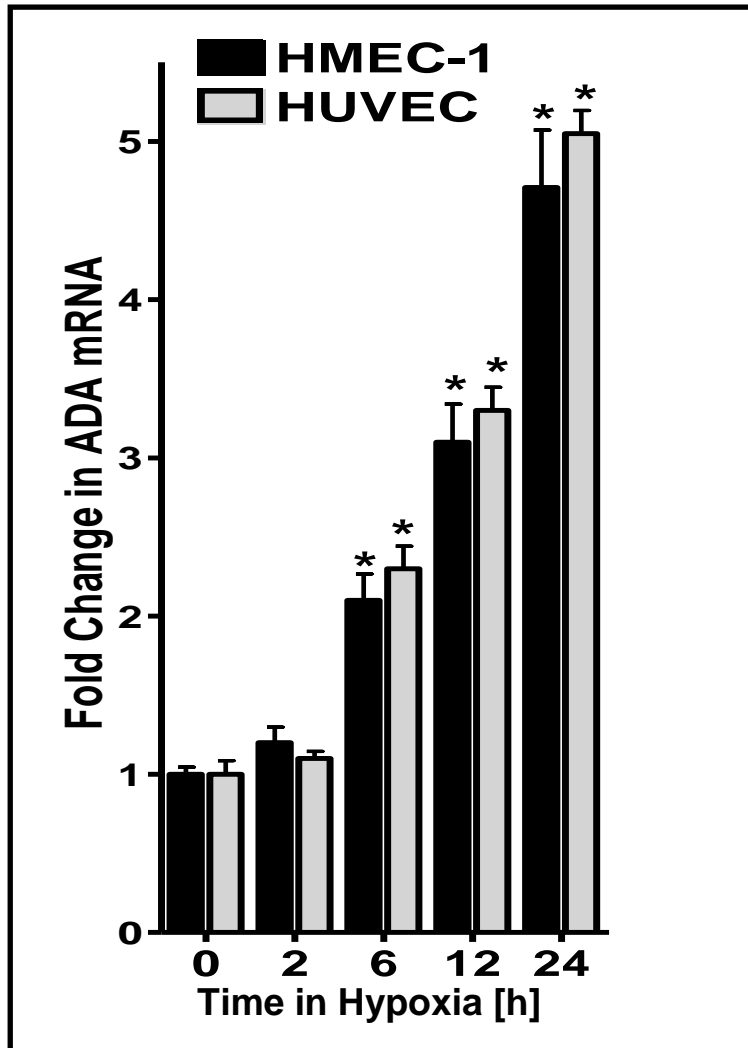


**Figure 1b:** Total RNA from confluent HMEC-1 and HUVEC monolayers exposed to normoxia or hypoxia for indicated time periods, was isolated, and ADA mRNA levels were determined by real-time RT-PCR. Data were calculated relative to internal housekeeping gene ( $\beta$ -actin) and are expressed as fold increase over normoxia  $\pm$  SD at each indicated time. Results are derived from three experiments in each condition (\*  $p < 0.01$ ).

Based on these findings, next step was to examine ADA protein levels in hypoxia. Western blot analysis of total ADA protein revealed a time-dependent induction of ADA (range 12–48 hours), maximal protein levels were observed at 48 hours (Figure 1c). There was no additional increase at 72 hours (data not shown).

Based on previous reports that ADA can be localized to the cell surface via interaction with CD26 (123), the possibility that such increases in ADA protein levels may be localized to the cell surface, had to be examined. As shown in Figure 1d, immunoprecipitation of ADA from surface-biotinylated protein revealed a time-dependent induction of surface ADA (range 12–48 hours), with maximal protein levels observed at 48 hours (Figure 1d). Taken together, these results demonstrate that ADA is rapidly induced by hypoxia, and such increases of ADA protein are demonstrable at the cell surface.

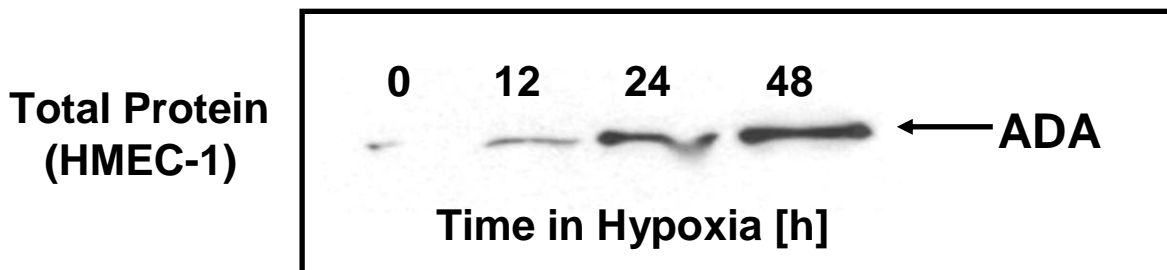


**Figure 1c:** Confluent HMEC-1 monolayers were exposed to indicated time periods of hypoxia (0 – 72 hours), washed and lysed. Lysates were resolved by NuPAGE<sup>®</sup> Novex Bis-Tris gel and resultant western blots were probed with a rabbit polyclonal antibody against human ADA. A representative experiment of three is shown.

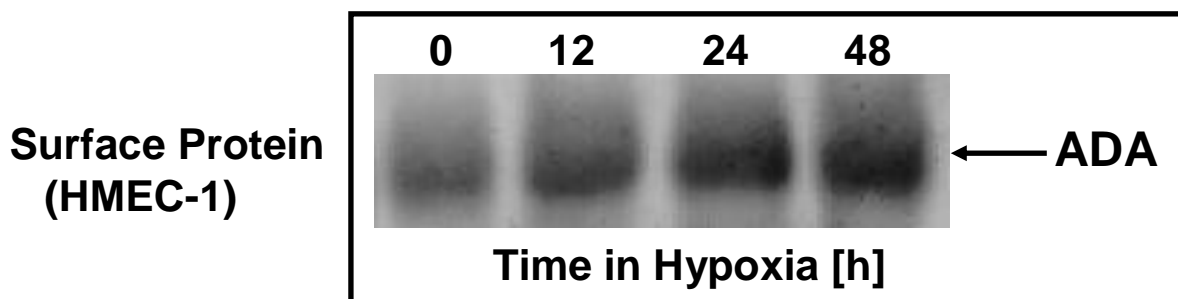


**Figure 1d:** Confluent HMEC-1 monolayers were exposed to indicated time periods of hypoxia (0 – 48 hours), monolayers were washed, surface proteins were biotinylated and cells were lysed. ADA was immunoprecipitated with a rabbit polyclonal ADA-antibody. Immunoprecipitates were resolved by NuPAGE<sup>®</sup> Novex Bis-Tris gel and resultant western blots were probed with streptavidin. Three experiments were done.

### 3.2 Functional results for hypoxia induced ADA

Next step was to determine whether hypoxia-inducible ADA was enzymatically active. To measure ADA function on the endothelial surface, HMEC-1 were exposed over different time periods to hypoxia (exposure time of 12 to 72 hours). Following hypoxia exposure, the time-dependent generation of inosine from exogenous adenosine (50  $\mu$ M final concentration) was measured by HPLC and was used to determine ADA activity.

Ultraviolet absorption spectra were measured at 260 nm at 37° C, with a retention time for inosine of 3.2 minutes and for adenosine of 3.7 minutes (see HPLC tracing, Figure 2a).

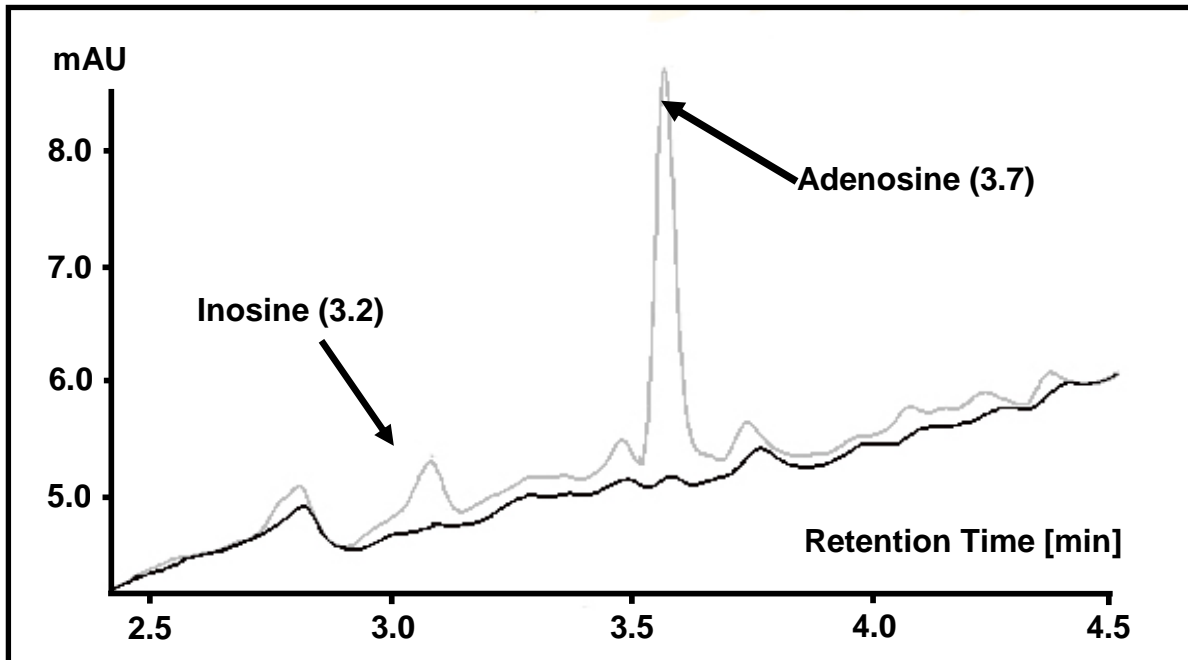


**Figure 2a:** To measure ADA enzyme activity on the endothelial surface, HMEC-1 were exposed to indicated time periods to hypoxia and 50  $\mu\text{M}$  adenosine was added to the supernatant (HBSS) of intact HMEC-1, and inosine generation was measured via HPLC. The HPLC tracing obtained from the supernatant is displayed and retention times for inosine (3.2 minutes) and for adenosine (3.7 minutes) are indicated (black line: HBSS alone; grey line: HBSS after addition of 50  $\mu\text{M}$  adenosine).

As shown in Figure 2b, measurements of total ADA activity from hypotonic lysates of hypoxic endothelia (exposure time of 48 hours) revealed a hypoxia-dependent increase of total ADA activity, with maximal increases of  $7.1 \pm 0.52$ -fold over normoxia controls ( $p < 0.01$ ). Same experiments were done in addition of the ADA-inhibitor deoxycoformycin. ADA activity was inhibited >95% by deoxycoformycin (Figure 2b).

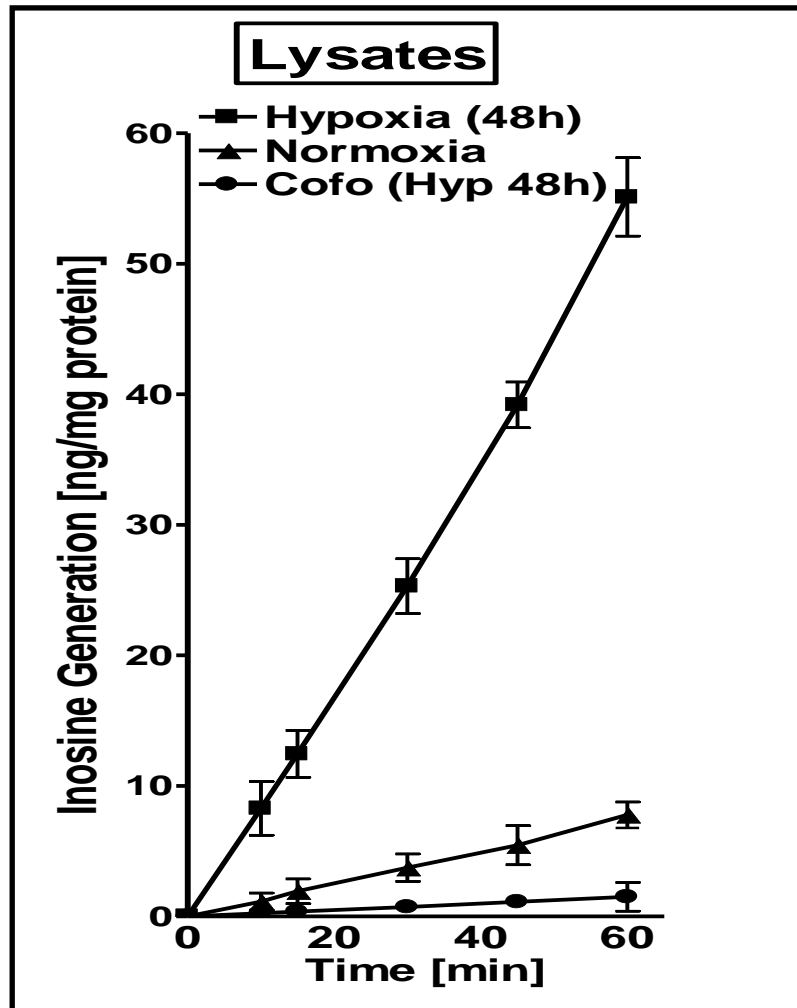


**Figure 2b:** HMEC-1 endothelia were exposed to normoxia and hypoxia (48 hours), washed and lysed. Then adenosine (50  $\mu$ M) was added and inosine generation was measured via HPLC to indicated time points (10, 15, 30, 45 and 60 minutes). Controls were performed in hypoxic endothelia with 100 nM deoxycoformycin (Cofo). So it was shown that ADA activity is induced in lysates of endothelia by hypoxia.

Recent experiments have shown that ADA is also localized at the cell surface (Figure 1d). Based on these findings next step was now to determine whether hypoxia-dependent increases of cell surface ADA were evident on intact



endothelial cells. To do this, the time-dependent generation of inosine from exogenous adenosine (50  $\mu\text{M}$  final concentration) was examined in the presence of 10  $\mu\text{M}$  dipyridamole, which inhibits adenosine uptake by ENT1 and ENT2. As shown in Figure 2c, cell surface ADA activity was increased in a hypoxia time-dependent fashion with maximal induction after 48 hours of hypoxia exposure ( $5.0 \pm 0.61$  fold over normoxia;  $p < 0.01$  by ANOVA). No additional increases with 72 hours hypoxia exposure were observed (data not shown). Same experiments were also done in addition of deoxycoformycin. Such surface ADA activity was inhibited by >95% by deoxycoformycin (Figure 2c).

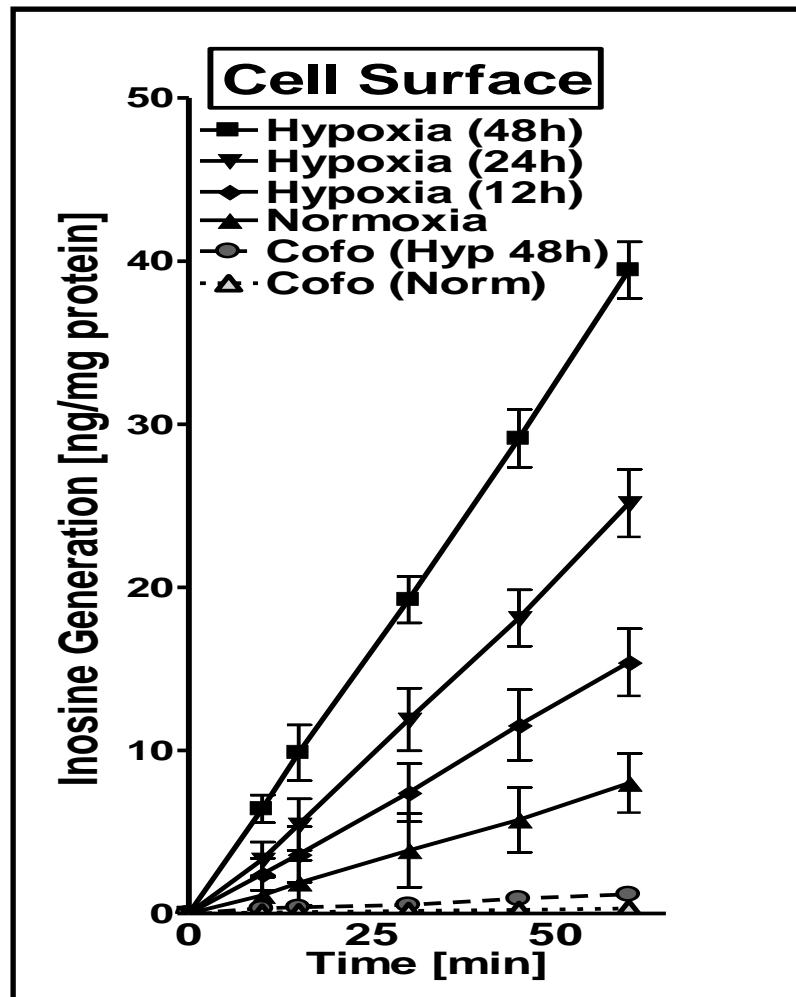


**Figure 2c:** HMEC-1 were exposed to normoxia and indicated times of hypoxia (12, 24, 48 and 72 hours) and washed in HBSS<sup>+</sup>. Then 10  $\mu$ M dipyridamole (to prevent endothelial adenosine uptake by ENT1 and ENT2) was added. 5 minutes later, 50  $\mu$ M adenosine was added in the supernatant and inosine generation was measured via HPLC to indicated time points (10, 15, 30, 45 and 60 minutes). To confirm that the observed increase in inosine generation with hypoxia exposure reflects ADA activity, controls with 100 nM deoxycoformycin (Cofc) were performed in normoxic and 48 hours hypoxic endothelia.

Previous reports have indicated that ADA may be released into the extracellular milieu (124, 125). To examine whether soluble supernatants contain measurable ADA activity, and whether hypoxia might increase soluble ADA activity, HMEC-1 were exposed to hypoxia for 44 hours, after which medium was replaced with hypoxic pre-equilibrated HBSS<sup>+</sup>. After additional 4 hours of hypoxia, cell-free supernatants were harvested and ADA activity was determined by examining the generation of inosine from exogenous adenosine. As shown in Figure 2d, soluble ADA activity increased  $2.3 \pm 0.11$ -fold relative to normoxia controls ( $p < 0.025$ ). Same like at the cell surface (see Figure 2c), soluble ADA activity was inhibited by >95% with the addition of deoxycoformycin (Figure 2d).

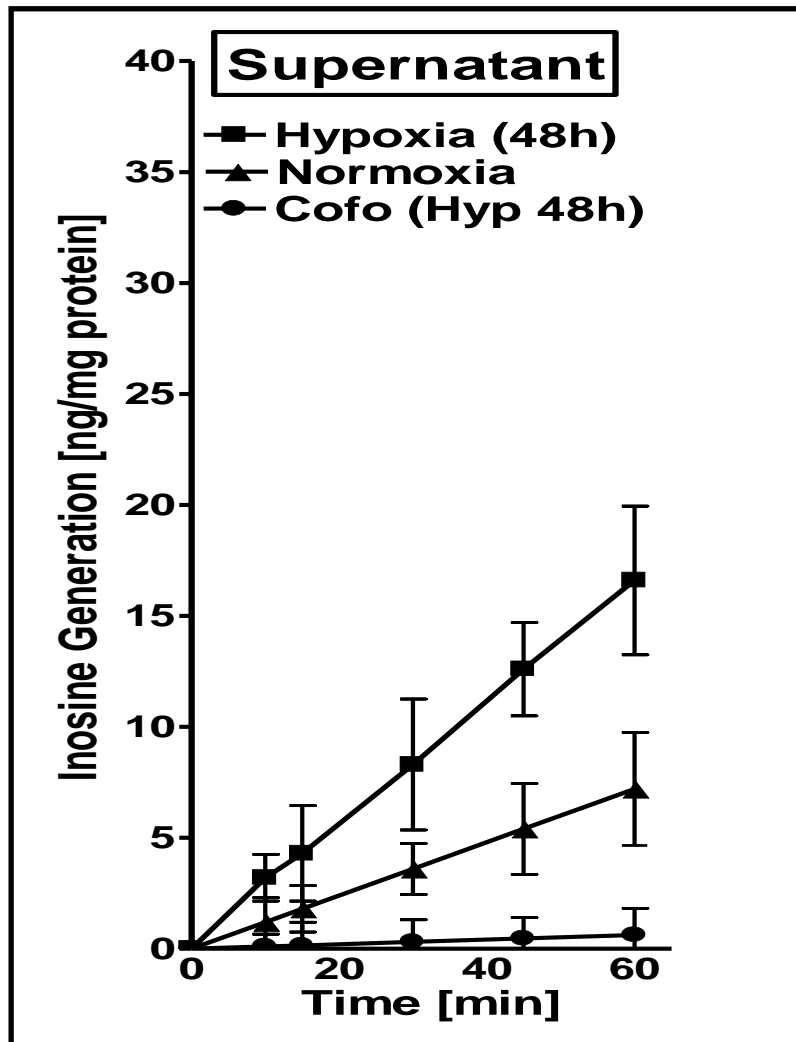


**Figure 2d:** For this purpose, HMEC-1 were exposed again to hypoxia for 48 hours. During the last 4 hours cell medium was replaced with HBSS<sup>+</sup> supplemented with 10 mM HEPES (pH 7.4). After that time the supernatant (HBSS<sup>+</sup>/Hepes) was collected from the cells, 50  $\mu$ M adenosine was added and inosine generation in the supernatant was measured via HPLC to indicated time points (10, 15, 30, 45 and 60 minutes). ADA activity was also measured in the supernatant of normoxic endothelia. Experiments were also done in addition of the ADA inhibitor deoxycoformycin (Cofo) to confirm the previous measurements of ADA activity.

Taken together, this analysis of functional ADA activity confirms the last findings of increased ADA mRNA and protein expression.

### **3.3 Transcriptional induction of the ADA complexing protein CD26 is coordinated by hypoxia**

There is no evidence that ADA can be expressed as an integral membrane protein. Therefore, given the findings of increased surface and soluble ADA activity (Figures 2c and 2d), the question was whether ADA might be complexed at the cell surface. Significant evidence suggested that surface ADA activity can be associated with the dipeptidyl peptidase CD26 (126) in various cell types, including epithelia (127) and endothelia (128-130). Here, the possibility was considered that expression of CD26 may parallel the ADA induction profile observed in hypoxia. To do this, CD26 expression was determined in HMEC-1 and HUVEC by real-time RT-PCR after exposing to hypoxia. This analysis revealed an early and prominent induction, with maximal expression of  $8.2 \pm 1.1$  and  $5.8 \pm 1.2$  fold induction in HMEC-1 and HUVEC, respectively, after 2 hours exposure to hypoxia (Figure 3a).

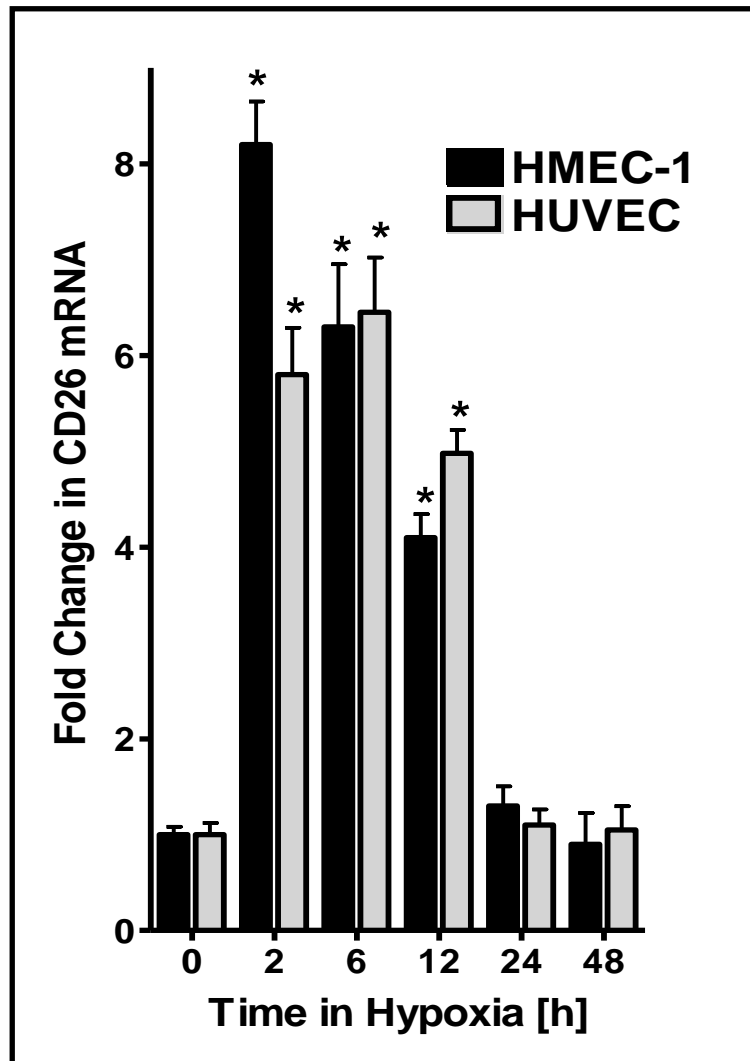


**Figure 3a:** Confluent HMEC-1 and HUVEC monolayers were exposed to normoxia or hypoxia for indicated time periods (2, 6, 12, 24 or 48 hours), total RNA was isolated and CD26 mRNA levels were determined by real time RT-PCR.  $\beta$ -actin transcripts were determined in parallel and used as a control. Data were calculated relative to internal housekeeping gene ( $\beta$ -actin) and are expressed as fold increase over normoxia  $\pm$  SD at each indicated time. Results are derived from three experiments in each condition (\*  $p < 0.01$ ).

Based on these results CD26 function was examined by immunoblotting experiments. Total protein analysis via western blot and immunoprecipitation of biotinylated surface protein confirmed CD26 induction by hypoxia and demonstrated its localization to the cell membrane (Figure 3b and c).

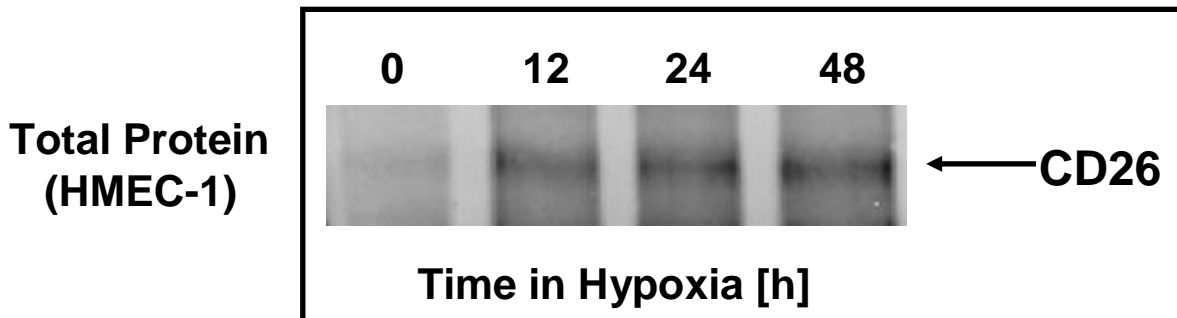


**Figure 3b:** Confluent HMEC-1 monolayers were exposed to indicated time periods of hypoxia (0 – 48 hours), washed and lysed. Lysates were resolved by NuPAGE<sup>®</sup> Novex Bis-Tris gel and resultant western blots were probed with a rabbit polyclonal antibody against human CD26. A representative experiment of three is shown.

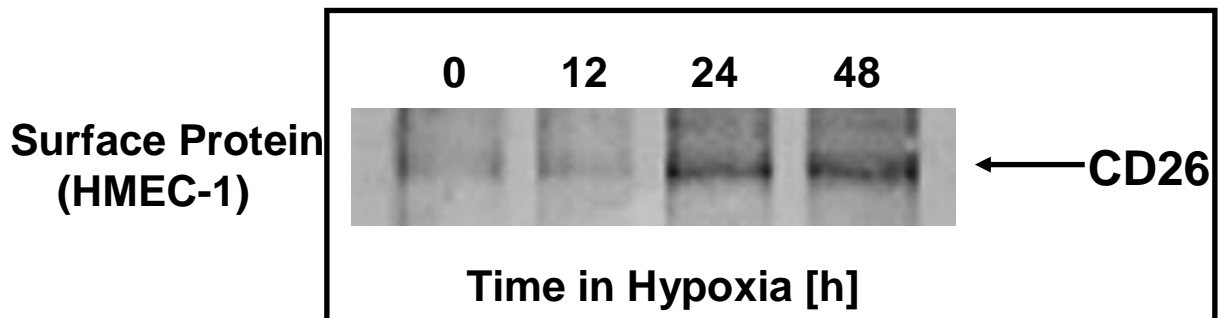


**Figure 3c:** Confluent HMEC-1 monolayers were exposed to indicated time periods of hypoxia (0 – 48 hours), monolayers were washed, surface proteins were biotinylated and cells were lysed. CD26 was immunoprecipitated with a rabbit polyclonal CD26-antibody. Immunoprecipitates were resolved by NuPAGE<sup>®</sup> Novex Bis-Tris gel and resultant western blots were probed with streptavidin. Three experiments were done.

Next experiments were done to confirm that the observed increase in functional cell surface ADA is bound to hypoxia-induced CD26. Therefore the interaction of ADA with CD26 was inhibited by the HIV-1 envelope glycoprotein gp120, a specific inhibitor (131-133). Cell surface ADA activity (see Figure 2c) was now examined in the presence of 100 nM HIV-1 gp120, a concentration previously shown to inhibit ADA interaction with CD26 effectively (132). As shown in Figure 3d, the observed induction of ADA by hypoxia was nearly completely abolished by HIV-1 gp120 ( $p < 0.01$ ). Moreover, after addition of HIV-1 gp120 surface ADA activity of control normoxic endothelia was also significantly reduced ( $p < 0.025$ ) (Figure 3d). Controls were done with equivalent amounts of non-specific protein (BSA), but no influence on surface ADA activity was shown (data not included). Taken together these data indicate that ADA induction by hypoxia is functional and localized to the cell surface via its counterligand CD26. These studies also suggest a coordinated induction of ADA and the ADA-complexing protein CD26 by hypoxia.

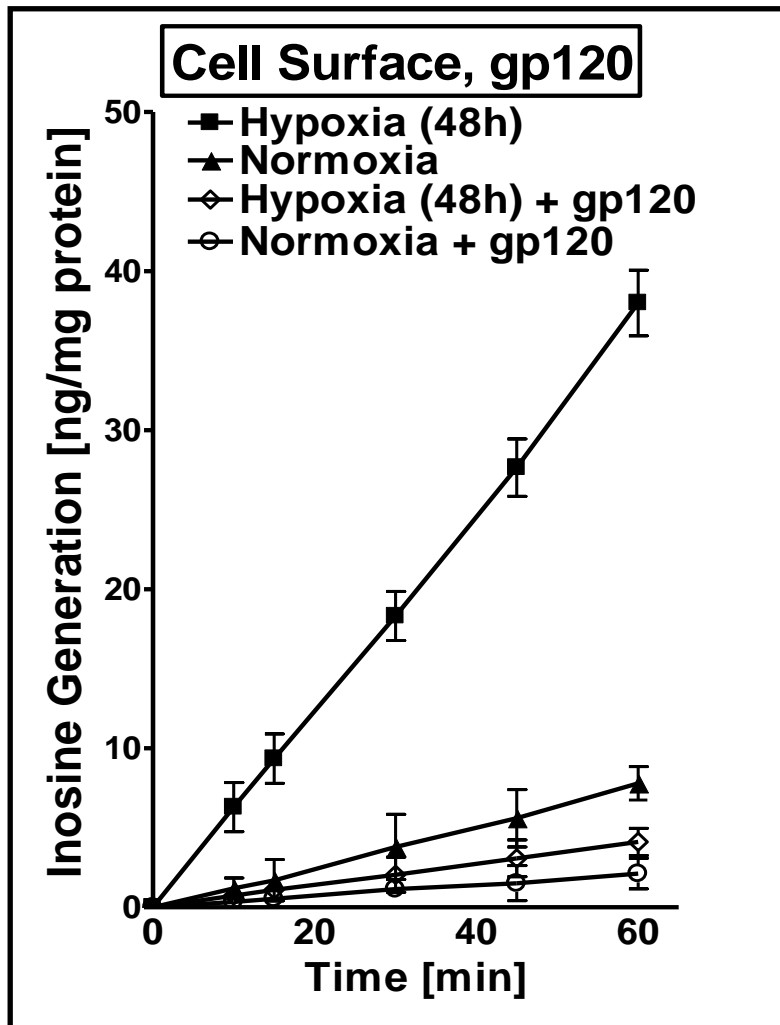


**Figure 3d:** HMEC-1 were exposed to normoxia and 48 hours of hypoxia and one part of endothelia were incubated in 100 nM HIV-1 gp120 diluted in HBSS<sup>+</sup> at 37° C for 10 minutes. Then 10  $\mu$ M dipyridamole (to prevent endothelial adenosine uptake by ENT1 and ENT2) is added. 5 minutes later, 50  $\mu$ M adenosine is added in the supernatant and inosine generation is measured via HPLC to indicated time points (10, 15, 30, 45 and 60 minutes).



### 3.4 Influence of ADA activity on endothelial adenosine signaling

After having shown that endothelial ADA induction is functional and localized to the endothelial surface (see 3.2), next experiments were done to examine if ADA activity could influence endothelial signaling mediated by extracellular adenosine. Previous studies have shown (97) that vascular permeability is controlled by adenosine. To investigate this possibility, responses of normoxic and posthypoxic endothelia after adding various concentrations of adenosine (0 – 100  $\mu\text{M}$ ) were compared by macromolecule paracellular permeability assay (see 2.4.11). Barrier function was determined by transendothelial flux of 70 kD FITC-dextran. The examinations showed that adenosine enhanced barrier function (i.e. inhibited flux of 70 kD FITC-dextran) to a greater extent in post-hypoxic HMEC-1 (48 hours) than in normoxic HMEC-1.  $\sim 30 \mu\text{M}$  and  $\sim 1 \mu\text{M}$  adenosine in post-hypoxia decreased transendothelial flux respectively (Figure 4a).

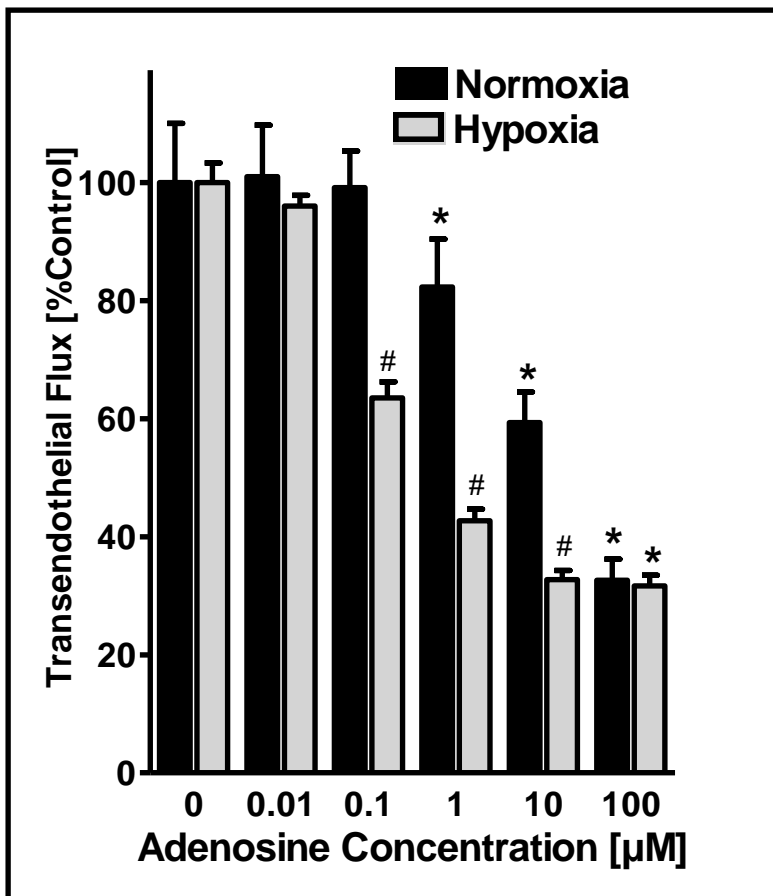


**Figure 4a:** Indicated concentrations (0 – 100  $\mu\text{M}$ ) of adenosine diluted in 100  $\mu\text{l}$  HBSS<sup>+</sup> were added to the surface of confluent normoxic or post-hypoxic (exposure time 48 hours) HMEC-1 which were grown to full confluency on an apical portion of a permeable support system. Endothelial permeability was quantified by 70 kD FITC-labeled dextran (3.5  $\mu\text{M}$ ) which was added to fluids within the apical portion of the insert at the start of the assay. Fluids from the opposing well were sampled 3 times over 60 minutes, fluorescence intensity was measured and FITC-dextran concentrations were determined. Transendothelial flux was calculated by linear regression. Data were derived from 6 monolayers in each condition.

Data are expressed as mean  $\pm$  SD of percent control flux with HBSS<sup>+</sup> only. Asterisk (\*) indicates significant differences from baseline ( $p < 0.05$ ) and cross (#) indicates differences from baseline and from normoxia ( $p < 0.05$ ).

Next step was to investigate the effect of extracellular ADA on paracellular permeability. Therefore ADA concentrations were measured in the supernatant of posthypoxic endothelia by comparing deoxycoformycin inhibited inosine generation with known solutions of bovine ADA. In fact, ADA concentrations in supernatants of posthypoxic HMEC-1 (exposure time 12 hours) were approximately 1, 25, 50 and 60 piccoM with 2, 4, 8 and 12 hours of exposure time (data not shown). Based on these findings, the influence of extracellular ADA (using concentrations 1, 10 and 100 piccoM) on paracellular adenosine responses in normoxic endothelia were examined. As shown in Figure 4b, adenosine-induced enhancement of the endothelial barrier function was significantly decreased in the presence of 0.1 nM ADA (estimated  $\text{EC}_{50} \sim 700 \mu\text{M}$ ). Similarly, when using lower concentrations of ADA, the  $\text{EC}_{50}$  of adenosine was increased from  $\sim 30 \mu\text{M}$  to  $\sim 50$  and  $\sim 100 \mu\text{M}$  with 1 and 10 piccoM ADA concentrations (data not shown).

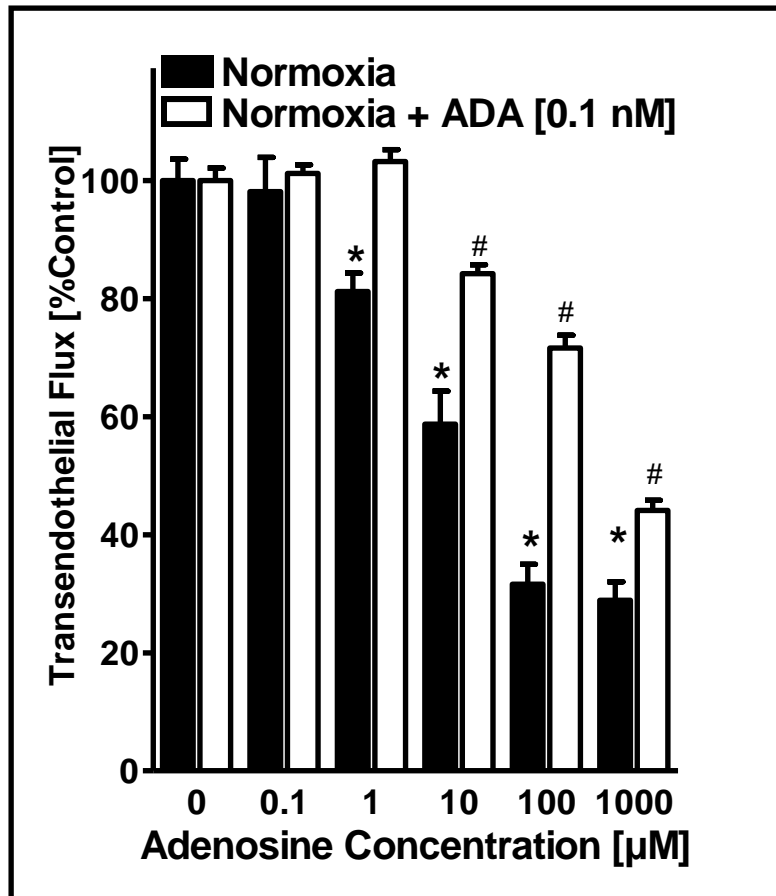


**Figure 4b:** Indicated concentrations (0 – 1000 µM) of adenosine diluted in 100 µl HBSS<sup>+</sup> were added to the surface of confluent normoxic endothelia grown in a permeable support system. Measurements of adenosine elicited barrier responses were done with and without addition of 0.1 nM bovine ADA. With these conditions endothelial permeability was quantified by 70 kD FITC-labeled dextran (3.5 µM) which was added to fluids within the apical portion of the insert at the start of the assay. Fluids from the opposing well were sampled 3 times over 60 minutes, fluorescence intensity was measured and FITC-dextran concentrations were determined. Transendothelial flux was calculated by linear regression. Data were derived from 6 monolayers in each condition.

Asterisk (\*) indicates significant differences from baseline ( $p < 0.05$ ) and cross (#) indicates differences from baseline and from untreated controls ( $p < 0.05$ ).

Further experiments were done to measure adenosine-elicited barrier responses in posthypoxic endothelia (48 hours hypoxia exposure) in the presence of the highly specific ADA inhibitor deoxycoformycin. As shown in Figure 4c, adenosine-elicited barrier responses were significantly increased in the presence of 100 nM deoxycoformycin. Adenosine endothelial concentration  $EC_{50}$ 's of  $\sim 1 \mu\text{M}$  for post-hypoxia without and post-hypoxia with deoxycoformycin was respectively different (Figure 4c).

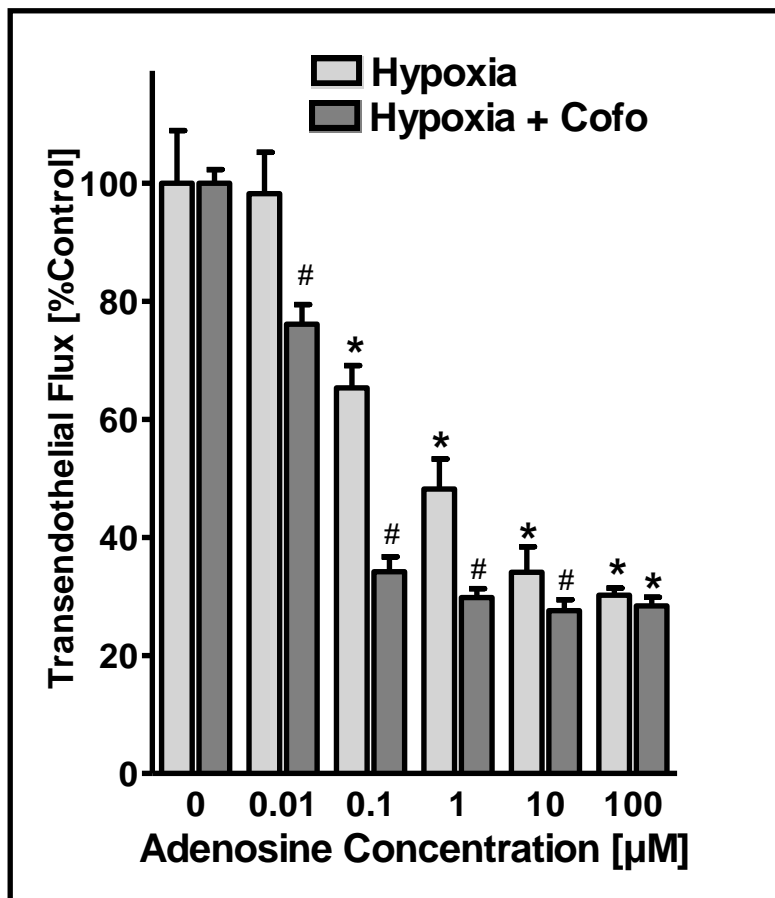


**Figure 4c:** Adenosine barrier function was measured in the presence of the highly specific ADA inhibitor deoxycoformycin (Cofo) (100 nM) and in hypoxic controls without addition of deoxycoformycin. Concentrations of adenosine (0 – 100  $\mu\text{M}$ ) were diluted in 100  $\mu\text{l}$  HBSS<sup>+</sup> and were added after deoxycoformycin to the surface of the confluent hypoxic HMEC-1 (48 hours) grown in a permeable

*support system. Endothelial permeability was quantified by 70 kD FITC-labeled dextran (3.5  $\mu$ M) which was added to fluids within the apical portion of the insert at the start of the assay. Fluids from the opposing well were sampled 3 times over 60 minutes, fluorescence intensity was measured and FITC-dextran concentrations were determined. Transendothelial flux was calculated by linear regression. Data were derived from 6 monolayers in each condition.*

*Asterisk (\*) indicates significant differences from baseline ( $p < 0.05$ ) and cross (#) indicates differences from baseline and from untreated controls ( $p < 0.05$ ).*

Similar results were found when adding 100 nM HIV-1 gp120 (inhibitor of ADA and CD26 interaction) to the permeable support system with hypoxic endothelia (Figure 4d). This confirmed the recent studies that ADA is just in combination of CD26 functional. Therefore the binding of ADA and CD26 are involved in regulating vascular adenosine responses.

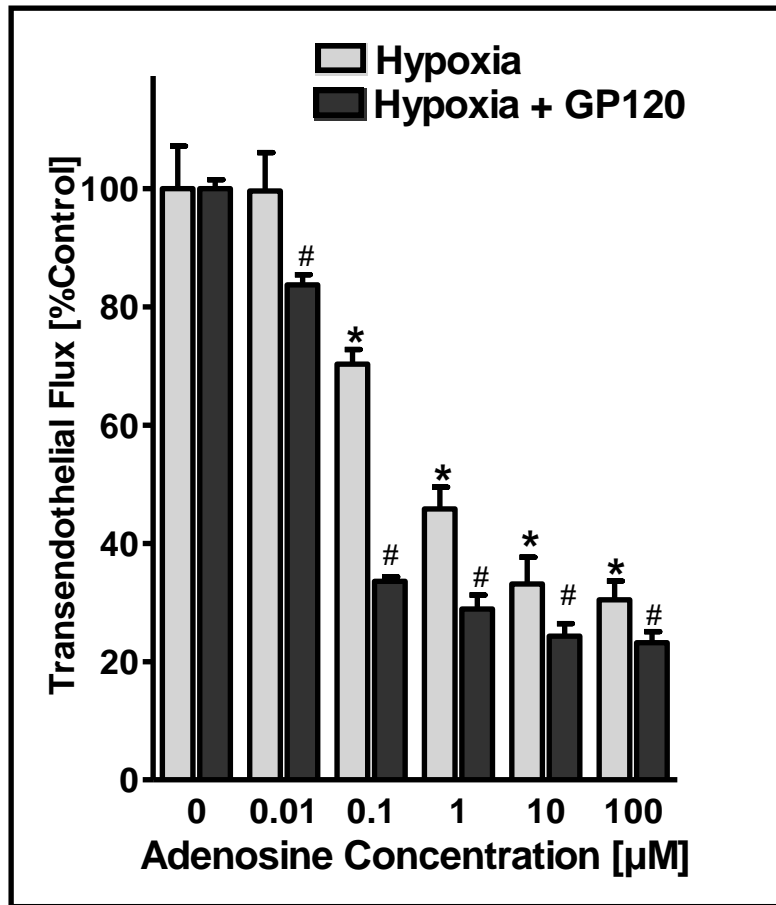


**Figure 4d:** Adenosine elicited barrier responses were measured with and without addition of HIV-1 gp120 which inhibits the ADA binding to the ADA complexing protein CD26. For that hypoxic endothelia (48 hours exposure time) were washed with 100 nM HIV-1 gp120 diluted in HBSS<sup>+</sup> and indicated concentrations (0 – 100 µM) of adenosine diluted in 100 µl HBSS<sup>+</sup> were added to the surface of hypoxic endothelia grown in a permeable support system. With these conditions endothelial permeability was quantified by 70 kD FITC-labeled dextran (3.5 µM) which was added to fluids within the apical portion of the insert at the start of the assay. Fluids from the opposing well were sampled 3 times over 60 minutes, fluorescence intensity was measured and FITC-dextran concentrations were determined. Transendothelial flux was calculated by linear regression. Data were derived from 6 monolayers in each condition.

*Asterisk (\*) indicates significant differences from baseline ( $p < 0.05$ ) and cross (#) indicates differences from baseline and from untreated controls ( $p < 0.05$ ).*

All these findings suggest that extracellular ADA, at levels observed with exposure to hypoxia, significantly influences endpoint adenosine responses, i.e. increased ADA activity dampens adenosine-elicited barrier function because adenosine itself stabilizes endothelial permeability.

### **3.5 In vivo model for endothelial permeability and PMN tissue accumulation**

Other authors have shown that hypoxia promotes vascular leak and tissue PMN accumulation in murine models (13, 14, 94, 95, 97, 134-136). Prompted by the above in vitro findings of attenuated adenosine-elicited barrier responses with increased ADA activity, and previous studies suggesting an improvement of endothelial function and decreased vascular leakage during sepsis with ADA inhibition (137-139), ADA could be pursued as a pharmacological target in a previously described murine in vivo model of hypoxia (13, 97).

As first step, mice were injected with the ADA inhibitor deoxycoformycin (1 mg/ kg intraperitoneally and 1 mg/ kg subcutaneously) or PBS<sup>+</sup> for control and then exposed to either normoxia (room air) or normobaric hypoxia (8% O<sub>2</sub> and 92% N<sub>2</sub>) for 4 hours. Pulmonary edema was assessed by determining lung water content (wet : dry ratio). As shown in Figure 5a, hypoxia increased pulmonary water content by 61±8.9% ( $p < 0.025$ ). Such increases in lung water were significantly decreased (51±6.3% decrease,  $p < 0.01$ ) by administration of deoxycoformycin in hypoxia, thereby indicating that pharmacological inhibition of ADA is associated with a significant decrease in lung water during hypoxia (Figure 5a).

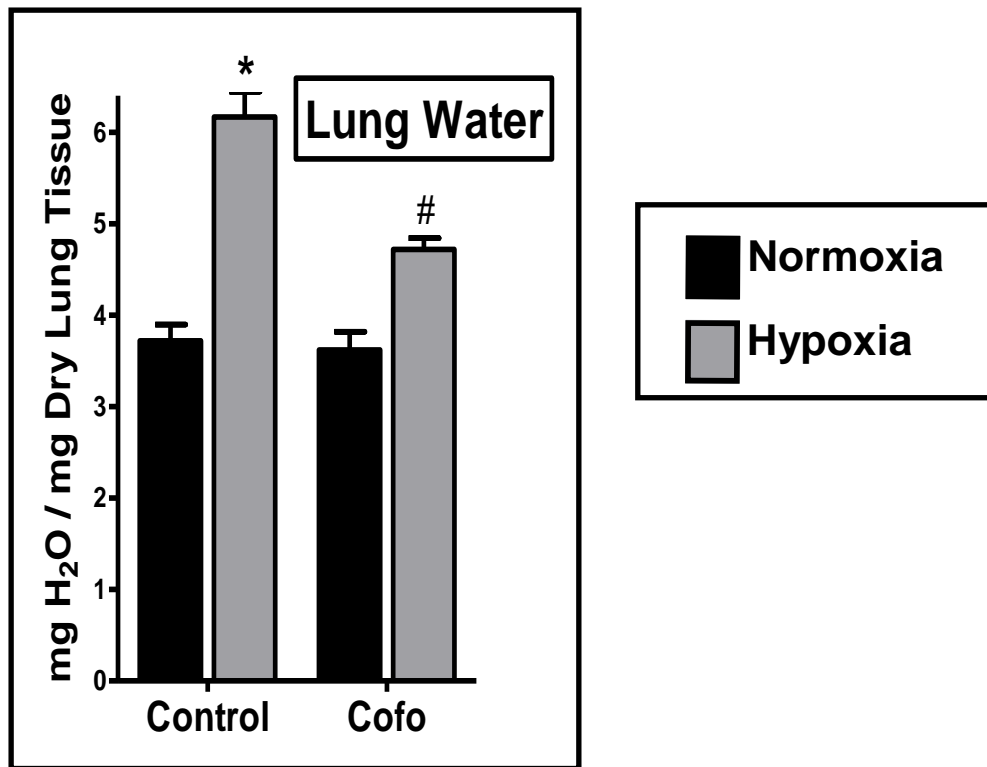


**Figure 5a:** Pulmonary edema was assessed in normoxia and hypoxia. For this purpose, C57BL/6/129 svj mice were injected with deoxycoformycin (Cofo) (1 mg/kg intraperitoneally, and 1 mg/kg subcutaneously) or PBS<sup>+</sup> for control. Then animals were exposed to either normoxia (room air) (black bars) or normobaric hypoxia (8% O<sub>2</sub>, 92% N<sub>2</sub>) (grey bars) for 4 hours. After that animals were sacrificed and lungs were collected, weighed and dried. Weight differences before and after drying were used to calculate lung water content.

Data are expressed as mean  $\pm$  SD mg H<sub>2</sub>O / mg dry lung tissue and are pooled from 6 animals per each condition. Asterisk (\*) indicates significant differences between hypoxia and normoxia ( $p < 0.025$ ) and cross (#) indicates significant differences between deoxycoformycin (Cofo) treatment and control treatment with PBS<sup>+</sup> ( $p < 0.025$ ).



To assess vascular leak in this in vivo model, the albumin marker Evan's blue was administered before hypoxia exposure. Comparative analysis of basal permeability (i.e. in normoxia) revealed no deoxycoformycin-elicited changes in any of the organs examined (lung, colon and liver). By contrast, deoxycoformycin significantly protected animals from hypoxia-induced vascular leak, i.e. decreased permeability (Figure 5b). Such protective influence of deoxycoformycin was observed in all organs examined, and was particularly evident in the lung.

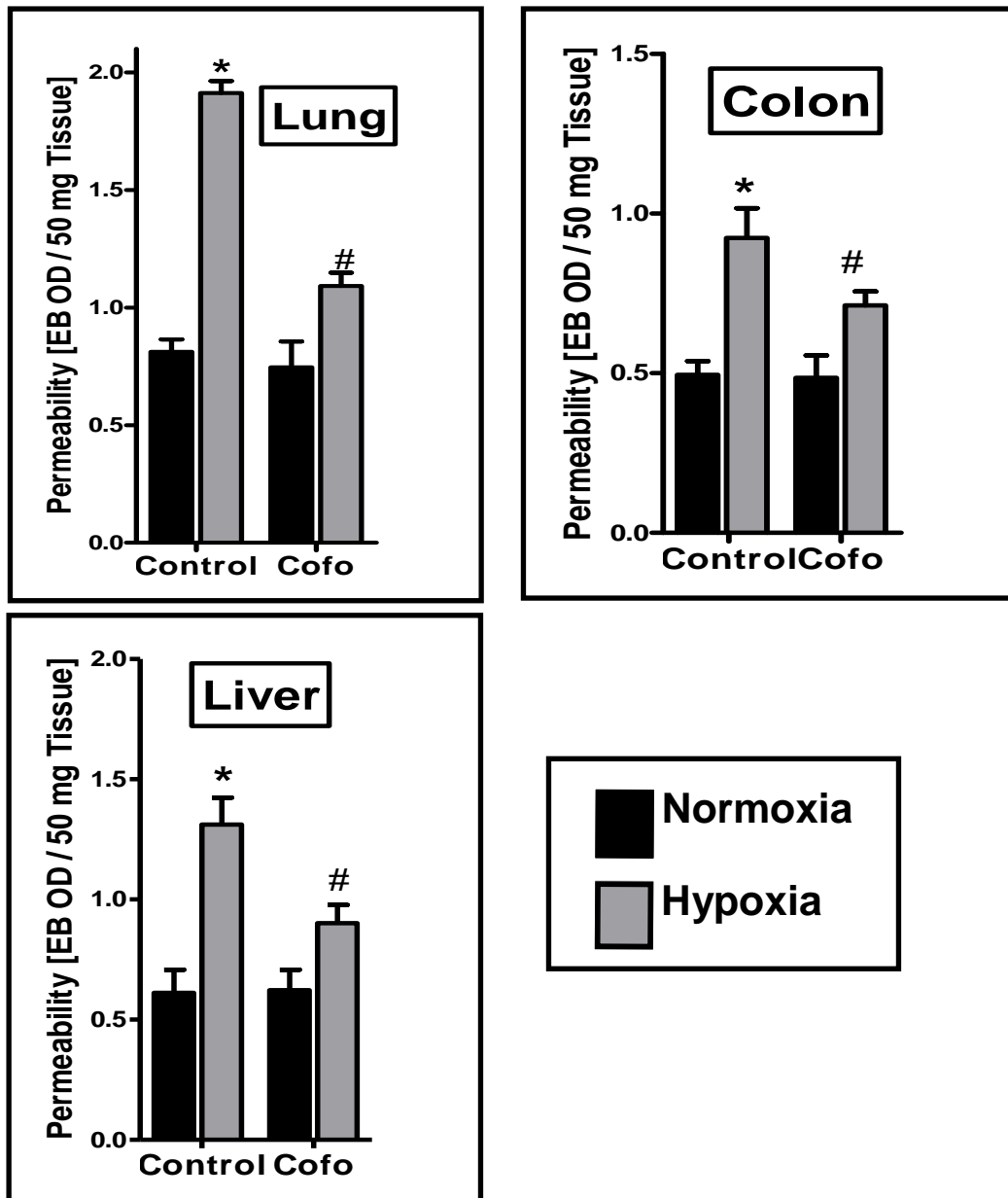


**Figure 5b:** *Vascular barrier function was assessed by intravascular administration of Evan's blue. Animals were injected with deoxycoformycin (Cofc) (1 mg/ kg intraperitoneally and 1 mg/ kg subcutaneously) or PBS<sup>+</sup>. For the purpose of quantifying vascular permeability, 0.2 ml of Evan's blue (0.5% in PBS<sup>+</sup>) were administered intravenously before exposure to normobaric hypoxia (8% O<sub>2</sub>, 92% N<sub>2</sub>) or room air (normoxia) for 4 hours. Then mice were sacrificed and the lungs, liver and colon were harvested. Organ Evan's blue concentrations were quantified following formamide extraction (55° C for 2 hours) by measuring absorbances at 610 nm with subtraction of reference absorbance at 450 nm.*

*Data are expressed as mean ± SD Evan's blue (EB) OD / 50 mg wet tissue and are pooled from 6 animals per condition. Asterisk (\*) indicates significant differences between normoxia and hypoxia exposure (p<0.01), cross (#) indicates significant differences between deoxycoformycin (Cofc) and control treatment with PBS<sup>+</sup> (p<0.025).*

Last studies have demonstrated that inhibition of ADA function is associated with decreased vascular leakage (see Figure 5b), so it could be hypothesized that a reduction of adenosine metabolism at the vascular surface may also function as anti-inflammatory response during hypoxia, particularly given the anti-inflammatory properties of adenosine (62). To test this hypothesis, multiple mucosal organs (lung, colon, liver) were screened for PMN accumulation following administration of deoxycoformycin (Figure 5c). Agreeing with previous studies (95, 140), the PMN marker myeloperoxidase (MPO) significantly increased after hypoxia exposure in all animals. However deoxycoformycin treated animals showed a lesser extent of the PMN marker MPO compared to PBS<sup>+</sup> controls (p<0.05 for all organs).

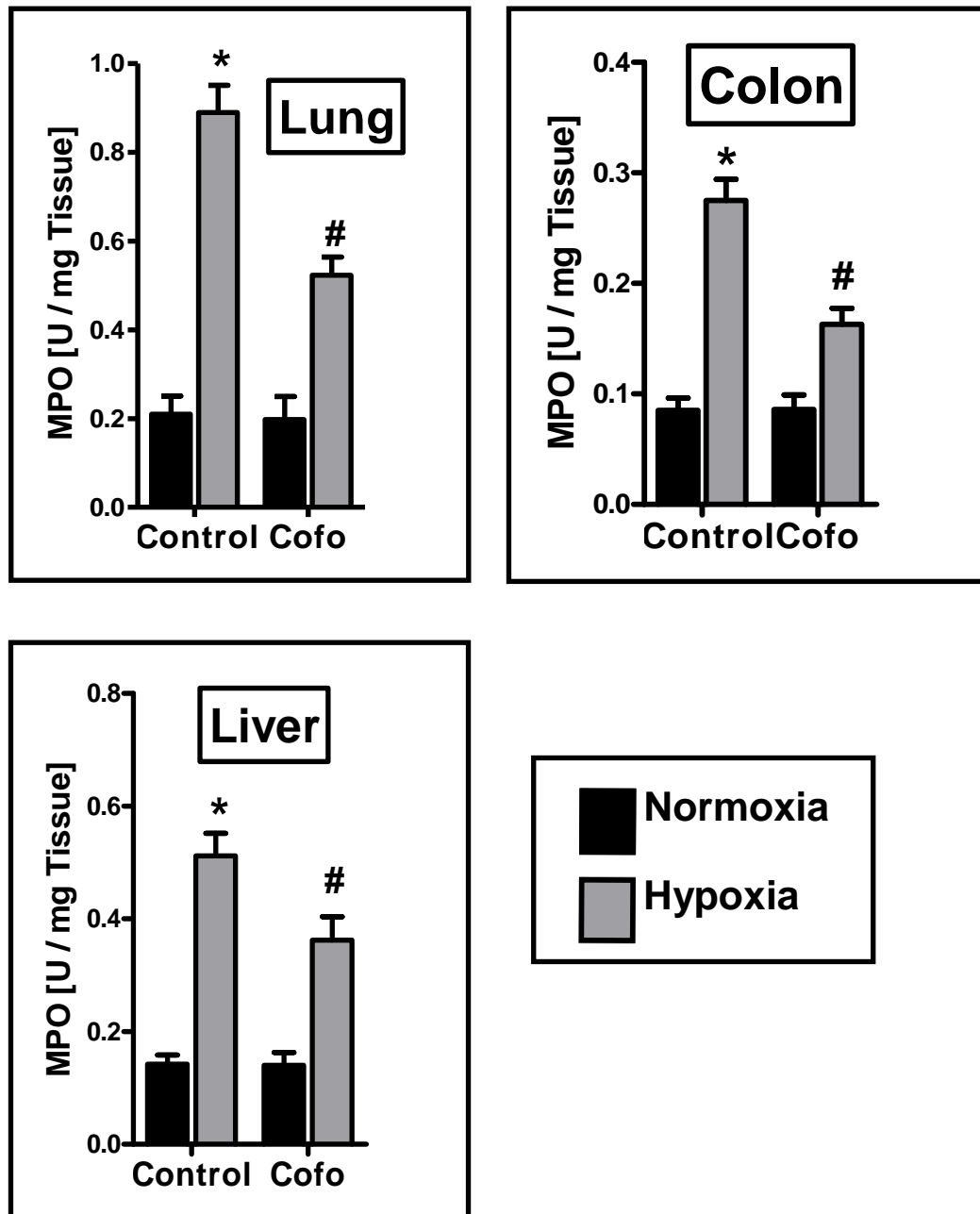


**Figure 5c:** Assessment of PMN accumulation by myeloperoxidase (MPO) measurements after hypoxic exposure. To quantify PMN tissue concentrations, animals were administered deoxycoformycin (Cofo) or PBS<sup>+</sup> for control, exposed to normobaric hypoxia (8% O<sub>2</sub>, 92% N<sub>2</sub>) or room air for 4 hours. Then they were sacrificed, organs were harvested and the PMN marker myeloperoxidase (MPO)

was quantified. After solubilization of the organs with 0.5% Triton X-100 each sample was mixed with a solution of 1 mM 2,2-azino-di-(3-ethyl) di-thiazoline sulfonic acid and 10 mM H<sub>2</sub>O<sub>2</sub> in 100 mM citrate buffer (pH 4.2, 20° C). Then colour development was measured at 405 nm.

Data are expressed as mean  $\pm$  SD U / mg tissue and are pooled from 6 animals per condition. Asterisk (\*) indicates significant differences between normoxia and hypoxia exposure ( $p < 0.01$ ), cross (#) indicates significant differences between deoxycoformycin (Cofo) and control treatment with PBS<sup>+</sup> ( $p < 0.025$ ).

These in vivo findings support the hypothesis that adenosine metabolism via ADA is a critical control-point in the regulation of both vascular leak and PMN accumulation within hypoxic tissues, and suggest that inhibition of ADA might represent a therapeutic target in the treatment of hypoxia associated vascular leak syndrome and excessive inflammatory cell accumulation.

## 4 Discussion

Results from these studies indicate that hypoxia transcriptionally induces endothelial ADA, and that such increased ADA is tethered via CD26 to form an extracellular complex which can diminish adenosine signaling by converting adenosine to inosine. Similarly, plasma ADA activity was increased *in vivo* in a murine model of acute hypoxia, thereby providing an important mechanism to balance extracellular adenosine levels in conditions of high adenine nucleotide metabolism (Figure 6).

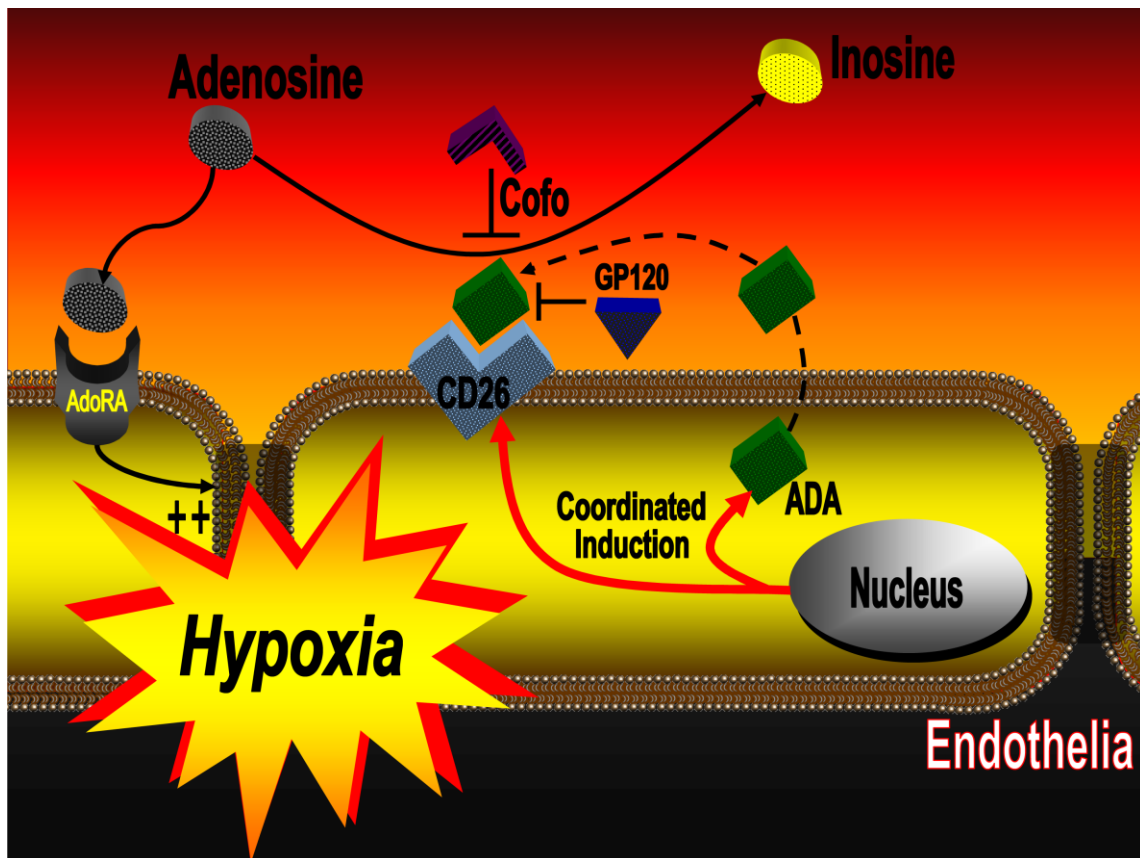


**Figure 6:** Proposed model of coordinated induction of adenosine deaminase (ADA) and CD26. Hypoxia coordinates the induction of endothelial ADA and CD26. After transcriptional induction of ADA, the enzyme is released from the endothelial cell and binds to its cell surface receptor CD26. Under hypoxic

*conditions vascular adenosine signaling is modulated by the increase of endothelial cell surface ADA. In general, extracellular adenosine can activate endothelial adenosine receptors, which stabilize endothelial barrier function. Due to increased ADA surface activity during hypoxia, adenosine is metabolized to inosine via ADA, so vascular adenosine signaling is terminated and extracellular inosine concentration is increasing. Inhibition of ADA with deoxycoformycin (Cofo) or inhibition of ADA binding to its receptor CD26 with the glycoprotein HIV-1 gp120 can contribute to increasing vascular adenosine effects during acute hypoxia.*

Several previous studies have shown that acute hypoxia is associated with increased vascular adenosine levels (90, 108, 141). The present data show for the first time that there is a catabolic pathway to control vascular adenosine levels in hypoxia. Such increases in vascular adenosine generation and signaling are important to maintain vascular endothelial function and suppress excessive inflammation during conditions of acute hypoxia (13, 64, 95, 97, 103).

By contrast, elevated adenosine levels for a long-term period may be associated with adenosine receptor desensitization as well as the accumulation of toxic adenosine metabolites (e.g. deoxyadenosine). Pulmonary toxicity (116), fibrosis (115) or severe combined immunodeficiency (117, 118) are described results of chronic elevation of adenosine levels. Recent studies have shown how hypoxia elevates extracellular adenosine. First, acute hypoxia directly increases levels of the ecto-nucleotidases CD39 and CD73 (13, 95, 97, 136), surface enzymes which coordinate adenosine generation from precursor nucleotides. Both, CD39- and CD73-null mice show increased vascular permeability, tissue edema and PMN tissue accumulation during acute hypoxia exposure, and such observations implicate protective influences of adenosine on multiple physiologic pathways associated with hypoxia (13, 95, 97). Moreover, hypoxia also promotes adenosine signaling by selective adenosine receptor induction. Vascular endothelia express

more than one subtype of adenosine receptors (A1, A2a, A2b and A3), but only the A2b receptor is selectively up-regulated by hypoxia, and such increases in adenosine receptor expression are associated with increased vascular adenosine effects (13). In addition, a third mechanism of increasing vascular adenosine signaling has been found in recent studies, namely the hypoxia-mediated repression of equilibrative nucleoside transporters (ENT1 and ENT2) (109). So, molecular mechanisms are now understood, which explain the elevation of extracellular adenosine in hypoxia.

It is, however, not surprising that hypoxia coordinates transcriptional induction of metabolic pathways that terminate adenosine signaling. Adenosine receptors, like other G-protein-coupled receptors, are tightly regulated by ligand availability (142). With chronic exposure to ligand, regulatory pathways exist to attenuate signaling through these receptors, including both receptor desensitization and receptor internalization pathways mediated by the recruitment of  $\beta$ -arrestins (142-144). Additional studies have shown that following chronic receptor stimulation,  $\beta$ -arrestins also recruit phosphodiesterases to  $G\alpha_s$ -coupled receptors (e.g. adenosine A2a and A2b receptors), thereby coordinately blocking G-protein signaling and promoting cyclic AMP degradation (145).

In a similar way the induction of adenosine generating capacity by CD39 and CD73 and the induction of ADA may be coordinated. For example, maximal increases of endothelial ADA are seen after 24 hours of hypoxia exposure (Figure 1b). By contrast, earlier and more dramatic increases in endothelial CD39 and CD73 have been reported (13). For example, endothelial CD39 and CD73 are increased to 7- to 10-fold after 8 hours of hypoxia exposure (13), the induction of endothelial ADA is less than 3-fold at 8 hours. These observations suggest that ADA induction by hypoxia and localization to the endothelial cell surface may occur more delayed than hypoxia associated increases in nucleotide phosphohydrolysis and signaling. Thus, this time course of events suggest the possibility that the physiologic role of

ADA induction by hypoxia represents a catabolic pathway induced to prevent long-term increases of extracellular adenosine.

The observation that adenosine receptor mediated cellular function is altered by extracellularly localized ADA has already reported previously. Hashikawa et al. recently demonstrated that in CD26 transfected cells, extracellularly localized ADA can terminate adenosine signaling. However, this effect was dependent upon CD26 expression as well as on the extent of CD26 saturation (146). In addition, Martin et al. demonstrated that the expression of CD26 and the degree of ADA bound via CD26 to the T-cell surface increases upon T-cell activation (147). Such data indicate that ADA binding to CD26 produces a co-stimulatory response that is enhanced by T cell activation. Moreover, ADA bound to CD26 was found to also influence co-stimulatory signals of the immunological synapse (148). Such studies highlight the critical role of CD26 induction by hypoxia. But only via their coordinated induction, CD26 and ADA together can cause an increase in cell surface ADA activity, thereby modulating endothelial adenosine signaling.

In the present study it is demonstrated that hypoxia coordinates the induction of cell surface localized ADA, thereby increasing the endothelial capacity to metabolize adenosine to inosine. Through this mechanism, induction of ADA modulates vascular adenosine signaling by decreasing the amount of extracellular adenosine available to activate adenosine receptors. The way how ADA is exported from inside the cells to cell surface and how it becomes bound to CD26 is still not known.

However, at the same time, this transcriptionally regulated metabolic pathway also introduces the possibility that hypoxia promotes extracellular inosine production and may promote inosine signaling. But no specific inosine receptors have yet been characterized. However, Jin et al. observed that that like adenosine, inosine can also elicit vasoconstriction of hamster cheek pouch arterioles as a result of mast cell degranulation (149). In this work, it was shown that inosine binds to A<sub>3</sub> adenosine receptors and thereby stimulates the observed degranulation of mast cells. Moreover, the effect of inosine on mast-cell degranulation was lost in mice



that lack the adenosine A<sub>3</sub> receptor (150). Thus, the ratio of the local concentrations of adenosine and inosine likely determine signaling events. For example, the outcome of the mast-cell response depends on the adenosine to inosine ratio, as inosine appears to bind to A<sub>3</sub> receptors, thus, enhancing mast-cell degranulation, whereas adenosine can also bind to A<sub>2a</sub> receptors, which decreases mast-cell degranulation (151). In contrast to the pro-inflammatory effects on mast cells, inosine has also been found to act as powerful anti-inflammatory agent in macrophages and lymphocytes. Inosine treatment, for instance, has been associated with inhibition of the production of pro-inflammatory cytokines (e.g. tumor necrosis factor- $\alpha$ , interleukin-1 and macrophage inflammatory protein) (152). Moreover, during conditions of hypoxia, ischemia and reperfusion, exogenous administration of larger doses of inosine were found to prevent ischemia–reperfusion related injury in several tissues, including the intestine, the heart and the brain (153-155). In the present study, specific effects of inosine generation related to increased ADA activity were not investigated.

Further studies were done in the studygroup of H. K. Eltzhig. For example, ADA levels in blood samples of chronically hypoxic children who were undergoing a cardiac surgery to repair congenital heart defects were examined. These results showed a more than 4-fold increase in circulating ADA levels in plasma of these chronically hypoxic children who had an approximately 15% decrease in mean oxygen saturation. It is important to note that circulating adenosine has strong cardiac influences. In particular, of its many central nervous actions, adenosine can induce hypotension and cardiac suppression (61), and thus, it is tempting to speculate that an important adaptive pathway for these patients is rapid adenosine clearance. Such clearance could be achieved through the ADA induction pathway. Further studies will be necessary to elucidate whether these patients benefit in other ways from increased circulating ADA levels.

In summary, the results of this study identify ADA induction by hypoxia as a transcriptionally regulated innate adaptation of the vascular endothelium to attenuate elevated extracellular adenosine levels. Through coordinated induction of the ADA complexing protein CD26 which is necessary for ADA function, ADA is localized to the endothelial surface and reduces the extracellular adenosine levels which increase during hypoxia. Further examinations of these findings will determine whether ADA inhibition may serve as a therapeutic target for disorders involving vascular leak syndrome or excessive inflammatory responses during acute hypoxia.

## 5 Summary

It is well known that extracellular levels of adenosine increase during limited oxygen availability. Acute increases of adenosine concentration are important to diminish excessive inflammation or vascular leakage in hypoxic tissue. Chronically elevated adenosine levels reveal toxic effects. Based on these facts, there must be clearance mechanisms which inhibit high adenosine concentrations during long-term hypoxic conditions.

Previous microarray analysis revealed a nearly 50-fold induction of the enzyme adenosine deaminase (ADA) mRNA in hypoxia which metabolizes adenosine to inosine. Guided by these results the following investigations were done.

First studies were done by real-time PCR and western blot. These findings confirmed the initial microarray results. The ADA mRNA was prominently induced by hypoxia and also the western blot analysis of total ADA protein indicated a time - dependent induction of ADA. Measurements of enzyme activity revealed in lysates as well as in supernatant and on cell surface hypoxia – dependent increases of ADA activity. Moreover, further examinations in human endothelia showed that the ADA – complexing protein CD26 is also induced by hypoxia. Furthermore ADA activity on cell surface was dependent on CD26 binding to ADA. Treatment with glycoprotein HIV-1 gp120, a specific inhibitor of ADA – CD26 interaction, showed an effective blocking of inosine generation.

Functional studies in *in vitro* as well as in *in vivo* models revealed that inhibition of ADA with deoxycoformycin enhances protective responses mediated by adenosine (e.g. vascular leak, neutrophil accumulation or pulmonary edema).

Altogether these findings reveal induction of ADA as an innate metabolism during conditions of limited oxygen supply to decrease elevated extracellular adenosine levels by converting adenosine to inosine and to protect in this way the organism from potentially deleterious effects of long-term increase of adenosine. In contrast, during acute hypoxia associated with excessive inflammation and vascular leakage, inhibition of ADA may serve as a new therapeutic strategy to enhance

adenosine signaling in endothelia and inhibit tissue permeability and accumulation of inflammatory cells.

## Zusammenfassung

Es ist bekannt, dass sich Adenosin, ein Abbauprodukt des Adenosintriphosphats (ATP), unter hypoxischen Bedingungen im extrazellulären Raum anreichert. Ein kurzfristiger Anstieg der Adenosinkonzentrationen im hypoxischen Gewebe hat einen positiven Effekt, da es die Ausbreitung der Entzündungsreaktion sowie die Endothelschädigung im Rahmen des Sauerstoffmangels reduziert. Über längere Zeit hinweg bestehende erhöhte Adenosinkonzentrationen zeigen hingegen toxische Wirkung. Aufgrund dieser Tatsachen war anzunehmen, dass es einen Mechanismus im Stoffwechsel gibt, der die Anhäufung von Adenosin unter längerandauerenden hypoxischen Bedingungen verhindert.

Vorbestehende Untersuchungen mittels Microarray-Analyse zeigten eine nahezu 50-fach gesteigerte Induktion des Enzyms Adenosindeaminase (ADA) unter Hypoxie, welches Adenosin zu Inosin abbaut. Diese Ergebnisse waren somit Grundlage dieser Arbeit.

Die weiteren Untersuchungen mittels real-time PCR und Western blot bestätigten die ersten Ergebnisse. Eine Induktion der Adenosindeaminase konnte sowohl auf mRNA-Ebene, Protein-Ebene als auch bei den funktionellen Messungen der ADA - Aktivität im Zelllysate, im Überstand als auch auf der Zelloberfläche nachgewiesen werden. Weitere Experimente zeigten ebenso eine Hypoxie-bedingte Induktion von CD26. Es konnte gezeigt werden, dass ADA auf der Zelloberfläche nur in Verbindung mit CD26 enzymatisch aktiv ist. Durch Hemmung des ADA - CD26 - Komplexes mit dem Glykoprotein HIV-1 gp120, einem spezifischen Inhibitor, konnte die Inosinentstehung fast vollständig gehemmt werden.

Bei weiterführenden Untersuchungen zeigte sich sowohl im *in vitro* als auch im *in vivo* Modell, dass durch eine spezifische Hemmung des Enzyms ADA mittels Deoxycoformycin die protektive Wirkung des Adenosins auf die Zellwandpermeabilität verstärkt werden konnte.

Zusammenfassend zeigen diese Ergebnisse einen angeborenen Metabolismus, der unter hypoxischen Bedingungen zu einer Induktion der Adenosindeaminase

---

führt, um die toxischen Wirkungen bei chronisch erhöhten Adenosinkonzentrationen durch Abbau zu Inosin zu verringern. Im Gegensatz dazu könnte bei akut aufgetretener Hypoxie die Hemmung der Adenosindeaminase ein möglicher therapeutischer Ansatz sein, um die Endothelschädigung als auch die Entzündungsreaktion im hypoxischen Gewebe zu mindern.

## 6 References

1. Dancey, J.T., Deubelbeiss, K.A., Harker, L.A., and Finch, C.A. 1976. Neutrophil kinetics in man. *J. Clin. Invest.* 58:705-715.
2. Ley, K. 2001. Pathways and bottlenecks in the web of inflammatory adhesion molecules and chemoattractants. *Immunol Res* 24:87-95.
3. Shimizu, Y., Rose, D.M., and Ginsberg, M.H. 1999. Integrins in the immune system. *Adv Immunol* 72:325-380.
4. Gonzalez-Amaro, R., and Sanchez-Madrid, F. 1999. Cell adhesion molecules: selectins and integrins. *Crit Rev Immunol* 19:389-429.
5. Ley, K. 2002. Integration of inflammatory signals by rolling neutrophils. *Immunol Rev* 186:8-18.
6. Dejana, E., Spagnuolo, R., and Bazzoni, G. 2001. Interendothelial junctions and their role in the control of angiogenesis, vascular permeability and leukocyte transmigration. *Thromb Haemost* 86:308-315.
7. Lennon, P.F., Taylor, C.T., Stahl, G.L., and Colgan, S.P. 1998. Neutrophil-derived 5'-Adenosine Monophosphate Promotes Endothelial Barrier Function via CD73-mediated Conversion to Adenosine and Endothelial A2B Receptor Activation. *J. Exp. Med.* 188:1433-1443.
8. Dejana, E., Corada, M., and Lampugnani, M.G. 1995. Endothelial cell-to-cell junctions. *FASEB J.* 9:910-918.
9. Lewis, R.E., and Granger, H.J. 1988. 4 (LTB<sub>4</sub>). *Micro. Res.* 35:27-47.
10. Meyrick, B., Hoffman, L.H., and Brigham, K.L. 1984. Chemotaxis of granulocytes across bovine pulmonary artery intimal explants without endothelial cell injury. *Tiss. Cell* 16:1-16.
11. Shaw, J.O., and Henson, P.M. 1982. Pulmonary intravascular sequestration of activated neutrophils. *Am. J. Pathol.* 108:17-23.
12. Huang, A., Furie, M., Nicholson, S., Fischbarg, J., Liebovitch, L., and Silverstein, S. 1988. Effects of human neutrophil chemotaxis across human endothelial cell monolayers on the permeability of these monolayers to ions and macromolecules. *J. Cell. Physiol.* 135:355-366.
13. Eltzschig, H.K., Ibla, J.C., Furuta, G.T., Leonard, M.O., Jacobson, K.A., Enjyoji, K., Robson, S.C., and Colgan, S.P. 2003. Coordinated adenine nucleotide phosphohydrolysis and nucleoside signaling in posthypoxic endothelium: role of ectonucleotidases and adenosine A2B receptors. *J Exp Med* 198:783-796.
14. Collard, C.D., Park, K.A., Montalto, M.C., Alapati, S., Buras, J.A., Stahl, G.L., and Colgan, S.P. 2002. Neutrophil-derived Glutamate Regulates Vascular Endothelial Barrier Function. *J. Biol. Chem.* 277:14801-14811.
15. Synnestvedt, K., Furuta, G.T., Comerford, K.M., Louis, N., Karhausen, J., Eltzschig, H.K., Hansen, K.R., Thompson, L.F., and Colgan, S.P. 2002. Ecto-5'-nucleotidase (CD73) regulation by hypoxia-inducible factor-1 (HIF-1) mediates permeability changes in intestinal epithelia. *J. Clin. Invest.* 110:993-1002.

16. Collard, C.D., Bukusoglu, C., Agah, A., Colgan, S.P., Reenstra, W.R., Morgan, B.P., and Stahl, G.L. 1999. Hypoxia-induced expression of complement receptor type 1 (CR1, CD35) in human vascular endothelial cells. *Am J Physiol* 276:C450-458.
17. Narravula, S., Lennon, P.F., Mueller, B.U., and Colgan, S.P. 2000. Regulation of endothelial CD73 by adenosine: paracrine pathway for enhanced endothelial barrier function. *J Immunol* 165:5262-5268.
18. Comerford, K.M., Lawrence, D.W., Synnestvedt, K., Levi, B.P., and Colgan, S.P. 2002. Role of vasodilator-stimulated phosphoprotein in protein kinase A-induced changes in endothelial junctional permeability. *Faseb J*.
19. Stevens, T., Garcia, J.G.N., Shasby, D.M., Bhattacharya, J., and Malik, A.B. 2000. Mechanisms regulating endothelial cell barrier function. *Am. J. Physiol. (Lung Cell Mol Physiol)* 279:L419-L422.
20. Stevens, T., Creighton, J., and Thompson, W.J. 1999. Control of cAMP in lung endothelial cell phenotypes. Implications for control of barrier function. *Am J Physiol* 277:L119-126.
21. Stan, R.V. 2002. Structure and function of endothelial caveolae. *Microsc Res Tech* 57:350-364.
22. Michel, C.C. 1998. Capillaries, caveolae, calcium and cyclic nucleotides: a new look at microvascular permeability. *J Mol Cell Cardiol* 30:2541-2546.
23. Worthylake, R.A., and Burridge, K. 2001. Leukocyte transendothelial migration: orchestrating the underlying molecular machinery. *Curr Opin Cell Biol* 13:569-577.
24. Schoenwaelder, S.M., and Burridge, K. 1999. Bidirectional signaling between the cytoskeleton and integrins. *Curr Opin Cell Biol* 11:274-286.
25. Tsukita, S., Furuse, M., and Itoh, M. 2001. Multifunctional strands in tight junctions. *Nat Rev Mol Cell Biol* 2:285-293.
26. Rubin, L.L. 1992. Endothelial cells: adhesion and tight junctions. *Curr. Opin. Cell Biol.* 4:830-833.
27. Janzer, R.C., and Raff, M.C. 1987. Astrocytes induce blood-brain barrier properties in endothelial cells. *Nature* 325:253-257.
28. Moore, T.M., Chetham, P.M., Kelly, J.J., and Stevens, T. 1998. Signal transduction and regulation of lung endothelial cell permeability. Interaction between calcium and cAMP. *Am J Physiol* 275:L203-222.
29. Burns, A.R., Bowden, R.A., MacDonell, S.D., Walker, D.C., Odeunmi, T.O., Donnachie, E.M., Simon, S.I., Entman, M.L., and Smith, C.W. 2000. Analysis of tight junctions during neutrophil transendothelial migration. *J Cell Sci* 113:45-57.
30. Minnear, F.L., DeMichele, M.A.A., Moon, D.G., Reider, C.L., and Fenton, J.W. 1989. Isoproterenol reduces thrombin-induced pulmonary endothelial permeability in vitro. *Am. J. Physiol.* 257:H1613-H1623.
31. Weinbaum, S., Zhang, X., Han, Y., Vink, H., and Cowin, S.C. 2003. Mechanotransduction and flow across the endothelial glycocalyx. *PNAS* 100:7988-7995.



32. Rehm, M., Zahler, S., Lotsch, M., Welsch, U., Conzen, P., Jacob, M., and Becker, B.F. 2004. Endothelial glycocalyx as an additional barrier determining extravasation of 6% hydroxyethyl starch or 5% albumin solutions in the coronary vascular bed. *Anesthesiology* 100:1211-1223.
33. Platts, S.H., and Duling, B.R. 2004. Adenosine A3 Receptor Activation Modulates the Capillary Endothelial Glycocalyx. *Circ Res* 94:77-82.
34. Cramer, T., Yamanishi, Y., Clausen, B.E., Forster, I., Pawlinski, R., Mackman, N., Haase, V.H., Jaenisch, R., Corr, M., Nizet, V., et al. 2003. HIF-1alpha is essential for myeloid cell-mediated inflammation. *Cell* 112:645-657.
35. Kong, T., Eltzschig, H.K., Karhausen, J., Colgan, S.P., and Shelley, C.S. 2004. Leukocyte adhesion during hypoxia is mediated by HIF-1-dependent induction of {beta}2 integrin gene expression. *PNAS*:0401339101.
36. Tamura, D.Y., Moore, E.E., Partrick, D.A., Johnson, J.L., Offner, P.J., and Silliman, C.C. 2002. Acute hypoxemia in humans enhances the neutrophil inflammatory response. *Shock* 17:269-273.
37. Colgan, S.P., Dzus, A.L., and Parkos, C.A. 1996. Epithelial exposure to hypoxia modulates neutrophil transepithelial migration. *J Exp Med* 184:1003-1015.
38. Collard, C.D., Park, K.A., Montalto, M.C., Alapati, S., Buras, J.A., Stahl, G.L., and Colgan, S.P. 2002. Neutrophil-derived Glutamate Regulates Vascular Endothelial Barrier Function. *J Biol Chem* 277:14801-14811.
39. Rui, T., Cepinskas, G., Feng, Q., Ho, Y.S., and Kvietys, P.R. 2001. Cardiac myocytes exposed to anoxia-reoxygenation promote neutrophil transendothelial migration. *Am J Physiol Heart Circ Physiol* 281:H440-447.
40. Madara, J.L. 1998. Regulation of the movement of solutes across tight junctions. *Annu Rev Physiol* 60:143-159.
41. Luscinskas, F.W., Ma, S., Nusrat, A., Parkos, C.A., and Shaw, S.K. 2002. The role of endothelial cell lateral junctions during leukocyte trafficking. *Immunol Rev* 186:57-67.
42. Luscinskas, F.W., Ma, S., Nusrat, A., Parkos, C.A., and Shaw, S.K. 2002. Leukocyte transendothelial migration: a junctional affair. *Semin Immunol* 14:105-113.
43. Carpenter, T.C., and Stenmark, K.R. 2001. Hypoxia decreases lung neprilysin expression and increases pulmonary vascular leak. *Am J Physiol Lung Cell Mol Physiol* 281:L941-948.
44. Schoch, H.J., Fischer, S., and Marti, H.H. 2002. Hypoxia-induced vascular endothelial growth factor expression causes vascular leakage in the brain. *Brain* 125:2549-2557.
45. Rippe, B., and Haraldsson, B. 1994. Transport of macromolecules across microvascular walls: the two-pore theory. *Physiol. Rev.* 74:163-219.
46. Lum, H., and Malik, A.B. 1994. Regulation of vascular endothelial barrier function. *Am. J. Physiol.* 267:L223-L241.

47. Eltzschig, H.K., and Collard, C.D. 2004. Vascular ischaemia and reperfusion injury. *Br Med Bull* 70:71-86.
48. Kloner, R.A., Ellis, S.G., Lange, R., and Braunwald, E. 1983. Studies of experimental coronary artery reperfusion: Effects on infarct size, myocardial function, biochemistry, ultrastructure and microvascular damage. *Circulation* 68(Suppl I):8-15.
49. Kloner, R.A., Ganote, C.E., and Jennings, R.B. 1974. The "no-reflow" phenomenon after temporary coronary occlusion in the dog. *J. Clin. Invest.* 54:1496-1508.
50. Maier, R.V., and Bulger, E.M. 1996. Endothelial changes after shock and injury. *New Horizons* 4:211-223.
51. Waxman, K. 1996. Shock: Ischemia, reperfusion and inflammation. *New Horizons* 4:153-160.
52. Gautam, N., Olofsson, A.M., Herwald, H., Iversen, L.F., Lundgren-Akerlund, E., Hedqvist, P., Arfors, K.E., Flodgaard, H., and Lindbom, L. 2001. Heparin-binding protein (HBP/CAP37): a missing link in neutrophil-evoked alteration of vascular permeability. *Nat Med* 7:1123-1127.
53. Pereira, H.A. 1995. CAP37, a neutrophil-derived multifunctional inflammatory mediator. *J Leukoc Biol* 57:805-812.
54. Lee, T.D., Gonzalez, M.L., Kumar, P., Chary-Reddy, S., Grammas, P., and Pereira, H.A. 2002. CAP37, a novel inflammatory mediator: its expression in endothelial cells and localization to atherosclerotic lesions. *Am J Pathol* 160:841-848.
55. Hayashi, M., Kim, S.W., Imanaka-Yoshida, K., Yoshida, T., Abel, E.D., Eliceiri, B., Yang, Y., Ulevitch, R.J., and Lee, J.D. 2004. Targeted deletion of BMK1/ERK5 in adult mice perturbs vascular integrity and leads to endothelial failure. *J Clin Invest* 113:1138-1148.
56. Webb, A.R. 2000. Capillary leak. Pathogenesis and treatment. *Minerva Anesthesiol* 66:255-263.
57. Michel, C.C., and Curry, F.E. 1999. Microvascular permeability. *Physiol Rev* 79:703-761.
58. Karhausen, J., Furuta, G.T., Tomaszewski, J.E., Johnson, R.S., Colgan, S.P., and Haase, V.H. 2004. Epithelial hypoxia-inducible factor-1 is protective in murine experimental colitis. *J Clin Invest* 114:1098-1106.
59. Baxter, G.F. 2002. Role of adenosine in delayed preconditioning of myocardium. *Cardiovasc Res* 55:483-494.
60. Mubagwa, K., and Flameng, W. 2001. Adenosine, adenosine receptors and myocardial protection: an updated overview. *Cardiovasc Res* 52:25-39.
61. Linden, J. 2001. Molecular approach to adenosine receptors: receptor-mediated mechanisms of tissue protection. *Annu Rev Pharmacol Toxicol* 41:775-787.
62. Hasko, G., and Cronstein, B.N. 2004. Adenosine: an endogenous regulator of innate immunity. *Trends Immunol* 25:33-39.

63. McCallion, K., Harkin, D.W., and Gardiner, K.R. 2004. Role of adenosine in immunomodulation: review of the literature. *Crit Care Med* 32:273-277.
64. Sitkovsky, M.V., Lukashev, D., Apasov, S., Kojima, H., Koshiba, M., Caldwell, C., Ohta, A., and Thiel, M. 2004. Physiological Control of Immune Response and Inflammatory Tissue Damage by Hypoxia-Inducible Factors and Adenosine A2A Receptors. *Annual Review of Immunology* 22:657-682.
65. Ohta, A., and Sitkovsky, M. 2001. Role of G-protein-coupled adenosine receptors in downregulation of inflammation and protection from tissue damage. *Nature* 414:916-920.
66. Hochachka, P.W., and Lutz, P.L. 2001. Mechanism, origin, and evolution of anoxia tolerance in animals. *Comp Biochem Physiol B Biochem Mol Biol* 130:435-459.
67. O'Farrell, P.H. 2001. Conserved responses to oxygen deprivation. *J Clin Invest* 107:671-674.
68. Boutilier, R.G. 2001. Mechanisms of cell survival in hypoxia and hypothermia. *J Exp Biol* 204:3171-3181.
69. Eltzschig, H.K., Thompson, L.F., Karhausen, J., Cotta, R.J., Ibla, J.C., Robson, S.C., and Colgan, S.P. 2004. Endogenous adenosine produced during hypoxia attenuates neutrophil accumulation: Coordination by extracellular nucleotide metabolism. *Blood*:2004-2006-2066.
70. Marcus, A.J., Broekman, M.J., Drosopoulos, J.H., Islam, N., Pinsky, D.J., Sesti, C., and Levi, R. 2003. Metabolic Control of Excessive Extracellular Nucleotide Accumulation by CD39/Ecto-Nucleotidase-1: Implications for Ischemic Vascular Diseases. *J Pharmacol Exp Ther* 305:9-16.
71. Robson, S.C., Enjyoji, K., Goepfert, C., Imai, M., Kaczmarek, E., Lin, Y., Sevigny, J., and Warny, M. 2001. Modulation of extracellular nucleotide-mediated signaling by CD39/nucleoside triphosphate diphosphohydrolase-1. *Drug Development Research* 53:193-207.
72. Robson, S.C., Kaczmarek, E., Siegel, J.B., Candinas, D., Koziak, K., Millan, M., Hancock, W.W., and Bach, F.H. 1997. Loss of ATP diphosphohydrolase activity with endothelial cell activation. *J Exp Med* 185:153-163.
73. Marcus, A.J., Broekman, M.J., Drosopoulos, J.H.F., Islam, N., Alyonycheva, T.N., Safier, L.B., Hajjar, K.A., Posnett, D.N., Schoenborn, M.A., Schooley, K.A., et al. 1997. The Endothelial Cell Ecto-ADPase Responsible for Inhibition of Platelet Function is CD39. *J. Clin. Invest.* 99:1351-1360.
74. Imai, M., Takigami, K., Guckelberger, O., Enjyoji, K., Smith, R.N., Lin, Y., Csizmadia, E., Sevigny, J., Rosenberg, R.D., Bach, F.H., et al. 1999. Modulation of nucleoside triphosphate diphosphohydrolase-1 (NTPDase-1)cd39 in xenograft rejection. *Mol Med* 5:743-752.
75. Gayle, R.B., 3rd, Maliszewski, C.R., Gimpel, S.D., Schoenborn, M.A., Caspary, R.G., Richards, C., Brasel, K., Price, V., Drosopoulos, J.H., Islam, N., et al. 1998. Inhibition of platelet function by recombinant soluble ecto-ADPase/CD39. *J Clin Invest* 101:1851-1859.

76. Koyamada, N., Miyatake, T., Candinas, D., Hechenleitner, P., Siegel, J., Hancock, W.W., Bach, F.H., and Robson, S.C. 1996. Apyrase administration prolongs discordant xenograft survival. *Transplantation* 62:1739-1743.
77. Pinsky, D.J., Broekman, M.J., Peschon, J.J., Stocking, K.L., Fujita, T., Ramasamy, R., Connolly, E.S., Jr., Huang, J., Kiss, S., Zhang, Y., et al. 2002. Elucidation of the thromboregulatory role of CD39/ectoapyrase in the ischemic brain. *J Clin Invest* 109:1031-1040.
78. Enjyoji, K., Sevigny, J., Lin, Y., Frenette, P.S., Christie, P.D., Esch, J.S., 2nd, Imai, M., Edelberg, J.M., Rayburn, H., Lech, M., et al. 1999. Targeted disruption of cd39/ATP diphosphohydrolase results in disordered hemostasis and thromboregulation. *Nat Med* 5:1010-1017.
79. Fabre, J.E., Nguyen, M., Latour, A., Keifer, J.A., Audoly, L.P., Coffman, T.M., and Koller, B.H. 1999. Decreased platelet aggregation, increased bleeding time and resistance to thromboembolism in P2Y1-deficient mice. *Nat Med* 5:1199-1202.
80. Napieralski, R., Kempkes, B., and Gutensohn, W. 2003. Evidence for coordinated induction and repression of ecto-5'-nucleotidase (CD73) and the A2a adenosine receptor in a human B cell line. *Biol Chem* 384:483-487.
81. Eltzschig, H.K., Ibla, J.C., Furuta, G.T., Leonard, M.O., Jacobson, K.A., Enjyoji, K., Robson, S.C., and Colgan, S.P. 2003.  $\alpha_2B$  receptors. *J. Ex. Med.* 198:783-796.
82. McDonald, D.M., Thurston, G., and Baluk, P. 1999. Endothelial gaps as sites for plasma leakage in inflammation. *Microcirculation* 6:7-22.
83. Takano, T., Clish, C.B., Gronert, K., Petasis, N., and Serhan, C.N. 1998. Neutrophil-mediated changes in vascular permeability are inhibited by topical application of aspirin-triggered 15-epi-lipoxin A4 and novel lipoxin B4 stable analogues. *J Clin Invest* 101:819-826.
84. Thompson, L.F., Eltzschig, H.K., Ibla, J.C., Van De Wiele, C.J., Resta, R., Morote-Garcia, J.C., and Colgan, S.P. 2004. Crucial role for ecto-5'-nucleotidase (CD73) in vascular leak during hypoxia. *J. Exp. Med.* 200:1395-1405.
85. Bear, J.E., Svitkina, T.M., Krause, M., Schafer, D.A., Loureiro, J.J., Strasser, G.A., Maly, I.V., Chaga, O.Y., Cooper, J.A., Borisy, G.G., et al. 2002. Antagonism between Ena/VASP proteins and actin filament capping regulates fibroblast motility. *Cell* 109:509-521.
86. Comerford, K.M., Lawrence, D.W., Synnestvedt, K., Levi, B.P., and Colgan, S.P. 2002. Role of vasodilator-stimulated phosphoprotein in protein kinase A-induced changes in endothelial junctional permeability. *FASEB J.*:01-0739fje.
87. Lawrence, D.W., Comerford, K.M., and Colgan, S.P. 2002. Role of VASP in reestablishment of epithelial tight junction assembly after Ca<sup>2+</sup> switch. *Am J Physiol Cell Physiol* 282:C1235-1245.

88. Kong, W., Engel, K., and Wang, J. 2004. Mammalian nucleoside transporters. *Curr Drug Metab* 5:63-84.
89. Archer, R.G., Pitelka, V., and Hammond, J.R. 2004. Nucleoside transporter subtype expression and function in rat skeletal muscle microvascular endothelial cells. *Br J Pharmacol* 143:202-214. Epub 2004 Aug 2002.
90. Saito, H., Nishimura, M., Shinano, H., Makita, H., Tsujino, I., Shibuya, E., Sato, F., Miyamoto, K., and Kawakami, Y. 1999. Plasma concentration of adenosine during normoxia and moderate hypoxia in humans. *Am J Respir Crit Care Med* 159:1014-1018.
91. Chaudary, N., Naydenova, Z., Shuralyova, I., and Coe, I.R. 2004. Hypoxia regulates the adenosine transporter, mENT1, in the murine cardiomyocyte cell line, HL-1. *Cardiovasc Res* 61:780-788.
92. Chaudary, N., Naydenova, Z., Shuralyova, I., and Coe, I.R. 2004. The adenosine transporter, mENT1, is a target for adenosine receptor signaling and protein kinase Cepsilon in hypoxic and pharmacological preconditioning in the mouse cardiomyocyte cell line, HL-1. *J Pharmacol Exp Ther* 310:1190-1198. Epub 2004 May 1106.
93. Eltzschig, H.K., Abdulla, P., Hoffman, E., Hamilton, K.E., Daniels, D., Schonfeld, C., Loffler, M., Reyes, G., Duszenko, M., Karhausen, J., et al. 2005. HIF-1-dependent repression of equilibrative nucleoside transporter (ENT) in hypoxia. *J. Exp. Med.* 202:1493-1505.
94. Ogawa, S., Koga, S., Kuwabara, K., Brett, J., Morrow, B., Morris, S.A., Bilezikian, J.P., Silverstein, S.C., and Stern, D. 1992. Hypoxia-induced increased permeability of endothelial monolayers occurs through lowering of cellular cAMP levels. *Am J Physiol* 262:C546-554.
95. Eltzschig, H.K., Thompson, L.F., Karhausen, J., Cotta, R.J., Ibla, J.C., Robson, S.C., and Colgan, S.P. 2004. Endogenous adenosine produced during hypoxia attenuates neutrophil accumulation: coordination by extracellular nucleotide metabolism. *Blood* 104:3986-3992.
96. Eltzschig, H.K., and Collard, C.D. 2004. Vascular ischaemia and reperfusion injury. *Br Med Bull* 70:71-86.
97. Thompson, L.F., Eltzschig, H.K., Ibla, J.C., Van De Wiele, C.J., Resta, R., Morote-Garcia, J.C., and Colgan, S.P. 2004. Crucial Role for Ecto-5'-Nucleotidase (CD73) in Vascular Leakage during Hypoxia. *J. Exp. Med.* 200:1395-1405.
98. Ockaili, R., Natarajan, R., Salloum, F., Fisher, B.J., Jones, D., Fowler, A.A., III, and Kukreja, R.C. 2005. HIF-1 activation attenuates postischemic myocardial injury: role for heme oxygenase-1 in modulating microvascular chemokine generation. *Am J Physiol Heart Circ Physiol* 289:H542-548.
99. Hotchkiss, R.S., and Karl, I.E. 2003. The Pathophysiology and Treatment of Sepsis. *N Engl J Med* 348:138-150.
100. Ware, L.B., and Matthay, M.A. 2000. The Acute Respiratory Distress Syndrome. *N Engl J Med* 342:1334-1349.

101. Thiel, M., Chouker, A., Ohta, A., Jackson, E., Caldwell, C., Smith, P., Lukashev, D., Bittmann, I., and Sitkovsky, M.V. 2005. Oxygenation inhibits the physiological tissue-protecting mechanism and thereby exacerbates acute inflammatory lung injury. *PLoS Biol* 3:e174.
102. Fink, M. 2002. Bench-to-bedside review: Cytopathic hypoxia. *Critical Care* 6:491 - 499.
103. Ohta, A., and Sitkovsky, M. 2001. Role of G-protein-coupled adenosine receptors in downregulation of inflammation and protection from tissue damage. *Nature* 414:916-920.
104. Taylor, C.T., and Colgan, S.P. 1999. Therapeutic targets for hypoxia-elicited pathways. *Pharm. Res.* 16:1498-1505.
105. Weissmuller, T., Eltzschig, H.K., and Colgan, S.P. 2005. Dynamic purine signaling and metabolism during neutrophil-endothelial interactions. *Purinergic Signalling* 1:229-239.
106. Kempf, V.A.J., Lebidziejewski, M., Alitalo, K., Walzlein, J.-H., Eehalt, U., Fiebig, J., Huber, S., Schutt, B., Sander, C.A., Muller, S., et al. 2005. Activation of Hypoxia-Inducible Factor-1 in Bacillary Angiomatosis: Evidence for a Role of Hypoxia-Inducible Factor-1 in Bacterial Infections. *Circulation* 111:1054-1062.
107. Peyssonnaud, C., Datta, V., Cramer, T., Doedens, A., Theodorakis, E.A., Gallo, R.L., Hurtado-Ziola, N., Nizet, V., and Johnson, R.S. 2005. HIF-1 $\alpha$  expression regulates the bactericidal capacity of phagocytes. *J. Clin. Invest.* 115:1806-1815.
108. Phillis, J.W., O'Regan, M.H., and Perkins, L.M. 1992. Measurement of rat plasma adenosine levels during normoxia and hypoxia. *Life Sci* 51:PL149-152.
109. Eltzschig, H.K., Abdulla, P., Hoffman, E., Hamilton, K.E., Daniels, D., Schönfeld, C., Löffler, M., Reyes, G., Duszenko, M., Karhausen, J., et al. 2005. HIF-1-dependent repression of equilibrative nucleoside transporter (ENT) in hypoxia. *J Exp Med* in press.
110. Blackburn, M.R. 2003. Too much of a good thing: adenosine overload in adenosine-deaminase-deficient mice. *Trends Pharmacol Sci* 24:66-70.
111. Driver, A.G., Kukoly, C.A., Ali, S., and Mustafa, S.J. 1993. Adenosine in bronchoalveolar lavage fluid in asthma. *Am Rev Respir Dis* 148:91-97.
112. Huszar, E., Vass, G., Vizi, E., Csoma, Z., Barat, E., Molnar Vilagos, G., Herjavec, I., and Horvath, I. 2002. Adenosine in exhaled breath condensate in healthy volunteers and in patients with asthma. *Eur Respir J* 20:1393-1398.
113. Fozard, J.R., and Hannon, J.P. 1999. Adenosine receptor ligands: potential as therapeutic agents in asthma and COPD. *Pulm Pharmacol Ther* 12:111-114.
114. Blackburn, M.R., Volmer, J.B., Thrasher, J.L., Zhong, H., Crosby, J.R., Lee, J.J., and Kellems, R.E. 2000. Metabolic Consequences of Adenosine Deaminase Deficiency in Mice Are Associated with Defects in Alveogenesis,

- Pulmonary Inflammation, and Airway Obstruction. *J. Exp. Med.* 192:159-170.
115. Chunn, J.L., Molina, J.G., Mi, T., Xia, Y., Kellems, R.E., and Blackburn, M.R. 2005. Adenosine-Dependent Pulmonary Fibrosis in Adenosine Deaminase-Deficient Mice. *J Immunol* 175:1937-1946.
  116. Sun, C.-X., Young, H.W., Molina, J.G., Volmer, J.B., Schnermann, J., and Blackburn, M.R. 2005. A protective role for the A1 adenosine receptor in adenosine-dependent pulmonary injury. *J. Clin. Invest.* 115:35-43.
  117. Buckley, R.H. 2000. Primary Immunodeficiency Diseases Due to Defects in Lymphocytes. *N Engl J Med* 343:1313-1324.
  118. Buckley, R.H. 2004. Molecular defects in human severe combined immunodeficiency and approaches to immune reconstitution. *Annu Rev Immunol* 22:625-655.
  119. Eltzschig, H.K. 2001. Anesthesia for trauma of the eye. In *Trauma of the eye*. J.M. Rohrbach, K.P. Steuhl, M. Knorr, and K. B., editors. Stuttgart, New York: Schattauer. 345-350.
  120. Robinson, K.A., Candal, F.J., Scott, N.A., and Ades, E.W. 1995. Seeding of vascular grafts with an immortalized human dermal microvascular endothelial cell line. *Angiology* 46:107-113.
  121. Barone, G.W., Farley, P.C., Conerly, J.M., Flanagan, T.L., and Kron, I.L. 1989. Morphological and functional techniques for assessing endothelial integrity: the use of Evans blue dye, silver stains, and endothelial derived relaxing factor. *J Card Surg* 4:140-148.
  122. Parkos, C.A., Delp, C., Arnaout, M.A., and Madara, J.L. 1991. Neutrophil migration across a cultured intestinal epithelium: Dependence on a CD11b/CD18 - mediated event and enhanced efficiency in the physiologic direction. *J. Clin. Invest.* 88:1605-1612.
  123. Kameoka, J., Tanaka, T., Nojima, Y., Schlossman, S.F., and Morimoto, C. 1993. Direct association of adenosine deaminase with a T cell activation antigen, CD26. *Science* 261:466-469.
  124. Dong, R.P., Kameoka, J., Hegen, M., Tanaka, T., Xu, Y., Schlossman, S.F., and Morimoto, C. 1996. Characterization of adenosine deaminase binding to human CD26 on T cells and its biologic role in immune response. *J Immunol* 156:1349-1355.
  125. Strauss, P.R. 1986. Murine lymphocytes and lymphocyte cell lines secrete adenosine deaminase. *Adv Exp Med Biol* 195 Pt B:275-282.
  126. Schrader, W.P., West, C.A., Miczek, A.D., and Norton, E.K. 1990. Characterization of the adenosine deaminase-adenosine deaminase complexing protein binding reaction. *J. Biol. Chem.* 265:19312-19318.
  127. Dinjens, W.N., ten Kate, J., van der Linden, E.P., Wijnen, J.T., Khan, P.M., and Bosman, F.T. 1989. Distribution of adenosine deaminase complexing protein (ADCP) in human tissues. *J. Histochem. Cytochem.* 37:1869-1875.

128. Gherzi, G., Chen, W.-T., Lee, E.W., and Zukowska, Z. 2001. Critical role of dipeptidyl peptidase IV in neuropeptide Y-mediated endothelial cell migration in response to wounding. *J. Biol. Chem.* 276:453.
129. Cheng, H.-C., Abdel-Ghany, M., Elble, R.C., and Pauli, B.U. 1998. Lung Endothelial Dipeptidyl Peptidase IV Promotes Adhesion and Metastasis of Rat Breast Cancer Cells via Tumor Cell Surface-associated Fibronectin. *J. Biol. Chem.* 273:24207-24215.
130. Hansen, L., Deacon, C.F., Orskov, C., and Holst, J.J. 1999. Glucagon-Like Peptide-1-(7-36)Amide Is Transformed to Glucagon-Like Peptide-1-(9-36)Amide by Dipeptidyl Peptidase IV in the Capillaries Supplying the L Cells of the Porcine Intestine. *Endocrinology* 140:5356-5363.
131. Blanco, J., Valenzuela, A., Herrera, C., Lluís, C., Hovanessian, A.G., and Franco, R. 2000. The HIV-1 gp120 inhibits the binding of adenosine deaminase to CD26 by a mechanism modulated by CD4 and CXCR4 expression. *FEBS Lett* 477:123-128.
132. Valenzuela, A., Blanco, J., Callebaut, C., Jacotot, E., Lluís, C., Hovanessian, A.G., and Franco, R. 1997. Adenosine deaminase binding to human CD26 is inhibited by HIV-1 envelope glycoprotein gp120 and viral particles. *J Immunol* 158:3721-3729.
133. Lambeir, A.M., Durinx, C., Scharpe, S., and De Meester, I. 2003. Dipeptidyl-peptidase IV from bench to bedside: an update on structural properties, functions, and clinical aspects of the enzyme DPP IV. *Crit Rev Clin Lab Sci* 40:209-294.
134. Lawson, C.A., Yan, S.D., Yan, S.F., Liao, H., Zhou, Y.S., Sobel, J., Kisiel, W., Stern, D.M., and Pinsky, a.D.J. 1997. Monocytes and Tissue Factor Promote Thrombosis in a Murine Model of Oxygen Deprivation. *J. Clin. Invest.* 99:1729-1738.
135. Pinsky, D.J., Naka, Y., Liao, H., Oz, M.C., Wagner, D.D., Mayadas, T.N., Johnson, R.C., Hynes, R.O., Heath, M., Lawson, C.A., et al. 1996. Hypoxia-induced Exocytosis of Endothelial Cell Weibel-Palade Bodies . A Mechanism for Rapid Neutrophil Recruitment after Cardiac Preservation. *J. Clin. Invest.* 97:493-500.
136. Synnestvedt, K., Furuta, G.T., Comerford, K.M., Louis, N., Karhausen, J., Eltzschig, H.K., Hansen, K.R., Thompson, L.F., and Colgan, S.P. 2002. Ecto-5'-nucleotidase (CD73) regulation by hypoxia-inducible factor-1 mediates permeability changes in intestinal epithelia. *J Clin Invest* 110:993-1002.
137. Law, W.R., Valli, V.E., and Conlon, B.A. 2003. Therapeutic potential for transient inhibition of adenosine deaminase in systemic inflammatory response syndrome. *Crit Care Med* 31:1475-1481.
138. Cohen, E.S., Law, W.R., Easington, C.R., Cruz, K.Q., Nardulli, B.A., Balk, R.A., Parrillo, J.E., and Hollenberg, S.M. 2002. Adenosine Deaminase Inhibition Attenuates Microvascular Dysfunction and Improves Survival in Sepsis. *Am. J. Respir. Crit. Care Med.* 166:16-20.



139. Adanin, S., Yalovetskiy, I.V., Nardulli, B.A., Sam, A.D., 2nd, Jonjev, Z.S., and Law, W.R. 2002. Inhibiting adenosine deaminase modulates the systemic inflammatory response syndrome in endotoxemia and sepsis. *Am J Physiol Regul Integr Comp Physiol* 282:R1324-1332.
140. Collard, C.D., Park, K.A., Montalto, M.C., Alipati, S., Buras, J.A., Stahl, G.L., and Colgan, S.P. 2002. Neutrophil-derived glutamate regulates vascular endothelial barrier function. *J Biol Chem* 2002:14801-14811.
141. Yamamoto, M., Nishimura, M., Kobayashi, S., Akiyama, Y., Miyamoto, K., and Kawakami, Y. 1994. Role of endogenous adenosine in hypoxic ventilatory response in humans: a study with dipyridamole. *J Appl Physiol* 76:196-203.
142. Lefkowitz, R.J., and Whalen, E.J. 2004. [beta]-arrestins: traffic cops of cell signaling. *16:162*.
143. Bohn Lm Fau - Gainetdinov, R.R., Gainetdinov Rr Fau - Lin, F.T., Lin Ft Fau - Lefkowitz, R.J., Lefkowitz Rj Fau - Caron, M.G., and Caron, M.G. Mu-opioid receptor desensitization by beta-arrestin-2 determines morphine tolerance but not dependence.
144. Bohn Lm Fau - Lefkowitz, R.J., Lefkowitz Rj Fau - Gainetdinov, R.R., Gainetdinov Rr Fau - Peppel, K., Peppel K Fau - Caron, M.G., Caron Mg Fau - Lin, F.T., and Lin, F.T. Enhanced morphine analgesia in mice lacking beta-arrestin 2.
145. Perry, S.J., Baillie, G.S., Kohout, T.A., McPhee, I., Magiera, M.M., Ang, K.L., Miller, W.E., McLean, A.J., Conti, M., Houslay, M.D., et al. 2002. Targeting of Cyclic AMP Degradation to beta 2-Adrenergic Receptors by beta - Arrestins. *Science* 298:834-836.
146. Hashikawa, T., Hooker, S.W., Maj, J.G., Knott-Craig, C.J., Takedachi, M., Murakami, S., and Thompson, L.F. 2004. Regulation of adenosine receptor engagement by ecto-adenosine deaminase. *Faseb J* 18:131-133.
147. Martin, M., Huguet, J., Centelles, J.J., and Franco, R. 1995. Expression of ecto-adenosine deaminase and CD26 in human T cells triggered by the TCR-CD3 complex. Possible role of adenosine deaminase as costimulatory molecule. *J Immunol* 155:4630-4643.
148. Pacheco, R., Martinez-Navio, J.M., Lejeune, M., Climent, N., Oliva, H., Gatell, J.M., Gallart, T., Mallol, J., Lluís, C., and Franco, R. 2005. CD26, adenosine deaminase, and adenosine receptors mediate costimulatory signals in the immunological synapse. *PNAS* 102:9583-9588.
149. Jin, X., Shepherd, R.K., Duling, B.R., and Linden, J. 1997. Inosine Binds to A3 Adenosine Receptors and Stimulates Mast Cell Degranulation. *J. Clin. Invest.* 100:2849-2857.
150. Tilley, S.L., Wagoner, V.A., Salvatore, C.A., Jacobson, M.A., and Koller, B.H. 2000. Adenosine and inosine increase cutaneous vasopermeability by activating A3 receptors on mast cells. *J. Clin. Invest.* 105:361-367.
151. Hasko, G., Sitkovsky, M.V., and Szabo, C. 2004. Immunomodulatory and neuroprotective effects of inosine. *Trends Pharmacol Sci* 25:152-157.

152. Hasko, G., Kuhel, D.G., Nemeth, Z.H., Mabley, J.G., Stachlewitz, R.F., Virag, L., Lohinai, Z., Southan, G.J., Salzman, A.L., and Szabo, C. 2000. Inosine Inhibits Inflammatory Cytokine Production by a Posttranscriptional Mechanism and Protects Against Endotoxin-Induced Shock. *J Immunol* 164:1013-1019.
153. Aussedat, J., Verdys, M., and Rossi, A. 1985. Adenine nucleotide synthesis from inosine during normoxia and after ischaemia in the isolated perfused rat heart. *Can J Physiol Pharmacol* 63:1159-1164.
154. Dowdall, J.F., Winter, D.C., and Bouchier-Hayes, D.J. 2002. Inosine modulates gut barrier dysfunction and end organ damage in a model of ischemia-reperfusion injury. *J Surg Res* 108:61-68.
155. Haun, S.E., Segeleon, J.E., Trapp, V.L., Clotz, M.A., and Horrocks, L.A. 1996. Inosine mediates the protective effect of adenosine in rat astrocyte cultures subjected to combined glucose-oxygen deprivation. *J Neurochem* 67:2051-2059.

## 7 Danksagung

Die vorliegende Arbeit wurde unter der Betreuung von Professor Dr. Holger Eltzschig aus der Abteilung für Anästhesiologie und Intensivmedizin der Universitätsklinik Tübingen durchgeführt. Für die Überlassung des interessanten Themas sowie die ausgezeichnete Betreuung danke ich ihm sehr. Im Besonderen möchte ich ihm dafür danken, dass er zu jeder Zeit für Fragen und Probleme ein offenes Ohr hatte und einem immer wieder mit Ratschlägen weiterhalf.

Ebenso gilt mein Dank den Mitarbeitern des Labors im Zentrum für Medizinische Forschung der Universitätsklinik Tübingen für die nette Zusammenarbeit. Alice Mager und Michaela Hoch-Gutbrod danke ich besonders für die hervorragende Einarbeitung in die labortechnischen Methoden sowie für die vielen freundschaftlichen Gespräche, Edgar Hoffmann und Marion Faigle für die Unterstützung bei den Experimenten und Christof Zanke sowie meinen Mitdoktoranden für so manche Hilfe bei diversen computertechnischen Problemen und für viele nette aufbauende Gespräche.

Bei meinen Eltern bedanke ich mich für die Unterstützung während des gesamten Studiums sowie der Familie Conzen für das Arbeiten an ihrem Computer in der letzten Ausarbeitungsphase der Dissertation, als mich mein eigenes Notebook im Stich ließ.

Zuletzt möchte ich einem ganz besonderen Freund danken, der mich während meiner ganzen Studienzeit begleitet hat und der immer an den Erfolg dieser Arbeit geglaubt hat.

## 8 Lebenslauf

Name: Simone Ulrike Knapp  
Geburtsdatum: 14. Juni 1980  
Geburtsort: Heilbronn

### Schulausbildung

---

August 1987 – Juli 1991 Michael-Beheim-Grundschule Obersulm  
August 1991 – Juni 2000 Justinus-Kerner-Gymnasium Weinsberg

### Studium

---

April 2001 Beginn des Studiums der Humanmedizin an der Eberhard-Karls-Universität Tübingen  
April 2003 Ärztliche Vorprüfung  
August 2006 – Dezember 2006 1.PJ-Tertial: Anästhesiologie am Universitätsklinikum Tübingen  
Dezember 2006. – April 2007 2.PJ-Tertial: Innere Medizin am Kantonsspital Liestal (Schweiz)  
April 2007 – Juli 2007 3.PJ-Tertial: Chirurgie am G.F. Jooste Hospital in Kapstadt (Südafrika)  
24. Juni 2008 2. Staatsexamen  
09. Juli 2008 Approbation als Ärztin

**Wissenschaftliche Tätigkeit**

---

März 2004 – April 2007

Promotion am Universitätsklinikum Tübingen,  
Abteilung für Anästhesiologie und  
Intensivmedizin

März 2007

Besuch des Kongresses medART am  
Universitätsspital Basel